THE THERMODYNAMIC MODEL

FOR

THE RECA/LEXA COMPLEX FORMATION

A Thesis Submitted to the College of

Graduate Studies and Research

In Partial Fulfillment of the Requirements

For the Degree of Masters of Science

In the Department of Biochemistry

University of Saskatchewan

Saskatoon

By

Ignace Adolfo Moya

PERMISSION TO USE

In presenting this thesis in partial fulfilment of the requirements for a Postgraduate degree from the University of Saskatchewan, I agree that the Libraries of this University may make it freely available for inspection. I further agree that permission for copying of this thesis in any manner, in whole or in part, for scholarly purposes may be granted by the professor or professors who supervised my thesis work; or in their absence, by the Head of the Department or the Dean of the College in which my thesis work was done. It is understood that any copying or publication or use of this thesis or parts thereof for financial gain shall not be allowed without my written permission. It is also understood that due recognition shall be given to me and to the University of Saskatchewan in any scholarly use which may be made of any material in my thesis.

Requests for permission to copy or to make other use of material in this thesis in whole or part should be addressed to:

Head of the Department of Biochemistry

University of Saskatchewan

Saskatoon, Saskatchewan, S7N 5E5

ABSTRACT

Escherichia coli RecA is a versatile protein that is involved in homologous recombination, and coordination of both the DNA damage response and translesion synthesis. Single-stranded DNA (ssDNA) that is generated at the site of double-stranded breaks serves as a signal to activate RecA. This allows RecA to form a long helical filament on the ssDNA, which is required in recombination, hydrolysis of ATP, and mediating the self-cleavage of some ser-lys dyad proteins such as the LexA repressor.

In this thesis, the formation of the RecA/LexA complex did not require preactivation by ssDNA, instead a volume excluding agent in the presence of LexA was able to stimulate its formation. These preliminary results led to a hypothesis that the formation of the RecA/LexA complex is a thermodynamic process that involves three steps: (1) a change in RecA's conformation towards the active form, (2) a change in LexA's conformation towards the cleavable form (*i.e.* burial of the ser-lys dyad catalytic residues), and (3) the binding between the active form of RecA and the cleavable form of LexA. Evidence for this model was shown by the ability of either NaCl, LexA K156A, an ATP substrate, or a volume excluding agent to enhance the stability of the RecA/LexA complex, which was detected by both the ATPase and coprotease assays. Hyper-active RecA mutants, isolated form the yeast two-hybrid screen, were also tested, however they did not enhance the stability of the complex. Additionally, RecA's binding preference for the monomer or dimer form of LexA was examined, since it is unknown which species of LexA is able to enhance the stability of the complex. To generate the monomer form of LexA, single point mutations were introduced at the dimer interface of the protein such that its dimerization was disrupted by charge-charge repulsions. Based

on the inhibition assay, RecA was found to bind preferentially to dimer form and not the monomer form of LexA, possible reasons for these results are discussed.

ACKNOWLEDGEMNTS

First of all, I would like to thank my supervisor Dr. Luo for letting me work on this project. He was very helpful in teaching me the theory and the experimental procedures behind this project. I also appreciated the lengthy conversations that we had (one to one and half hours in length) on a variety of topics including the project itself, daily news, and his stories from Alabama. I would also like to thank Dr. Geyer for both his guidance and materials for the yeast two-hybrid system.

I would like to thank my coworkers, Gloria Qian and John He for their help with the assays and protein purification; Karen Mochoruk for her work with the mass spectrometer; and Kris Barreto and Dr. Xianzhong Shi for their tips in PCR and the laborious techniques that were related to the yeast system. The summer students, James Zheng, Jiayi Han, and Sally Zhao were also helpful in relieving some of my workload in the lab, which allowed me to skip work on a few occasions.

Special thanks to my parents and friends in Saskatoon for all of their help and support during graduate studies.

DEDICATION

This thesis is dedicated to the memory of my friend Francisco Moran. I enjoyed all the times that I spent visiting and speaking to him in Spanish. It was the remedy that I needed to cure my homesickness.

TABLE OF CONTENTS

LIST OF TABLES

LIST OF FIGURES

LIST OF ABBREVIATIONS

A^-	Minus adenine
ADP	Adenosine diphosphate
Amp	Ampicillin
AMP-PNP	5'-adenylylimidodiphosphate
AMP-PCP	Adenosine 5'-(β,γ-methylene) triphosphate
ATP	Adenosine triphosphate
ATP-γ-S	Adenosine 5 -O-(3-thio)-triphosphate
B42AD	B42 activation domain
CFU	Colony forming units
CSM	Complete supplement mixture
CTP	Cytidine triphosphate
d	Deoxy prefix
DNA	Deoxyribonucleic acid
ds	Double-stranded prefix
E. coli	*Escherichia coli*
EcRecA	*Escherichia coli* RecA
EDTA	Ethylenediaminetetraacetic acid
gal	Galactose
glu	Glucose
H^-	Minus histidine
HEPES	N-(2-hydroxyethyl)-piperazine-N'-2-ethanesulfonic acid
HhH	Helix-hairpin-helix
Histag	Hexahistidine tag
IPTG	Isopropyl-thio-β-D-galactoside
Kan	Kanamycin
L^-	Minus leucine
LB	Luria Bertani
MES	N-(morpholino)ethanesulfonic acid
MvRadA	*Methanococcus voltae* RadA
NTP	Nucleoside triphosphate
OD	Optical density
ORF	Open reading frame
PCR	Polymerase chain reaction
PEG	Polyethylene glycol
P_i	Inorganic phosphate
RFI	Relative fluorescence increase

RNA	Ribonucleic acid
RMSD	Root-mean-square deviation
sac	Saccharose
SD	Synthetic defined
SDS	Sodium dodecyl sulphate
ser-lys	Serine-lysine
STE	Shiga toxin-producing *Escherichia coli*
STMP	Salt titration midpoint
ss	Single-stranded prefix
TAE	Tris-acetate-EDTA
Tris	Tris(hydroxymethyl)aminomethane
UTP	Uridine triphosphate
W^-	Minus tryptophan
X-Gal	5-bromo-4-chloro-3-indolyl-β-D-Galactopyranoside
YPD	Yeast/peptone/dextrose

1. INTRODUCTION

Escherichia coli RecA protein is a general recombinase that is involved in the repair of double-stranded DNA (dsDNA) breaks caused by DNA-damaging agents and natural processing events (Friedberg *et al.*, 1995). RecA also has a coprotease activity that is essential to coordinate the "SOS" regulon, a series of ~40 unlinked genes that are required for post-replication repair (Courcelle *et al.*, 2001; Friedberg *et al.*, 1995). The single-stranded DNA (ssDNA), generated at ends of the double-strand breaks, serves as a signal to activate RecA's coprotease activity (Kowalczykowski *et al.*, 1994). In turn, the LexA repressor becomes a target for RecA-mediated cleavage, which leads to the transcriptional derepression of the SOS regulon (Walker, 1985).

RecA's coprotease activity is believed to facilitate the self-cleavage of the LexA repressor by providing a hydrophobic pocket (Lin and Little, 1989), which reduces the energetic cost in the burial and deprotonation of the ε-amino group of K156 in LexA (Luo *et al.*, 2001). Alternatively, the LexA repressor can undergo self-cleavage in the absence of RecA at neutral pH *in vitro*, but its rate of self-cleavage is dramatically reduced by 10,000-fold (Roland *et al.*, 1992). Under the latter conditions, LexA exists in a non-cleavable conformation where the ε-amino group of the K156 residue is exposed to the aqueous environment (Figure 2.3).

In vitro, the inactive form of RecA is able to self-polymerize at high protein concentrations, or at low protein concentrations in the presence of Mg^{2+} ions (Brenner *et al.*, 1988). This occurs through the interaction between its N-terminal tail domain and its head (central) domain, which generates a right-handed helical filament (Story *et al.*, 1992; Takahashi *et al.*, 1996). Based on the small-angle neutron scattering studies, the self-polymer has a physical characteristic of 6.4 subunits per turn with a compressed helical pitch of <70 Å (DiCapua *et al.*, 1990b). The active form of RecA is correlated to its enzymatic activities (ATPase, coprotease, and recombinase), which requires the binding of ATP, excess Mg^{2+} ions, and ssDNA (Kowalczykowski *et al.*, 1994; Roman

and Kowalczykowski, 1986). Based on the electron microscopy structures and small-angel neutron scattering studies, all three enzymatic activities have a common physical characteristic of 6.2 subunits per turn with an extended helical pitch of >95 Å (DiCapua *et al.*, 1992; DiCapua *et al.*, 1990a; Yu and Egelman, 1992). RecA's active form can be deactivated upon hydrolysis of ATP to ADP, which compresses the helical pitch to ~80 Å and increases the number of subunits per turn to ~6.4 (DiCapua *et al.*, 1990b; Story *et al.*, 1992; Yu *et al.*, 2001). In general, the RecA filament exists in two conformations, a compressed or an extended helical pitch that is correlated to its inactive or active states respectively (DiCapua *et al.*, 1990b).

As mentioned above, the extended helical pitch of the RecA filament is correlated to its active form (*i.e.* its ATPase and coprotease activity), no matter how the activation is brought about (DiCapua *et al.*, 1992; DiCapua *et al.*, 1990a). This relationship, the level of RecA's ATPase and coprotease activity, was applied to this study in order to detect the formation of the RecA/LexA complex *in vitro*. It was found that RecA's enzymatic activities were stimulated with increasing concentrations of a volume-excluding agent, polyethylene glycol (PEG) in the presence of wild-type LexA, such that preactivation by ssDNA was not required. Therefore, it is proposed that the formation of a RecA/LexA complex is a thermodynamic process that can be broken down into three steps: (1) activation of RecA (the active form), (2) stabilization of LexA's cleavable conformation (the cleavable form), and (3) binding between the active form of RecA and the cleavable form of LexA. To provide evidence for this model, the stability of the RecA/LexA complex was enhanced by decreasing the energy barrier that was associated at each step in the thermodynamic process.

2. REVIEW OF LITERATURE

2.1. RecA Protein

Escherichia coli RecA protein is a multifunctional protein that is essential for three different biological functions: (1) general recombination, (2) coordination of unlinked DNA repair genes in response to DNA damage, and (3) coordination of translesion synthesis (Bianco and Kowalczykowski, 2001). Thus, RecA possesses a number of different enzymatic activities, such as homologous pairing and exchange of DNA, ATP- and DNA-dependent coproteolytic processing of effector proteins, and interacting with mutagenic protein factors that are involved in translesion synthesis (Kowalczykowski *et al.*, 1994).

Given RecA's essential role in maintaining the genomic integrity and consequent survival of the cell in response to DNA damaging agents, it is not surprising that the protein is conserved among a wide range of prokaryotic organisms. Additionally, RecA has a structural homology with other recombinases found in eukaryotic and archaeal organisms (Kowalczykowski and Eggleston, 1994). The conserved structure of RecA in various organisms suggests that all of the recombinases have evolved from a common ancestor (Kowalczykowski and Eggleston, 1994).

2.2. Overview of RecA's Biological Functions

RecA was first discovered by Clark and Margulies (1965) when screening bacterial cells that were defective in recombination. Later on, the protein was found to be essential for all pathways associated with homologous recombination, such as prophage production and DNA damage response (SOS induction) with the exception of *recET*-mediated plasmid recombination (Bianco *et al.*, 1998). For example, mutations in both *recA* and *uvrA* genes made the cells defective in specific types of DNA repair upon exposure to DNA damaging agents, such as the repair of DNA-cross links, double-stranded breaks, and bypass of modified DNA bases (Kowalczykowski *et al.*, 1994).

2.2.1. SOS Induction

The RecA protein and the LexA repressor play a central role in coordinating various unlinked DNA-repair genes in *E. coli*, which is collectively referred to as the SOS response (Figure 2.1) (Witkin, 1991). Activation of the SOS response involves the generation of ssDNA at the site of dsDNA breaks upon exposure to DNA damaging agents. This serves as a signal to activate RecA's coprotease activity, which is responsible for mediating the cleavage of the LexA repressor (Horrii *et al.*, 1981; Little *et al.*, 1980). The self-proteolytic cleavage of the LexA repressor occurs at the A84-G85 peptide, which separates its DNA binding domain from its dimerization domain (Slilaty and Little, 1987), and in turn leads to the transcriptional derepression of ~40 unlinked genes that belong to the SOS regulon (Courcelle *et al.*, 2001; Walker, 1985). RecA's coprotease activity also targets other LexA homologs such as the lytic repressor protein (either λ, ϕ80, 434, or P22) of lambdoid bacteriophages (Eguchi *et al.*, 1988; Roberts *et al.*, 1978; Sauer *et al.*, 1982), and a mutagenic factor (UmuD) that is involved in the error-prone DNA replicative bypass machinery (Rajagopalan *et al.*, 1992; Shinagawa *et al.*, 1988).

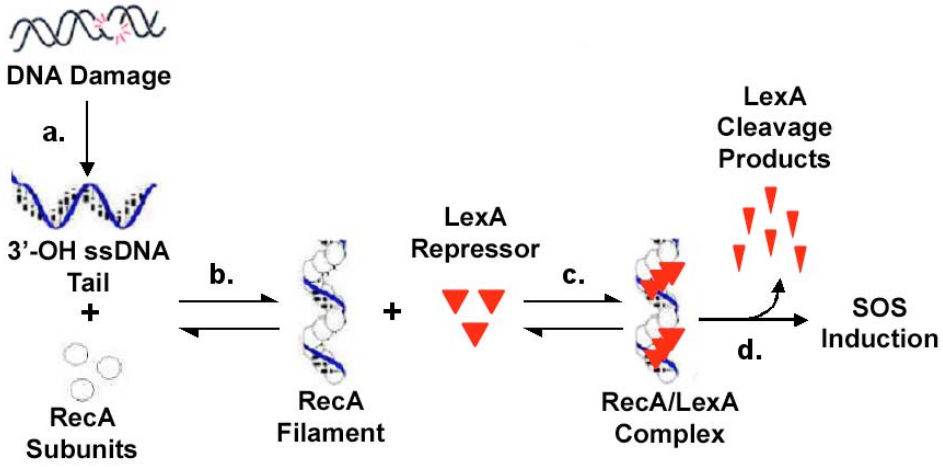

Figure 2.1. A cartoon diagram depicting the activation of the SOS response.

Upon exposure to DNA damaging agents, **(a)** the ends of the damaged dsDNA breaks are processed into 3'-OH ssDNA tails. **(b)** RecA's coprotease activity is activated when the protein binds to the 3'-OH ssDNA tails to form an extended RecA nucleofilament. **(c)** The nucleofilament binds to the LexA repressor to form a RecA/LexA complex, which **(d)** facilitates the self-cleavage of LexA, and consequently leads to the transcriptional derepression of the SOS genes (SOS induction). (The figure was modified from Bianco and Kowalczykowski, 1998).

Activation of the SOS response is also implicated in the epidemiology of Shiga toxin producing *E. coli* (STEC). Shiga toxins are encoded in the bacteriophage genes that are integrated in the host *E. coli* chromosome (Kuzminov, 1999) and they are the main cause of food borne illnesses in the developed countries (Haque *et al.*, 2003). The release of Shiga toxins into the gut can increase the risk for developing hemolytic anemia, thrombocytopenia, acute renal failure, and complications of the central nervous system (http://www.cdc.gov/epo/dphsi/casedef/hemolyticcurrent.htm). Presently, there is no conventional therapy for treating severe STEC infections, because certain antibiotics are known to increase the severity of the infection (Schuller *et al.*, 2005; Wong *et al.*, 2000). Antibiotics such as the quinolones can cause DNA damage in STEC, and in turn can lead to the activation of both the SOS response pathway and the lytic pathway of lambdoid bacteriophage that is integrated in the bacterial chromosome (Kimmitt *et al.*, 2000; Kuzminov, 1999; Quillardet and Hofnung, 1993). These two pathways are consequently activated by ssDNA when the integrity of the genome is compromised. The ssDNA serves as a signal to activate RecA-mediated cleavage of the CI phage repressor (Kim and Little, 1993), a LexA homolog, and in turn lead to the transcriptional derepression of phage particles (*e.g.* Shiga toxins) and host bacterial cell lysis (Kuzminov, 1999; Oppenheim *et al.*, 2005). Thus, drugs that target the RecA/CI phage repressor complex may be beneficial in treating severe STEC diseases.

2.2.2. RecA-mediated Cleavage of Wild-type LexA

The role of the activated RecA nucleofilament is believed to provide a hydrophobic pocket in the burial and deprotonation of the ε-amino group of the K156 residue in LexA (Lin and Little, 1989; Luo *et al.*, 2001). This shifts LexA's conformation towards the cleavable form, thereby increasing its rate of self-cleavage by 10,000-fold at neutral pH as predicted by the conformation-equilibrium model (Figure 2.2) (Roland *et al.*, 1992). The energy barrier, required to shift LexA's conformation from the non-cleavable form to the cleavable form (Figure 2.3), is believed to maintain LexA's self-cleavage reaction in check in the absence of RecA (Luo *et al.*, 2001). Additionally, RecA-mediated cleavage for all other LexA homologs are expected to follow a similar course as mentioned above. They all share a common fold at the

cleavage site region (β strand b3-loop-β strand b4 motif) and a ser-lys dyad catalytic mechanism when compared to the LexA crystal structure (Luo *et al.*, 2001).

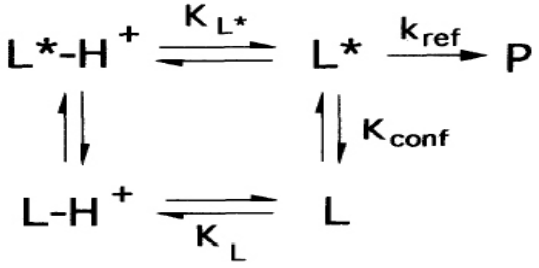

Figure 2.2. The conformation-equilibrium model for LexA self-cleavage and RecA-mediated cleavage.

The model represents two interconvertible conformations of LexA, a non-cleavable conformation (L) and a cleavable conformation (L^*) that can exist in the presence or absence of RecA. The interconversion between the two conformations is controlled by the specific local environment around the active site residues (S119 and K156). The ratio $[L^*]/[L]$ is defined by the equilibrium constant (K_{conf}), and the self-cleavage of LexA in the L* form follows a first ordered rate constant (k_{ref}). P represents the cleavage products of the reaction. (The figure was modified from Roland *et al.*, 1992).

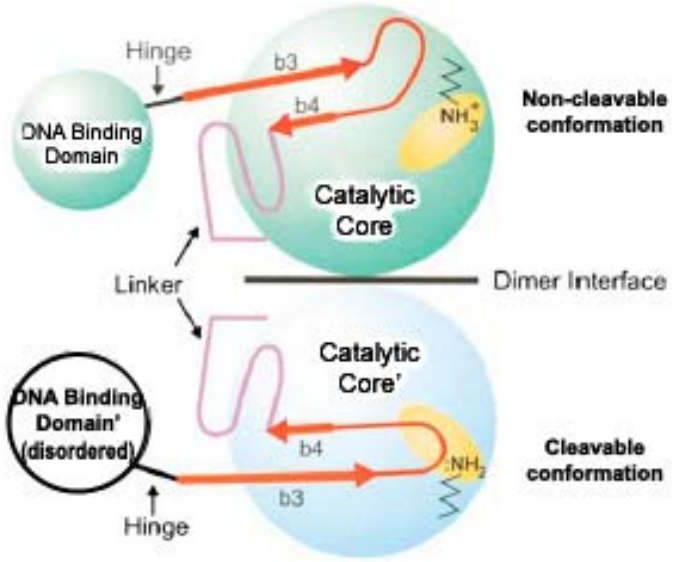

Figure 2.3. A cartoon picture depicting the two interconvertible conformations of the LexA homodimer.

In the top subunit, LexA exists in the non-cleavable conformation when the positively charged ε-amino group of K156 is exposed to the solvent. In the bottom subunit, LexA exists in the cleavable conformation when the cleavage site region (orange) buries and deprotonates the ε-amino group of K156. (The figure was modified from Luo *et al.*, 2001).

As mentioned above, the self-cleavage mechanism in LexA consists of a ser-lys dyad that is conserved among certain ser-lys proteases (Luo *et al.*, 2001; Slilaty and Little, 1987; Slilaty and Vu, 1991). In the LexA protein, the ε-amino group of K156 is deprotonated and buried in the oxyanion hole, which serves as a general base to increase the nucleophilicity of S119 that is responsible for the cleavage of the A84-G85 peptide bond (Figure 2.4). The end products for this cleavage reaction are an N-terminal DNA binding domain and a C-terminal fragment (Little, 1993). The loss of the C-terminal (dimerization) domain reduces the N-terminal DNA binding domain's affinity for its operator site and also its half-life (Bertrand-Burggraf *et al.*, 1987; Little, 1983). This allows the two DNA strands to melt (Silva and Silveira, 1993) and allow the bound RNA polymerase to isomerize from a closed to an open complex (Vershon *et al.*, 1987), in order to transcriptional derepress the SOS genes.

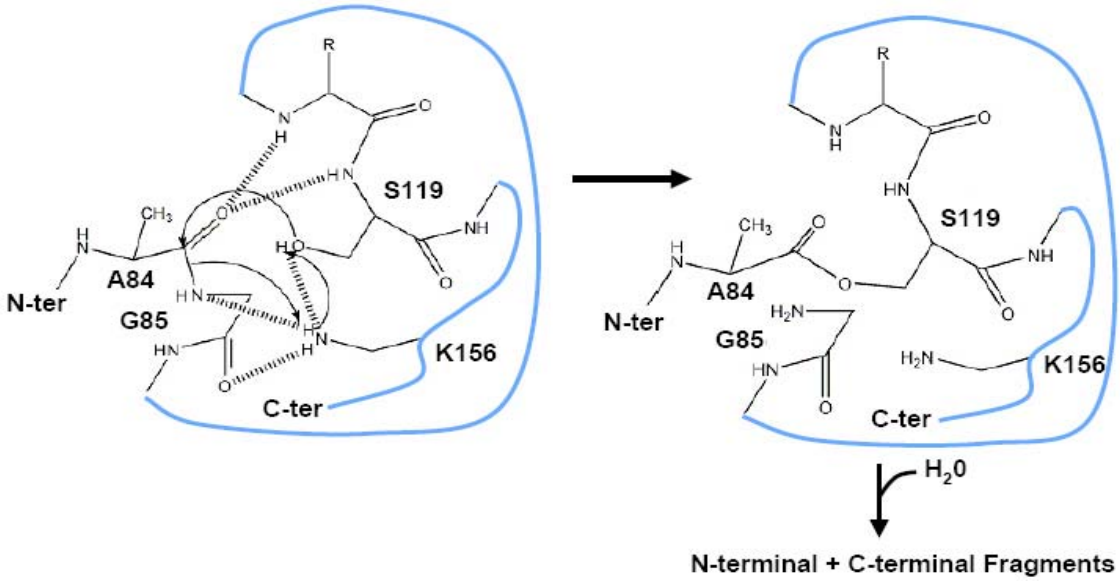

Figure 2.4. The catalytic mechanism proposed for the self-cleavage of the LexA repressor.

(The figure was modified from Slilaty and Little, 1987).

2.2.3. SOS Mutagenesis

SOS mutagenesis is an error-prone replication process that allows specific types of UV-induced DNA lesions to be bypassed by the DNA repair machinery (Walker, 1985). Initiation of this process involves the transcriptional derepression of the SOS operon; this includes the cleavage of the LexA repressor at the *umuDC* operon in order to

produce UmuD and UmuC. These proteins are able to associate and form an $UmuD_2UmuC$ heterotrimer, which is responsible for initiating the DNA damage cell cycle checkpoint (Opperman *et al.*, 1999). In the presence of the activated RecA nucleofilament, UmuD undergoes RecA-mediated cleavage (removal of its N-terminal 24 amino acids) to generate either a UmuD/UmuD' heterodimer or a $UmuD'_2$ homodimer (Burckhardt *et al.*, 1988; Nohmi *et al.*, 1988; Shinagawa *et al.*, 1988). The $UmuD'_2UmuC$ heterotrimer constitutes a functional DNA polymerase V that is responsible for bypassing DNA lesions that can not be replicated by DNA Polymerase III (Reuven *et al.*, 1999; Tang *et al.*, 2000; Tang *et al.*, 1999). Once the regions of the DNA-damaged bases are filled in, the RecA nucleofilament can no longer mediate the cleavage of UmuD. The remaining UmuD'-UmuD heterodimers lead to the inhibition of translesion synthesis (Battista *et al.*, 1990). Eventually, they are removed from the cell by the ATP-dependent protease, ClpXP, which turns off SOS mutagenesis (Gonzalez *et al.*, 2000).

2.2.4. Homologous Recombination

The pairing and complete exchange of DNA strands occur in a series of kinetically defined steps (Figure 2.5) (Kowalczykowski, 1987b). In the first step, presynapsis requires the formation of a stoichiometric complex of RecA proteins and ssDNA (where one RecA monomer will bind to 3-4 nucleotide residues in a 5' to 3' direction), which is facilitated by single-stranded DNA binding protein (SSB). In the second step, synapsis requires the binding of the RecA/ssDNA complex to dsDNA, where the first contacts are not necessarily homologous in nature. This leads to a nonhomologous paired complex known as coaggregates that is responsible for increasing the local concentration of DNA, and in turn increases the rate of homologous pairing (Gonda and Radding, 1986). Following homologous alignment, there are two types of joint molecules that can form depending on the topological constraints. (1) Paranemic joints occur when the incoming ssDNA is not topologically intertwined at the internal site of the complementary dsDNA. (2) Plectonemic joints occur when the incoming ssDNA winds freely around the ends of the complementary dsDNA. The final step involves RecA-mediated branch migration, where the heteroduplex region in the joint molecule is

extended unidirectionally (5' to 3' direction relative to the incoming ssDNA) until the complete exchange of the ssDNA occurs.

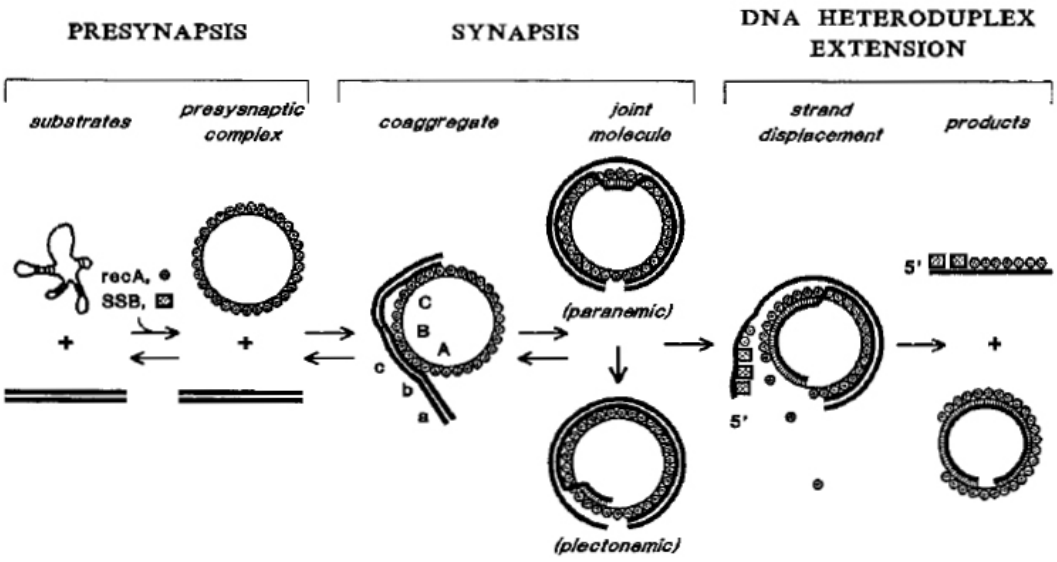

Figure 2.5. A schematic representation of the DNA strand exchange reaction catalyzed by RecA.

A simplified version of the kinetic steps involved in the protein-catalyzed exchange of DNA strands between circular single-stranded and linear double-stranded DNA molecules in the presence of SSB protein. Upon complete exchange of DNA strands, the linear ssDNA and nicked (or gapped) circular dsDNA products are formed. (The figure was taken from Kowalczykowski, 1991).

2.3. The Role of RecA's ATPase Activity

All of RecA's biological activities require the presence of ATP, which is responsible for the allosteric transition into a conformation that is referred to as a "high-affinity DNA binding state" (Menetski and Kowalczykowski, 1985). Under these conditions, the RecA nucleofilament has an extended helical pitch of >95 Å with an average of 6.2 subunits per turn (Figure 2.6) (DiCapua *et al.*, 1992; DiCapua *et al.*, 1990b; Yu *et al.*, 2001). This extension in the RecA/ATP filament is correlated to its tight binding affinity for ssDNA, which in turn is able to promote DNA strand-exchange activities and mediate the cleavage of some ser-lys proteases.

The binding of ATP and not its hydrolysis has been found to promote RecA's DNA strand exchange reaction (Menetski *et al.*, 1990). For example, less than 3 $x10^{-3}$ molecules of ATP-γ-S are hydrolyzed per base pair of DNA heteroduplex formed in 3.4

kb pairs of DNA heteroduplex. Thus, the slowly hydrolysable ATP analog, ATP-γ-S [adenosine-5'-O-(3-thiotriphosphate)] is able to promote RecA's DNA strand exchange activities with no input of free energy (Cox and Lehman, 1981; Honigberg *et al.*, 1985; Menetski *et al.*, 1990; Riddles and Lehman, 1985) because the reaction is isoenergetic (*i.e.* the free energy of the substrates and products are identical, because the number of base pairs is conserved through the reaction) (Kowalczykowski, 1991). The free energy in the DNA strand-exchange step is obtained from the binding of ATP, which results in an allosteric conformational change. The energy derived from the binding of ATP is required for the input of free energy in: (a) displacing SSB protein from ssDNA, (b) unwinding of dsDNA, and (c) pairing and stabilizing the three-stranded DNA intermediate (Kowalczykowski, 1991).

In the absence of ATP or in the presence of ADP, the RecA filament exists in a "low-affinity DNA binding state" (Menetski and Kowalczykowski, 1985). Under these conditions, the RecA filament has a collapsed helical pitch of <82 Å with an average of 6.4 subunits per turn (Figure 2.6) (DiCapua *et al.*, 1990b; Story *et al.*, 1992; Yu *et al.*, 2001). This collapse in RecA's helical structure is correlated with its low DNA binding affinity (Menetski and Kowalczykowski, 1985), which allows RecA to dissociate from the DNA (*i.e.* the displacement of DNA strands).

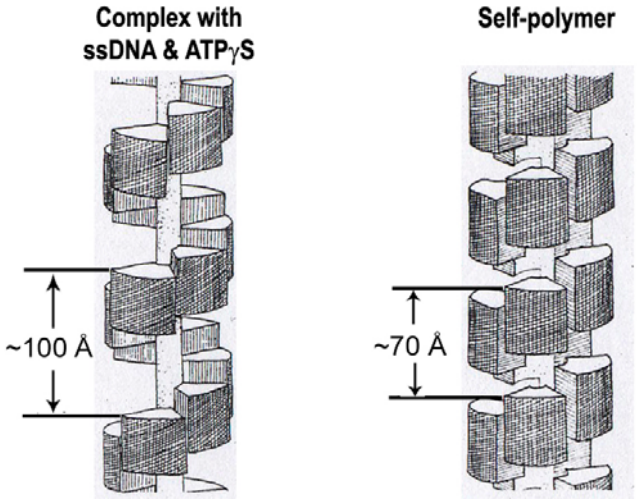

Figure 2.6. The inactive and active structure of the RecA filament.
(a) The active state of the RecA filament (complex with ssDNA and ATP-γ-S) has an extended pitch of ~100 Å. **(b)** The inactive state of the RecA self-polymer has a compressed pitch of ~70 Å. (The figure was modified from DiCapua *et al.*, 1990).

In general, the hydrolysis of ATP to ADP accomplishes two tasks: (1) it destroys the ATP effector molecule and (2) it produces a new ADP effector molecule (Kowalczykowski, 1991). It also solves the "tight binding dilemma" for a protein that is expected to bind tightly to its DNA substrate and yet be able to dissociate and act on a different molecule (Kowalczykowski, 1987a).

2.3.1. Regulating RecA's Coprotease Activity

The same allosteric conformational changes that are associated with RecA's DNA strand-exchange activities upon ATP binding can also be applied to its coprotease activity. Based on small angle neutron scattering and electron microscopy studies, RecA's coprotease activity is correlated to the extended helical pitch that is seen for RecA/ATP nucleofilaments (*i.e.* >95 Å with an average of 6.2 subunits per turn) (DiCapua *et al.*, 1992; VanLoock *et al.*, 2003a; Yu and Egelman, 1992). Also, the binding of ATP-γ-S in the presence of high salt concentrations can stimulate RecA's coprotease activity that would otherwise require ssDNA preactivation (DiCapua *et al.*, 1990a). Thus, the extended helical pitch of the RecA filament is a requirement for its coprotease activity, no matter how these allosteric conformational changes are brought about.

Theses changes may be responsible for the spacing within the helical groove of RecA in order to accommodate the LexA repressor (Story *et al.*, 1992; Yu and Egelman, 1993) and also a hydrophobic environment in order to shift LexA's conformation towards the cleavable form (Lin and Little, 1989). Thus, the formation of a stable RecA/LexA complex requires the extended helical pitch of RecA (DiCapua *et al.*, 1992) and it may also require the cleavable form of the LexA protein (Luo *et al.*, 2001).

The structural changes associated with the hydrolysis of ATP to ADP will most likely decrease the spacing within the helical groove of RecA, as a result of the collapse in its helical pitch (Yu and Egelman, 1992). Thus, the RecA/ADP nucleofilament is not expected to bind to the incoming LexA repressor nor mediate its self-cleavage, since the repressor will not be able to fit inside RecA's helical groove.

2.4. Modulating the Structure and Stability of the RecA/DNA Complex by Nucleotide Cofactors

2.4.1. Structural Transitions in the RecA/DNA Complex

The electron microscopy images of the RecA/DNA complex shows a structure that is filamentous, and a morphology that is dependent on the nucleotide cofactor present (DiCapua *et al.*, 1992; Heuser and Griffith, 1989; Yu and Egelman, 1992). In the absence of a nucleotide cofactor or in the presence of ADP, the complex has a compact helical pitch of 55-83 Å (Heuser and Griffith, 1989; Story *et al.*, 1992; Yu and Egelman, 1992). This compact helical pitch is also consistent with the small-angle neutron scattering studies, but the complex is formed in the absence of ATP and in the presence or absence of ssDNA (DiCapua *et al.*, 1990b). Based on the electron microscopy and small-angle neutron scattering studies, the compact structure is able to accommodate six nucleotide residues per RecA monomer. Also in the same study, the RecA/DNA complex in the presence of either ATP or ATP-γ-S has an extended helical pitch of ~100 Å that is able to accommodate three nucleotide residues per RecA monomer. Thus, the data suggest that the conformation of the RecA nucleofilament can exist in two different structures, a compact or extended state. Additionally, the ATP-dependent transition into the extended state cannot occur in the absence of ssDNA. Therefore, the extended state of the RecA/ATP complex requires the preactivation by ssDNA.

The extension of RecA/ATP complexes upon ssDNA binding has also been observed with various binding assays. For example, the RecA protein has been studied with the fluorescent properties of etheno M13 ssDNA. The fluorescence of the etheno M13 DNA is found to increase upon binding of the RecA filament (Menetski and Kowalczykowski, 1985; Silver and Fersht, 1982, 1983). (The secondary structure of the etheno DNA has no effect on the binding parameters). The ratio of the fluorescence of the saturated RecA/etheno M13 DNA complex to RecA-free DNA [referred to as the relative fluorescence increase; (RFI)] is dependent on the nucleotide cofactor used (Menetski and Kowalczykowski, 1985; Silver and Fersht, 1982). In the presence of ADP or in the absence of a nucleotide cofactor, the RFI value is low; while in the presence of ATP or ATP-γ-S, the RFI value is high (Menetski and Kowalczykowski, 1985). The interconversion between the two RFI values can occur by allowing ATP to hydrolyze into

ADP. These changes correspond to different conformations that are consistent with the structural data mentioned earlier (Kowalczykowski, 1991), since the changes in etheno fluorescence occur upon nucleotide base unstacking (Leonard, 1984). Therefore, either structural or DNA binding methods are able to detect a compact or an extended helical structure that is dependent on the nucleotide cofactor used.

2.4.2. Stability of the RecA/ssDNA complex

As mentioned above, the nucleotide cofactor not only affects the conformation of the RecA/DNA complex, but also its stability (Menetski and Kowalczykowski, 1985). The stability of the complex has been examined by salt titration midpoint (STMP) (Kowalczykowski, 1986), where the salt concentration is quantitated for the amount that is required to dissociate half of the RecA/DNA complex. For example, the STMP for the RecA/DNA-free form is 450 mM NaCl for 0.5 mM ATP, >2.5 M NaCl for 0.5 mM ATP-γ-S, and 160 mM for 0.5 mM ADP. The STMP values also display ligand binding-specificity, since the ligand concentrations are hyperbolic for ADP (Menetski and Kowalczykowski, 1985) and sigmoidal for ATP (Menetski *et al.*, 1988). Thus, relative to the ligand free form, ATP or ATP-γ-S increases whereas ADP decreases the stability of the RecA/DNA complex.

2.5. Modulating RecA's DNA Binding Affinity with Nucleotide Cofactors

The binding affinity of adenine-containing nucleotide cofactors is correlated to their effectiveness in inducing the high-affinity DNA state of RecA as follows: ATP-γ-S > dATP > ATP > AMP-PNP >>AMP-PCP (Kowalczykowski, 1986). This correlation is also true for the binding affinity of other nucleotide triphosphate (NTP) cofactors (Kowalczykowski, 1991). The hierarchy implies that there is a relationship between the binding affinity of ATP substrate, the induction of the high affinity state, and RecA strand-exchange activities. These relationships can be easily understood in context to a model, which links the free energy of nucleotide binding to both DNA binding affinity and structural transitions (Figure 2.7) (Menetski *et al.*, 1988). The hierarchy arises from the fact that the total free energy (derived from nucleotide binding) is influenced by the binding constant and free nucleotide concentration (Kowalczykowski, 1991). This

implies that a higher concentration of NTP is required for a NTP that has a lower binding affinity (discussed below).

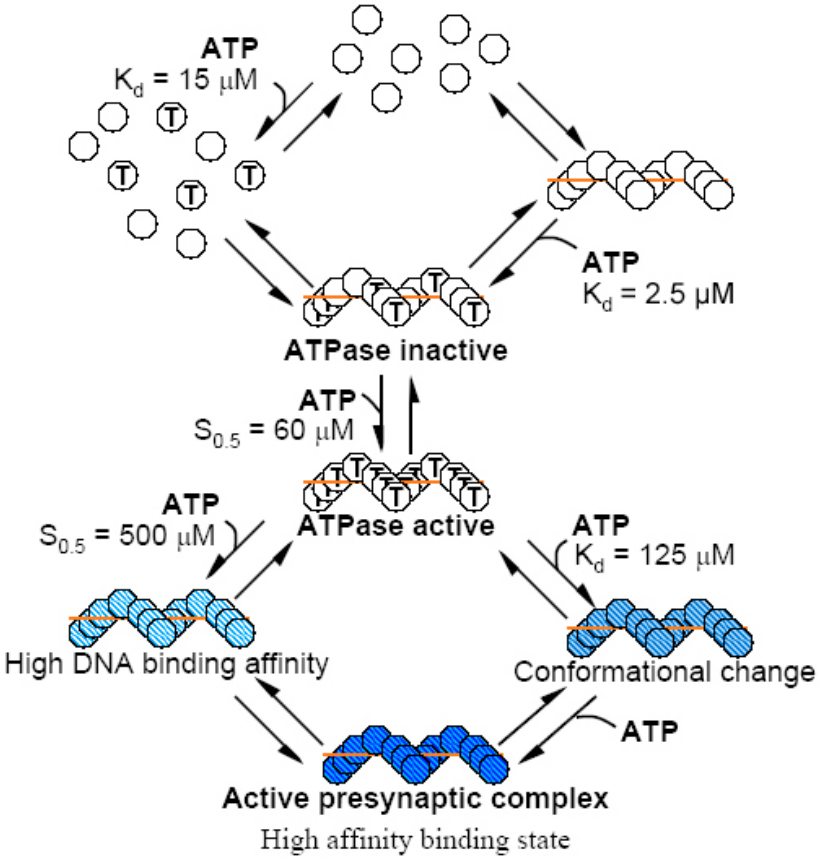

Figure 2.7. ATP concentration-dependent changes in RecA's structure, stability and ssDNA binding affinity.

Open circles represent nucleotide-fee RecA protein; circles labeled *T* represent the RecA/ATP complex; orange lines represent ssDNA; and shaded circles represent the different conformations of the RecA/ATP complex. Each step represents the steady-state properties. (The figure was modified from Kowalczykowski, 1991).

The binding of ATP by free protein (K_d ~15 μM) or by RecA/DNA complex (K_d ~ 2.5 μM) is a thermodynamic process (Kowalczykowski, 1986). This is also true for the binding of ADP, but it decreases RecA's affinity for ssDNA (Cotterill *et al.*, 1982). On the other hand, ATP hydrolysis shows a sigmoidal dependence on ATP concentrations ($S_{0.5}$ ~60 μM) and is not detectable until a concentration of 25 μM ATP is achieved (Menetski and Kowalczykowski, 1987). As the concentrations of ATP are increased, there is a change in the stability and structure of the RecA/DNA complex. This structural

transition has a higher affinity for ssDNA and a sigmoidal dependence on ATP concentrations (>100 μM). An even more stable RecA/DNA complex occurs at higher ATP concentrations (Menetski *et al.*, 1988), resulting in a fully extended structure that has a hyperbolic dependence on higher ATP concentrations (K_d ~125 μM). Thus, all of these changes must involve independent structural changes because their dependence on ATP concentrations is different at each stage (Kowalczykowski, 1991).

Apparently all of these transitions are required in the formation of an active presynaptic complex (Kowalczykowski, 1991), however, there is no evidence to suggest that these transitions are required for RecA's coprotease activity. For example, RecA is able to hydrolyze other NTPs in a DNA-dependent manner, such as dUTP, UTP, dCTP and CTP (Weinstock *et al.*, 1981b). The binding affinities for these NTPs are sufficient to promote RecA-mediated cleavage of the lambda repressor (Phizicky and Roberts, 1981), but not sufficient to promote its DNA strand exchange activity (Kowalczykowski, 1991). These results suggest that the binding of NTPs is able to facilitate the extended state of the RecA/DNA complex, but further structural transitions that are associated with the binding of either ATP or dATP (in RecA's DNA strand exchange activity) may not be required for its coprotease activity.

2.6. Subunit Rotations in the Active RecA/ssDNA/ATP Complex

Spectroscopic evidence for the RecA filament formed on ssDNA in the presence of ATP-γ-S indicates that there are significant rotations in the subunits with respect to the RecA crystal filament (Morimatsu *et al.*, 2002). A change in angle of ~15º for 20 dipole moments was observed between these transition moments relative to the axes of the active filament and the RecA crystal structure (Morimatsu *et al.*, 2002). These large changes were also consistent with the building of the RecA filament model (VanLoock *et al.*, 2003b), which lead to very different subunit-subunit interface than that seen with the RecA crystal filament.

2.7. Residues involved in ATP Binding

The residues K216, F217, R222, K248, K250, and P254 are conserved among all bacterial RecA sequences (Karlin and Brocchieri, 1996), but they are not in close contact with ATP in the RecA crystal structure (Story *et al.*, 1992). In the electron microscopy

generated RecA filament model, the six residues are situated on the adjacent subunit and in close proximity to the triphosphate of ATP (Figure 2.8) (VanLoock *et al.*, 2003b). Mutations at the residues K216, F217, and R222 had been found to impair RecA's ATPase activity and filament formation in the absences of ssDNA (Logan *et al.*, 1997; Skiba and Knight, 1994). Additionally, replacing Phe-217 with Tyr in the RecA filament model allows the OH group on the phenylalanine ring to be in close proximity to the ATP phosphate backbone and potentially act as a H-bond donor (VanLoock *et al.*, 2003b). This is supported by other studies, where the F217Y mutant was found to enhance RecA's DNA recombination and SOS induction *in vivo* (Skiba and Knight, 1994), and ATP-mediated filament assembly *in vitro* (De Zutter *et al.*, 2001). Also, disulfide mutations at RecA's subunit interface place the F217C mutant near the ATPase core *in vitro* (Skiba et al., 1999). The remaining residues (K248, K250, P254) in the RecA filament model were in close proximity to the adenosine base of ATP in the adjacent subunit (VanLoock *et al.*, 2003b). It is suggested that the K248 residue interacts with ATP in trans (Wu *et al.*, 2005), since the K248R/E96D double mutant partially restores

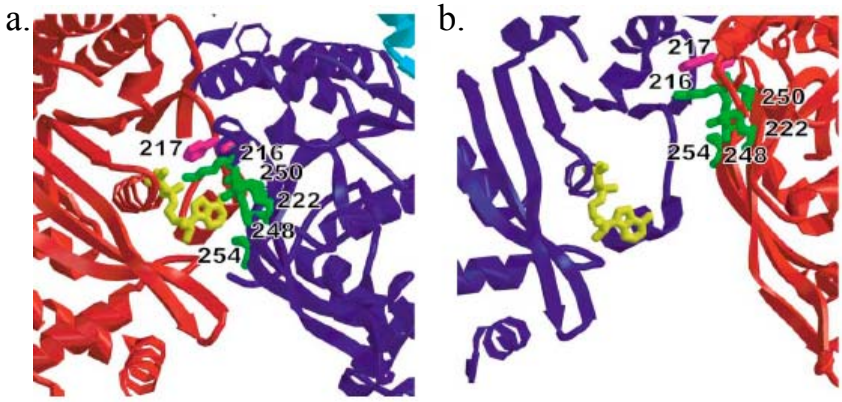

Figure 2.8. Location of the six conserved residues in the RecA filament model and crystal structure.

(a) In the RecA filament model, the six conserved residues found in all of the bacterial RecA proteins (216, 222, 248, 250, and 254 in green; and 217 in magenta) are interacting with the ATP substrate (yellow) on the adjacent subunit interface. **(b)** On the other hand, the RecA crystal structure, the six conserved residues are situated away from the ATP substrate. (The figure was modified from VanLoock *et al.*, 2003b).

ATP hydrolysis (Cox *et al.*, 2006). Also, single point mutations at K248 reduces the rate of ATP hydrolysis, ssDNA binding and filament formation (Nguyen *et al.*, 1993). In general, the RecA filament model suggests that the six conserved residues make important contacts with ATP, and provide stabilization at the subunit-subunit interface (*i.e.* important in filament formation). The residues in the crystal structure, on the other hand, are not involved in subunit-subunit contacts that are associated with the bound ATP (Story *et al.*, 1992).

2.8. Filament Assembly in RecA and RecA-homologs

In a recent paper published by our lab, the crystal structure for *methanococcus voltae* RadA (MvRadA; a RecA homolog) confirmed the location of the six conserved residues in the RecA filament model (K216, F217, R222, K248, K250, and P254), and also their role in ATP-mediated filament formation. The counterpart residues in MvRadA (G279, H280, R285, D302, H305, and P307) are in close proximity to the bound ATP analog (Wu *et al.*, 2004). Additionally, the ATP substrate is bridged by the solvent rich interface, which explains why filament assembly is extremely sensitive to ATP hydrolysis, and the variations in helical pitch that is observed for all documented RecA-homologs (Wu *et al.*, 2004).

2.9. The MvRadA-based RecA Dimer Model

The crystal structure of MvRadA was also used to generate an MvRadA-based RecA dimer model (RecA dimer model) on the conserved ATPase cores and C-terminal domains of EcRecA. The RecA dimer model was found to be structurally similar to the electron microscopy RecA filament model (3.5 Å RMSD), while both RecA dimer and RecA filament models had very little structural similarities with the EcRecA crystal structure (6.5 Å and 7.2 Å respectively; Figure 2.9) (Wu *et al.*, 2004). Additionally, both models have an extended helical pitch (~106 Å for MvRadA and 91 Å for EcRecA) that is associated with the active form of RecA, while the crystal structure of the RecA/ADP complex has a collapsed helical pitch of 82 Å that is associated with the inactive form of RecA. Therefore, these models may represent an allosteric conformational change that is associated with the active form of RecA. On the other hand, the crystal structure of the

RecA/ADP complex represents an allosteric conformational change that is associated with the inactive form of RecA.

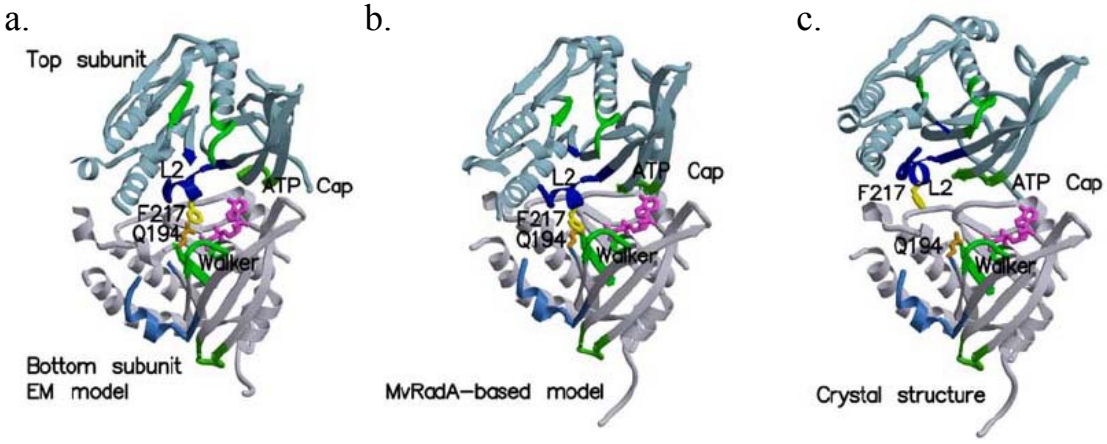

Figure 2.9. The different conformations adopted at RecA's ATPase core.

The ATPase cores of EcRecA are shown in ribbons, and the AMP-PNP substrates are shown in ball-and-stick. **(a)** The electron microscopy model for the active RecA filament, **(b)** the RecA dimer model for the active RecA filament, and **(c)** the crystal structure for the inactive RecA filament. The electron microscopy and RecA dimer models have a similar ATP-mediated interface and disposition of the helix G motif/L2 region. While the RecA crystal structure does not resemble either one of the two models. (The figure was taken from Wu *et al*., 2004).

In the RecA dimer model, three out of the six conserved residues (K248, K250, and P254) are situated in close proximity to the ATP analog/ATP core (residues 302-308) on the adjacent subunit, and the remaining conserved residues (K216, F217, and R222) are more distant from the phosphate backbone of the ATP analog when compared to the RecA filament model. The latter differences may be attributed to the potential allosteric conductance site at the helix G region that harbours the conserved residues (*e.g.* F217Y mutant increases the hyper-activity of RecA's ATPase activity). In general, the MvRadA-based and RecA filament model place the helix G region within the vicinity of the phosphate backbone of the ATP analog. Also, the N-terminal region of the ATPase core between bacterial and non-bacterial recombinases are structurally different, which may suggest an allosteric effect or simply a difference in orientation (Wu *et al.*, 2004). There is evidence to support the former since the N-terminal region is sensitive to trypsin digestion, which suggests that the region is exposed and flexible (Mikawa *et al.*, 1998; VanLoock *et al.*, 2003b).

2.10. Allosteric Changes in MvRadA

The differences between archaeal/eukaryal and bacterial recombinases are the location of the implicated dsDNA binding domain and cation dependent activity. RadA is known to be a stringent K^+-dependent ATPase, any other monovalent cation results in a 200-fold decrease in its ATPase activity (Wu *et al.*, 2005). The ATPase activity of MvRadA, EcRecA, yeast, and human Rad51 can also be stimulated by high salt concentrations, since the anionic species are believed to mimic the polyanionic phosphate backbone of DNA (Liu *et al.*, 2004; Pugh and Cox, 1988; Tombline *et al.*, 1990; Wu *et al.*, 2005).

In the MvRadA K^+-rich crystal structure, the L2 region (N256-R285) becomes ordered and there is a conformational change in the helix G region (G275-A282) (Wu *et al.*, 2005). At the helix G region, the side chain of H280 (equivalent F217 in EcRecA) forms a hydrogen bond with the γ-phosphate of the ATP analog. Also, the R285-F107 cation-π pair is partially vacated to allow two K^+ ions to be incorporated near the γ-phosphate binding site, which bridges the γ-phosphate with the carbonyl moieties at the C-terminus of the helix G region. This allows the γ-phosphate to make extensive contacts around the Helix G/L2 region with: a hydrogen bond by H280, a K^+ bridge with the helix G harbouring the H280 residue and a water nucleophile that is hydrogen bonded with the Q257 residue, and another separate K^+ bridge with the D302 residue (Wu *et al.*, 2005). Thus, there is a long-range conformational change upon binding of K^+ ions, which orders and stacks the putative ssDNA-binding L1 and L2 regions along the helical axis. These conformational changes suggest that there is cross-talk between the binding of potassium at the ATP site and the ssDNA-binding L2 region (Wu *et al.*, 2005).

RecA and other bacterial homologs do not require monovalent cations. The crystal structures of RecA-like homologs reveal that cationic side chains on the adjacent subunit make contact with the γ-phosphate in trans. For example, the circadian clock protein KaiC has a Lys-Arg pair (K457 and R459) that makes contact with the γ-phosphate in trans (Pattanayek *et al.*, 2004). Also, the RecA filament model has K248 (equivalent D302 in MvRadA) and K250 in close proximity to ATP in the adjacent subunit (VanLoock *et al.*, 2003b), and mutational studies suggest that K248 binds to ATP in trans (Cox *et al.*, 2006). Thus, the cationic side chains in the ATPase site of RecA and

RecA-like homologs make it unlikely for the protein to accommodate monovalent cations (Wu *et al.*, 2005). This may explain why RecA is able to maintain its ATPase activity in the absence of monovalent cations.

2.11. ATPase Catalytic Mechanism in MvRadA

The residues E151 and Q257 in MvRadA (equivalent to E96 and Q194 in EcRecA) are candidates for activating the hydrolyzing water (Story *et al.*, 1992), because these residues form hydrogen bonds with water. The residues are also found to cooperate with the P-loop motif (Wu *et al.*, 2005) that is responsible for wrapping around the triphosphate of ATP and making amide-phosphate hydrogen bonds. The contacts made at the ATP binding site by the ε-amino group of K111, side chain of H280, Mg^{2+} ion, and two K^+ ions are likely to create an electron withdrawing effect on the oxygen atoms of the γ-phosphate of ATP (Figure 2.10a) (Wu *et al.*, 2005). This polarizes the γ-phosphate of the ATP analog, allowing for nucleophilic attack by the hydrolyzing water molecule. (This also justifies why MvRadA is a K^+-dependent ATPase). Following hydrolysis of ATP to ADP, a negative charge is expected to build up at the β-phosphate of the leaving ADP molecule. The latter reaction is likely to be stabilized by the electron withdrawing Mg^{2+} ion; and the amide groups, along with the ε-amino group of K111 in the conserved P-loop motif (Figure 2.10b) (Wu *et al.*, 2005).

2.12. DNA Binding Domains in RecA

In the RecA crystal structure, the disordered loop regions, L1 (residues 157-164) and L2 (residues 195-209), were proposed to be the secondary dsDNA and primary ssDNA binding sites respectively (Story *et al.*, 1992). This proposal was based on various mutagenesis studies on the L1 and L2 regions of RecA. For example, the single point mutant, RecA E207Q (L2 region) was found to inhibit SOS response and homologous recombination activities *in vivo* (Larminat *et al.*, 1992). The mutant was found to be functional in its biochemical activities associated with primary ssDNA binding *in vitro*, but etheno DNA binding studies indicated that the mutant lacked one of the two ssDNA binding sites (Cazaux *et al.*, 1998). Also, mutagenesis studies on the L2 residues (N193, Q194, R196, T209, G211, and G212) were found to lead to defects in

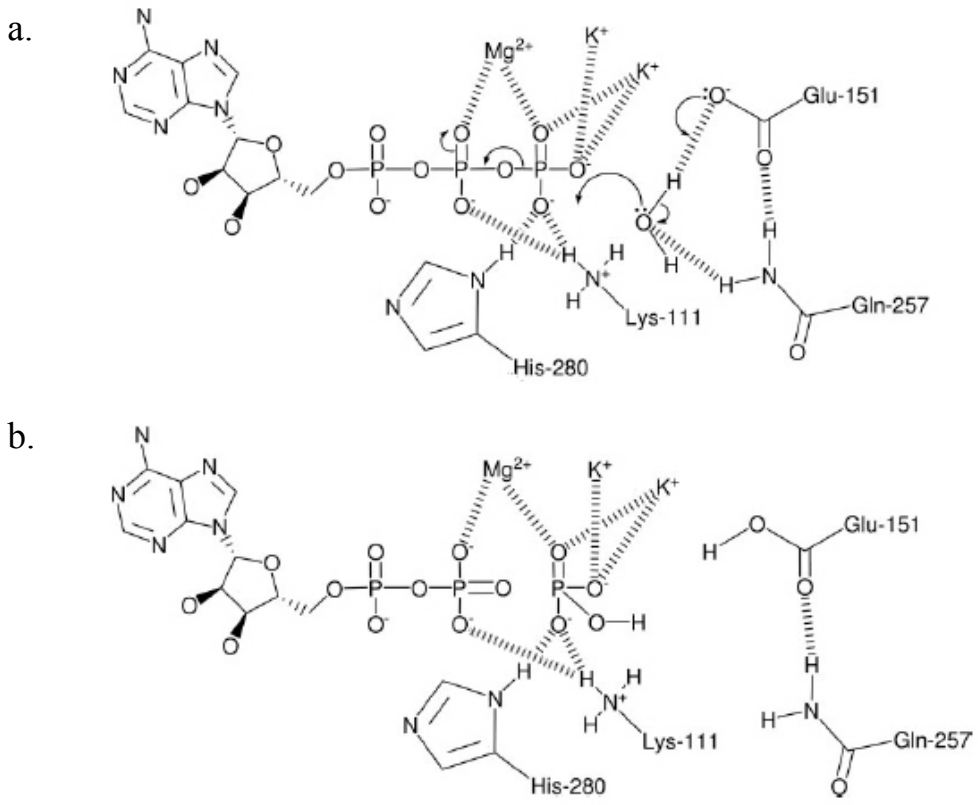

Figure 2.10. The proposed catalytic mechanism for ATP hydrolysis.

(a) The residue E151 acts as a general base in the activation of the hydrolyzing water molecule, and E151 and Q257 form hydrogen bonds with the hydrolyzing water molecule, in order to align it for nucleophilic attack. On the other hand, K111, H280, Mg^{2+} ion and the two K^{+} ions polarize the γ-phosphate of ATP. **(b)** Following hydrolysis of ATP, the Mg^{2+} ion and K111 stabilizes the negative charge build up at the β-phosphate of ADP. (The figure was modified from Wu *et al.*, 2005).

lambdoid bacteriophage recombination and recombinational DNA repair *in vivo* (Hörtnagel *et al.*, 1999). These two experiments suggest that the L2 region is involved in primary ssDNA binding.

On the other hand, the single point mutations at the L1 region in RecA were found to have constitutive coprotease activity (*i.e.* indicating that RecA has a ssDNA-dependent ATP hydrolysis), but lacked recombination *in vivo* (Wang and Tessman, 1986). This implies that the primary ssDNA site is functional, while the secondary dsDNA site is defective. Therefore, the L1 region may be involved in secondary dsDNA binding. Finally, a double substitution at the L1 region (E156L and G157V) in EcRecA was found to reduce the level of recombination and constitutive coprotease behaviour *in vitro*

(Mirshad and Kowalczykowski, 2003). This suggests that the L1 region is involved in both primary ssDNA and secondary dsDNA binding.

The L2 region in RecA has also been defined by a synthetic peptide (residues 193-212). This peptide was able to bind to ssDNA cooperatively (Gardner *et al.*, 1995), form a secondary structure in the presence of ssDNA (Selmane *et al.*, 1999), and promote joint molecule formation between single-stranded oligonucleotides and a homologous site on dsDNA (Voloshin *et al.*, 1996). Cross-linking studies with 5-iodouracil oligonucleotides on synthetic peptides containing either L1 or L2 regions were found to be covalently linked at the amino acid residues M164 (L1 region) and M202 (L2 region) (Malkov and Camerini-Otero, 1995). These results suggest that both L1 and L2 regions may be involved in primary ssDNA binding. It is also worth mentioning that the functional 5-iodouracil base and the reactive amino acid are cross-linked, because of the close proximity between each group (4-5 Å in distance) (Dong *et al.*, 1994). Thus, RecA is most likely to bind to the phosphodiester backbone of DNA rather than to the nucleotide base that is positioned for homologous pairing (Leahy and Radding, 1986).

In general, the majority of the research on the DNA binding sites suggests that the L1 region is involved in secondary dsDNA binding and possibly primary ssDNA binding, while the L2 region is involved in primary ssDNA binding

2.13. Homologous Strand Exchange in RecA and RecA-homologs

The extended recombinase filament serves as a scaffold in facilitating strand exchange between primary ssDNA and secondary homologous dsDNA. Given that this extended structure of the recombinase filament is conserved among archaeal, bacterial, and eukaryal organisms, this suggests that the conformation may have been shaped in order to accommodate the extended form of B-DNA for compatible homologous strand exchange (Egelman, 2001).

The N-terminal domain of archaeal and eukaryal recombinases, and the C-terminal domain of bacterial recombinase have lobes that are situated on a relatively smooth core filament between the associated ATPase domains. However, these lobe-like domains between archaeal/eukaryal and bacterial recombinase are different in topology and are located on opposite rims in the respective core filaments. NMR chemical shift perturbation mapping of the DNA binding and mutagenesis studies on a truncated N-

terminal lobe in HsRad51 (a MvRadA homolog) show that the HhH motif has a positively charged surface, and that it is involved in the binding of dsDNA (Aihara *et al.*, 1999). The spacing between HhH motifs is ~35 Å in the MvRadA K^+-free crystal structure, which may allow for flexibility in the dsDNA to contact the axial ssDNA (Wu *et al.*, 2004). A similar surface patch has been found on the C-terminal lobe of EcRecA (residues G301 and K302) (Aihara *et al.*, 1997), and mutations at the C-terminal domain of EcRecA (K286N and K302N) is found to reduce homologous pairing (Tateishi *et al.*, 1992). In either of the cases, the structural studies on archaeal, eukaryal and bacterial recombinase all have a lobe region that is implicated in the binding of dsDNA, and they are all located outside of their respective filament axis (Aihara *et al.*, 1997).

In the MvRadA K^+-free crystal structure, the subunit interface of the N-terminal elbow of L1 in one subunit, and the C-terminal elbow of L2 in the adjacent subunit are situated in close proximity to the helical axis (Wu *et al.*, 2004). The special arrangement between the L1 and L2 regions implies that these regions are interacting directly with the ssDNA in the active filament. In the presence of potassium, there is a long-range conformational change that orders and stacks the putative ssDNA-binding regions of L1 and L2 along the helical axis, which creates a positively charged patch compatible for binding anionic DNA (Wu *et al.*, 2005). However, the exact role of the L1 and L2 regions in the MvRadA K^+-rich crystal structure are not clear, since the Cl^- ions were not observed at these regions. Thus, the arrangement of the DNA binding regions in MvRadA is consistent with the arrangement found in the RecA based and RecA filament models, and their role in ssDNA binding is also consistent with the biochemical studies (see section 2.12).

The distance between HhH motifs and the L1 region is ~15 Å apart, which suggests that the L1 region may also be involved in the binding to dsDNA (Wu *et al.*, 2004). This is also consistent with mutagenesis in PfRad5, where R251 in the L1 region (equivalent R224 in MvRadA) is implicated in dsDNA binding (Shin *et al.*, 2003). Therefore, the results suggest that the dsDNA bound at the HhH motif may be brought into the groove through a wide opening in the filament axis, in order for the L1 region to bind to dsDNA in both EcRecA and MvRadA. However, the different polarities for dsDNA binding in EcRecA and MvRadA suggests two possibilities. (1) They utilize

different mechanisms and dsDNA binding lobes participate in ssDNA invasion into a homologous stretch of dsDNA. (2) They share similar mechanisms, but the dsDNA lobes play a less direct role (Wu *et al.*, 2004).

Despite the weak sequence similarities, the MvRadA crystal structure and the active RecA filament model both have a similar structure, which suggests that the two proteins are structural homologs. Therefore all RecA-like recombinases may have a conserved regulatory role at the ATPase core, which is responsible for re-orienting the L1 and L2 regions for DNA strand exchange (Wu *et al.*, 2004).

2.14. RecA's Binding Site for the LexA Repressor

Based on the RecA crystal structure, a "notch" region, situated between adjacent lobes of RecA, has been proposed as the binding site for the LexA repressor (Story *et al.*, 1992). The notch region is large enough to accommodate smaller proteins, and mutational studies on residues situated at this site are found to differentially affect RecA-mediated cleavage of the LexA repressor and its homologs *in vivo*. For example, R243L prevents cleavage of ϕ_{80} repressor and UmuD protein (Dutreix *et al.*, 1989), and G229S prevents cleavage of ϕ_{80} repressor (Ogawa and Ogawa, 1986). However, other residues at the notch region are also situated at the subunit-subunit interface in the active RecA filament model. For example, S25F (Wang and Tessman, 1986) and C116S (Weisemann and Weinstock, 1988) mutations lead to a constitutive coprotease activity for LexA homologs, and S117F (Dutreix *et al.*, 1989) leads to a defective coprotease activity for the LexA repressor. When these residues are examined in the active RecA filament model, they are situated at the subunit-subunit interface. Therefore, the latter mutations are not likely to play a direct role in RecA's coprotease activity.

Based on the electron microscopy studies on the RecA/LexA complex (VanLoock *et al.*, 2003a; Yu and Egelman, 1993), LexA appears to be in close proximity to some areas in the notch region (residues 229 and 243) and the secondary DNA-binding site (residues 154-156 and 165; *i.e.* L1 region [residues 157-164]). This can be seen in the reconstituted/modified crystal density diagram (Figure 2.11). The residues implicated in the binding of LexA are also consistent with mutational studies on RecA's coprotease activity, such as R243L (Dutreix *et al.*, 1989), G229S (Ogawa and Ogawa, 1986) and G154-E158 substitutions (Nastri *et al.*, 1997). Therefore, LexA appears to be binding at

both the inner surface of the C-terminal lobe and the N-terminal L1 region of RecA (Yu and Egelman, 1993).

The inability for the inactive RecA filament to promote the mediated cleavage of the LexA repressor can be explained by the overlap of electron density observed when the LexA subunit is positioned within the RecA crystal and the electron microscopy structures (Yu and Egelman, 1993). Therefore, the LexA repressor is unable to fit into the compressed helical groove of RecA.

Interestingly, the regions that are implicated in dsDNA binding (L1 region; and C-terminal lobe, residues 268 to 330) are also within the binding vicinity of the LexA repressor. This may explain why dsDNA (Takahashi and Schnarr, 1989) and high concentrations of ssDNA (Rehrauer *et al.*, 1996) are able to inhibit RecA-mediated cleavage of the LexA repressor. It also may explain why the non-cleavable LexA S119A mutant is able to act as a competitive inhibitor in RecA's DNA strand exchange activities (Harmon *et al.*, 1996).

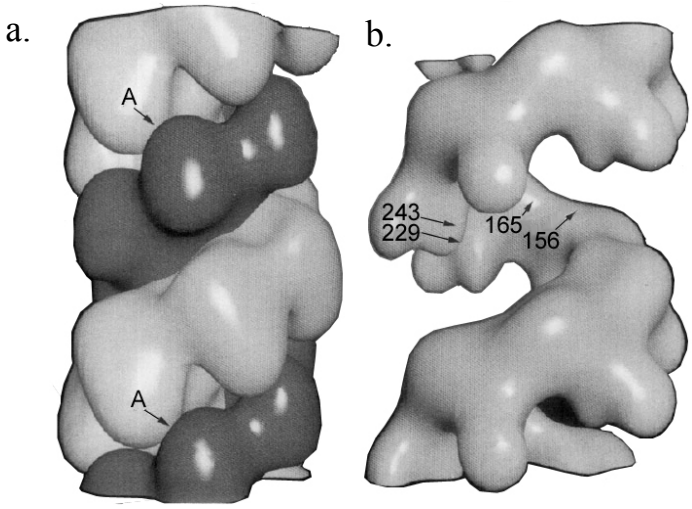

Figure 2.11. The electron microscopy image of the RecA/LexA complex.
(a) The 3-dimensional surfaces of the RecA-dsDNA filament (light gray) and the helically averaged LexA repressor difference density (dark gray) within the helical groove of RecA. The superimposition of the two structures generates the density of the LexA repressor with an apparent binding stoichiometry 1:1 (RecA:LexA). The arrows that are labeled as A indicate the position of the strong contacts, which corresponds to the residues 229 and 243. **(b)** A low resolution of the RecA crystal structure with the approximate positions of the residues 229, 243, 156 and 165 that are in close proximity to the LexA repressor. (The figure was modified from Yu and Egelman, 1993).

3. OBJECTIVES

The overall objective of this study was to examine the thermodynamic model for the formation of the RecA/LexA complex by reducing the energy barrier involved at each step in the thermodynamic process.

To achieve this goal, the energy barrier at each step was reduced by:

(1) High salt concentrations and/or a hyper-active RecA mutant in order to preactivate RecA.
   (a) A non-cleavable LexA mutant was used as bait in the yeast two-hybrid system, in order to isolate a hyper-active RecA mutant.

(2) LexA S119A and K156A in order to influence LexA's conformation.

(3) A volume-excluding agent (polyethylene glycol) in order to force the binding between the preactivated RecA protein and the cleavable conformation of LexA.

(4) Introducing different single-point mutations at LexA's dimer interface, in order to determine RecA's preference for the monomer or dimer form of LexA. This experiment was also related to the thermodynamic model, since the dimer or monomer form of LexA was expected to influence the energy barrier involved in the formation of the RecA/LexA complex.

4. MATERIALS AND METHODS

4.1. Cell lines

The strains used in the yeast monohybrid system were *S. cerevisiae* strain EY111 (*MATα his3 trp1 ura3*::*URA3-LexA8op-lacZ ade2*::*URA3-LexA8op-ADE2 leu2*::*LexA6op-LEU2*) and *S. cerevisiae* strain EY93 (*MATa ura2 his3 trp1 leu2 ade2*::*URA3*). Both yeast strains were a gift from Dr. Geyer's Lab. The *E. coli* strain XL1-Blue (electroporation-competent) (Stratagene) was used in making multiple copies of the plasmid of interest, and *E. coli* strain BL21 (DE3) (Novagen) was used in producing the protein of interest.

4.2. Materials

The items mentioned in the materials and methods are listed in Table 4.1.

Table 4.1. A list of items used in the experimental procedures.

Item	Supplier
Chemicals and Reagents	
ATP	Sigma
ATP-γ-S	Sigma
AMP-PNP	Sigma
Agarose	Invitrogen Life Technologies
Acetic acid, glacial	EMD Chemicals Inc
Acrylamide, electrophoresis grade	Sigma
Ammonium persulfate	EMD Chemicals Inc
Ammonium sulfate	EMD Chemicals Inc
Ammonium molybdate	EMD Chemicals Inc
Ampicillin, sodium salt	BioShop
Bradford reagent	Bio-Rad
Bromophenol blue	Alfa Aesar

Chloroform	Amresco
Coomassie Brilliant Blue R-250	AnaSpec
Dimethyl formaldehyde	Laboratory Plus
dNTP set	Amersham Biosciences
Ethidium Bromide	Sigma
Ethyl alcohol 95%	Commercial Alcohols Inc.
EDTA (ethylenediaminetetraacetic acid)	EMD Chemicals Inc
D-Galactose	BD Biosciences
Glycerol	EMD Chemicals Inc
Hydrochloric acid	BDH Inc.
HEPES (N-2-hydroxyethylpeperazine-N'-2-ethane-sulfonic acid)	BioShop
Imidazole	Avocado Research Chemicals ltd
Isoamyl alcohol	Amresco
Isopropyl alcohol	EMD Chemicals Inc
IPTG (Isopropyl-thio-β-D-galactoside)	EMD Chemicals Inc
Kanamycin sulfate	Bioshop
Lithium acetate	EMD Chemicals Inc
Malachite green oxalate	Avocado Research Chemicals Inc.
Magnesium chloride, hexahydrate	EMD Chemicals Inc
Magnesium sulfate	EMD Chemicals Inc
MES [2-(N-morpholino)-ethane sulfonic acid monohydrate]	EMD Chemicals Inc
2-Mercaptoethanol	Bioshop
Nickel sulfate, hexahydrate	EMD Chemicals Inc
Phenol	Amresco
Polyethylene glycol 400	Fluka Chemical
Polyethylene glycol 3500	Fluka Chemical
Potassium phosphate, dibasic	EMD Chemicals Inc
Potassium dihdrogen orthophosphate	BDH Inc.
Saccharose	EMD Chemicals Inc
Sodium chloride	EMD Chemicals Inc
SDS (sodium dodecyl sulfate)	Calbiochem
Sodium hydroxide	EMD Chemicals Inc
Sucrose	EMD Chemicals Inc
TRIS [Tris (hydroxymethyl) aminomethane]	EMD Chemicals Inc
Urea	EMD Chemicals Inc
X-Gal (5-bromo-4chloro-indoyl-β-D-galactopyranoside)	Eppendorf

Media

Agar	BD Biosciences
LB agar	EMD Chemicals Inc
LB Miller broth	EMD Chemicals Inc
Peptone	BD Biosciences
Yeast extract	BD Biosciences
Yeast nitrogen without amino acids	BD Biosciences
CSM, drop out supplements	Biol 101 Inc

Enzymes & Enzyme Buffers

10X DNA ligase buffer	MBI Fermentas
10X Thermopol reaction buffer	New England Bio Labs
BamH I	New England Bio Labs
10X Buffer R	MBI Fermentas
EcoR I	New England Bio Labs
Nco I	MBI Fermentas
10X NEBuffer #2	New England Bio Labs
Pfu DNA polymerase	MBI Fermentas
T4 DNA Ligase	MBI Fermentas
Taq DNA polymerase	New England Bio Labs
Thrombin	Sigma
Xho I	MBI Fermentas

Equipment & Miscellaneous Items

ÄKTA Prime Protein Purification System	Amersham Biosciences
Allegra X-22R Centrifuge	Beckman Coulter
Avanti J-25 Centrifuge	Beckman Coulter
Centrifuge 5415	Eppendorf
DU-40 Spectrophotometer	Beckman Coulter
Electroporator 2510	Eppendorf
Falcon tube, 50 ml	Becton Dickinson
Glass beads, 425–600 μm in diameter	Sigma
HiPrep 16/60 Sephacryl S-100 High Resolution	Amersham Pharmacia Biotech
HiPrep 16/60 Sephacryl S-300 High Resolution	Amersham Pharmacia Biotech
Mastercycler Gradient	Eppendorf

Micropipettors	Biohit
Micromass LTC Mass Spectrometer	Waters Corp
Orbit Environ Shaker	Lab-Line
Protein-Pak 125	Waters Corp
QIAgen Miniprep Kit	QIAgen
QIAquick Gel Extraction Kit	QIAgen
QIAquick PCR Purification Kit	QIAgen
Sonic Dismembrator Model 500	Fisher Scientific
Symmetry 400 C4 3.5 mm	Waters Corp

Resin

DE52 anion exchanger, DEAE cellulose	Whatman
Chelating Sepharose fast flow	Amersham Biosciences

DNA

pEG202 vector	Dr. R. Geyer
pET28a vector	Novagen
pJG4-5 vector	Dr. R. Geyer
ssDNA, dT_{36}	Integrated DNA technologies Inc
ssDNA, spermadine trihydrochloride	Sigma
Synthetic oligonucleotides	Integrated DNA technologies Inc

4.3. Common Procedures

4.3.1. Agarose Gel Electrophoresis

The DNA samples were mixed in a final concentration of 1X loading buffer [0.04% (w/v) bromophenol blue, 5% (v/v) glycerol], and ~4 µl of the mixture was loaded into the agarose gel. The samples were resolved on the agarose gel at 120V for 12 min in 1X TAE buffer (40 mM Tris-acetate, 1 mM EDTA pH 8.0), and visualized with a UV-lamp at 365 nm. The agarose gels consisted of 1.0% to 1.4% (w/v) agarose, 1X TAE buffer, and 0.5 µg/ml ethidium bromide.

4.3.2. Colony PCR

To ensure that the insert was successfully cloned into the plasmid, colony PCR was preformed on each single colony-forming unit (CFU) on the Lauria-Bertani (LB) agar plate that contained the appropriate antibiotic. A sterile pipette tip was used for

picking each CFU, and each CFU was resuspended in 6 µl of sterile double-distilled water. Four microliters of the resuspended colony was added to the PCR mixture in a 25 µl final reaction volume that consisted of 1 Unit *Taq* DNA Polymerase, 100 µM of each dNTP, 1X Thermo-Pol Reaction Buffer, 1 µM of each N_{for} and C_{rev} oligonucleotides (Table 4.2). The insert was amplified in a PCR Thermocycler by using the following conditions: 94°C, 2 min; 30X [94°C, 45 sec; 55°C, 1 min; 72°C, 1 min]; 72°C, 10 min; and then held at 4°C. The PCR products were visualized on a 1.5% agarose gel (section 4.3.1), in order to determine if the size of the insert corresponded to the gene of interest.

Table 4.2. Oligonucleotides used in detecting the *recA* insert in the pET28a and pJG4-5 plasmids, and *lexA* inserts in the pET28a and pEG202 plasmids.

PCR Step	Oligonucleotide Label	Oligonucleotide Sequence (5'-3')	Template
1. N_{for} C_{rev}	T7 Pro T7 Ter	taa tac gac tca cta tag gg gct agt tat tgc tca gcg g	PET28a plasmid Containing *recA* or *lexA*
1. N_{for} C_{rev}	ADH1 Pro (for) ADH Ter (rev)	tat acc aag cat aca atc aac tcc ata aga aat tcg ccc gg	pEG202 plasmid Containing *lexA*
1. N_{for} C_{rev}	GAL1 Pro (for) P2 RecA-XhoI (rev)	taa tac ttt caa cat ttt cg ccg ctc gag tta aaa atc ttc gtt agt-ttc tgc	pJG4-5 plasmid Containing *recA*

4.3.3. SDS-gel Electrophoresis

Six microliters of the reaction was mixed in a final concentration of 1X Loading buffer [50 mM Tris-HCl pH 6.8, 1% (v/v) β-mercaptoethanol, 2% (w/v) SDS, 0.1% (w/v) bromophenol blue, 10% (v/v) glycerol]. The mixture was loaded into a SDS-polyacrylamide gel and resolved at 200V for ~60 min. The protein bands were visualized by staining the gel with Coomassie Brilliant Blue. The resolving gel was composed of 12% (w/v) acrylamide mix, 380 mM Tris-base pH 8.8, 0.1% (w/v) SDS, 0.1% (w/v) ammonium persulfate, and 0.04% (v/v) TEMED. The stacking gel was composed of 5% (w/v) acrylamide mix, 130 mM Tris-HCl pH 6.8, 0.1% (w/v) SDS, 0.1% (w/v) ammonium persulfate, and 0.1% (v/v) TEMED.

4.3.4. Synthetic Media

The following recipes for making the synthetic plates and liquid media in the yeast monohybrid system are described in Geyer and Brent (2000). Synthetic plates and liquid media were prepared in a 1 L final volume as described below.

YPD plates and liquid media:

Yeast extract	10 g
Peptone	20 g
Agar (plates only)	20 g
H_2O	950 ml

Autoclave YPD media for 20 minutes at 1.05 kg/cm^2 and add 50 ml 40% (w/v) glucose.

Dropout plates and liquid media:

Yeast nitrogen base without amino acids	6.7 g
Dropout base	*x*
Agar (plates only)	20 g
H_2O:	
(glucose plates or media)	950 ml
Or	
(galactose/saccharose plates or media)	925 ml

Where *x* is equal to the amount of the appropriate CSM (complete supplement mixture) dropout base: 0.77 g CSM –TRP, 0.74 g CSM –HIS, 0.62 g CSM –HIS –LEU –TRP, or 0.61 g CSM –ADE –HIS –LEU –TRP. Autoclave media for 20 minutes at 1.05 kg/cm^2 and add either 50 ml of 40% (w/v) glucose (glu), or 50 ml of 40% (w/v) galactose (gal) and 25 ml of 40% (w/v) saccharose (sac).

X-Gal plates:

Yeast nitrogen base without amino acids	6.7 g
Dropout base	*x*
Agar	20 g
H_2O:	
(glucose plates or media)	850 ml
or	
(galactose/saccharose plates or media)	825 ml

Where *x* is equal to the amount of the appropriate CSM dropout base: 0.74 g CSM –HIS, or 0.62 g CSM –HIS –LEU –TRP[*]. Autoclave media for 20 minutes at 1.05 kg/cm^2 and add either 50 ml of 40% (w/v) glu, or 50 ml of 40% (w/v) gal and 25 ml of 40% (w/v) sac. Cool media to 55°C and add 10X BU salts (see below). Add 4 ml of 5-bromo-4-chloro-3-indolyl-β-D-galactopyranoside (X-Gal; 20 mg/ml dissolved in dimethyl formamide).

10X BU salts:	
$Na_2PO_4 \cdot 7H_2O$	70 g
NaH_2PO_4	30 g
H_2O	900 ml

Adjust 10X BU salts to pH 7.0 and autoclave BU salts for 20 minutes at 1.05 kg/cm^2.

4.4. The Yeast Monohybrid Screen for Hyper-active RecA Mutants

4.4.1. Site Directed Mutagenesis by Overlap Extension PCR of *lexA*

Both *lexA* mutants, K156A and S119A were generated by site-directed mutagenesis by overlap extension PCR as described in Sambrook and Russell (2001b). Briefly, the overlap site in each 5'- and 3'-regions of the DNA fragments were generated from the template pEG202 vector with the N_{for}/N_{rev} (Table 4.3; PCR step 1a) and C_{for}/C_{rev} (Table 4.3; PCR step 1b) oligonucleotide pairs respectively. The conditions used in the first PCR step consisted of 94°C, 1 min; 30X [94°C, 45 sec; 55°C, 1 min; 72°C, 1 min]; 72°C, 10 min; and then held at 4°C. The mixture for the PCR reaction was made up to a

[*] If the yeast cells were not transformed with the pJG4-5 vector, then the media was supplemented with 100 mg TRP.

50 µl reaction volume that consisted of 1 Unit *PFU* DNA Polymerase, 100 µM of each dNTP, 1X Thermo-Pol Reaction Buffer, 1 µM of each N_{for} and N_{rev}, or C_{for} and C_{rev} oligonucleotides, and 500 ng pEG202 plasmid. In all cases the two gene fragments were purified from a 1% agarose gel with the QIAquick Gel Extraction Kit unless otherwise stated.

In the second PCR step, each 5'- and 3'-regions of the PCR fragments were fused together and amplified by the N_{for}/C_{rev} oligonucleotide pair (Table 4.3; PCR step 2), in order to generate the ORF of interest. The conditions and composition of the mixture used in the second PCR step were similar to the first PCR step, except that the extension time at 72°C was 2 min, the template DNA consisted of 200 ng of each 5'- and 3'-regions of the DNA fragments, and the ORF was amplified with 1 µM of each N_{for} and C_{rev} oligonucleotides. The resulting ORFs from the PCR were not purified in order to maximize the cloning of the ORF into pEG202 plasmid *via* homologous recombination in yeast (discussed later).

4.4.2. Random Mutagenic PCR of *recA*

The *recA* library was generated from the wild-type *recA* or *recA* E96D template by random mutagenic PCR with the N_{for}/C_{rev} oligonucleotide pair (Table 4.3; PCR step 2). The conditions and composition of the mixture used in PCR are described in section 4.4.1, except that the extension time at 72°C was 2 min, 1 Unit *Taq* DNA Polymerase was used in the reaction mixture, and the template DNA consisted of 200 ng of wild-type *recA* or *recA* E96D. The resulting ORFs from the PCR were not purified in order to maximize the cloning of the ORF into pJG4-5 plasmid *via* homologous recombination in the yeast cell (discussed later).

Table 4.3. Oligonucleotides and templates that were used in generating l*exA* K156A and *lexA* S119A inserts, and r*ecA* library.

PCR Step	Construct	Sequence (5'-3')	Template
	LexA K156A (Bait)		
1a. N_{for} N_{rev}	ADH1 Pro (for) LexA K156A (rev)	tat acc aag cat aca atc aac tcc gaa gtt acc gtt gct cgc ctg aaa aaa cag g	pEG202
1b. C_{for} C_{rev}	LexA K156A (rev) LexA *XhoI* ADH Ter (rev)	cag gcg agc aac ggt aac ttc gtc atc aat tcg ccc gga att agc ttg gct gca ggt cga-ctc gag tta cag cca gtc gcc gtt gc	pEG202

2. N_{for} C_{rev}	ADH1 Pro (for) LexA *XhoI* ADH Ter (rev)	tat acc aag cat aca atc aac tcc aat tcg ccc gga att agc ttg gct gca ggt cga- ctc gag tta cag cca gtc gcc gtt gc	5'-*lexA* K156A & 3'-*lexA* K156A
	LexA S119A (Bait)		
1a. N_{for} N_{rev}	ADH1 Pro (for) LexA S119A (rev)	tat acc aag cat aca atc aac tcc cga tat ctt tca tcg cca tcc cgc tga cgc	pEG202
1b. C_{for} C_{rev}	LexA S119A (for) LexA xhoI ADH Ter (rev)	cgt cag cgg gat ggc gat gaa aga tat cgg aat tcg ccc gga att agc ttg gct gca ggt cga- ctc gag tta cag cca gtc gcc gtt gc	pEG202
2. N_{for} C_{rev}	ADH1 Pro (for) LexA *XhoI* ADH Ter (rev)	tat acc aag cat aca atc aac tcc aat tcg ccc gga att agc ttg gct gca ggt cga- ctc gag tta cag cca gtc gcc gtt gc	5'-*lexA* S119A & 3'-*lexA* S119A
	RecA library (Prey)		
1. N_{for} C_{rev}	RecA pJG4-5 (for)-*EcoRI* site RecA pJG4-5 (rev)- *Xho*I site	tac cct tat gat gtg cca gat tat gcc tct ccc- gaa ttc atg gct atc gac gaa aac aaa c tga cca aac ctc tgg cga aga agt cca aag- ctt ctc gag tta aaa atc ttc gtt agt ttc	*RecA* E96D or wild-type *recA*

4.4.3. Restriction Endonuclease Digest

The appropriate plasmid for either *lexA* or *recA* ORFs (pEG202 or pJG4-5 respectively) was digested for 15 hr at room temperature (20°C) with the appropriate restriction endonucleases. The restriction digest for the pEG202 plasmid was made up to a 50 µl final reaction volume that consisted of 1.0 µg pEG202 plasmid, 25 Units EcoR I, 25 Units BamH I, and 1X NEBuffer #2. On the other hand, the restriction digest for the pJG4-5 plasmid was made up to a 50 µl final reaction volume that consisted of 1.0 µg pJG4-5 plasmid, 25 Units EcoR I, 25 Units XhoI, and 1X Buffer R^+. In all cases the digested products were purified from a 1% agarose gel (section 4.3.1) with the QIAquick Gel Extraction Kit unless otherwise stated.

4.4.4. Yeast Transformation

The procedures for transforming the yeast cells are described in the Lithium Acetate High Efficiency protocol (Schiestl and Gietz, 1989), which was used in three different situations. (1) Cloning the insert (either *recA* library, *lexA* K156A, or *lexA* S119A) into the vector of interest *via* homologous recombination in *S. cerevisiae* strain EY93. (2) Transforming the *lexA* K156A or *lexA* S119A pEG202 plasmid into *S. cerevisiae* strain EY111, which served as bait in screening for hyper-active RecA

mutants. (3) Transforming the isolated *recA* mutant pJG4-5 plasmid into *S. cerevisiae* strain EY111 that contained *lexA* K156A pEG202, such that the interaction between the bait and prey could be reconfirmed. Briefly, the yeast cells were grown in 50 ml media* until an OD_{600nm} of 0.6 to 0.8 was reached. The culture was then harvested by centrifugation at 3,901 xg for 4 min at 10°C. The cell pellet was resuspended with 100 mM lithium acetate in a 1 ml final volume, and subsequently centrifuged at 15,700 xg for 15 sec at 20°C. The cell pellet was resuspended again with 100 mM lithium acetate in a 500 µl final volume, then distributed into ten 50-µl aliquots (ten transformations), and centrifuged at 15,700 xg for 15 sec. The supernatant was removed and the ingredients listed below were added to the cell pellet in the following order:

50% (w/v) Polyethylene glycol 3500	240 µl
1 M Lithium acetate	36 µl
2 mg/ml ssDNA	25 µl
400 ng plasmid DNA or 400 ng plasmid DNA + 800 ng insert	50 µl

The sample was mixed by vortexing until the pellet was completely resuspended. The DNA of interest was transformed into the host cell by heat shock, where the mixture was incubated at 30°C for 30 min, and then heat shocked at 42°C for 20 min. The sample was centrifuged at 5,900 xg for 15 sec, and the cell pellet was suspended in 500 µl of sterile double-distilled water. The cell suspension was plated on the appropriate CSM dropout base media by using sterile glass beads, and then incubated at 30°C for 3 days. The CSM dropout base media used for plating the transformants were: SD H^- for yeast cells that contained the *lexA* K156A or *lexA* S119A pEG202 plasmid, SD W^- for the yeast strain EY93 that contained the *recA* library pJG4-5 plasmid, and SD H^- W^- for the yeast strain EY111 that contained the *recA* mutant pJG4-5 plasmid and the *lexA* K156A pEG202 plasmid.

4.4.5. Yeast Minipreparation

After cloning *lexA* K156A or *lexA* S119A into the pEG202 vector *via* homologous recombination, the *lexA* mutant plasmid was isolated as described in the Yeast

* The media consisted of YPD for either EY111 or EY93 cells, and SD H^- for EY111 cells that contained *lexA* K156A or *lexA* S119A pEG202 plasmid.

Minipreparation protocol (Geyer and Brent, 2000). Briefly, several colonies were picked from the SD H^- plates, and inoculated into 3 ml SD H^- media. [Also, a sample from a single colony that contained the *recA* library was picked from the master plate (section 4.4.8.1) and then inoculated into 3 ml SD W^- media]. The cells were grown overnight in a shaking incubator at 30°C, and on the following day the cells were harvested by centrifugation at 3,901 xg for 5 min. The cell pellet was resuspended in 200 µl of breaking buffer [2% (v/v) Triton X-100, 1% (v/v) SDS, 100 mM NaCl, 10 mM Tris-HCl pH 8.0, 1 mM EDTA], and followed by the addition of ~300 µg of glass beads (425–600 µm) and 200 µl of phenol-chloroform-isoamyl alcohol (25:24:1, v/v/v). The cell walls were then disrupted by vortexing the mixture vigorously for 2 min. One microliter of the aqueous mixture that contained the plasmid of interest was transformed into *E. coli* XL1 Blue by electroporation (5 msec at 1,700 volts). The transformants were incubated for 1 hr at 37°C, and then plated on LB media that contained 100 µg/ml ampicillin (amp). On the following day, the CFUs that contained the insert of interest was identified by Colony PCR (section 4.3.2), and subsequently inoculated in 5 ml LB media that contained 100 µg/ml amp. The cells were grown overnight in a shaking incubator at 37°C, and on the following day the plasmid DNA was extracted from the overnight culture with the QIAgen Miniprep Kit. The isolated plasmid DNA was then sent for sequencing at the National Research Council (Saskatoon, SK).

4.4.6. Harvesting and storing of the transformed Library

Following transformation of the *recA* library into the yeast strain EY93 (section 4.4.4), the cells were harvested and stored at –80°C as described in the Harvesting and Pooling Primary Transformants protocol (Serebriiskii *et al.*, 2005). Briefly, the CFUs on SD H^- W^- plates were suspended in sterile double-distilled water, and pooled in 50 ml falcon tubes. The cell suspension was centrifuged at 3,901 xg for 5 min at 20°C, and then the pellet was resuspended in 1 volume of freeze down solution [65% glycerol, 0.1 M $MgSO_4$, 25 mM Tris-HCl pH 8.0]. Two hundred microliters of the cells were then dispensed into Eppendorf tubes, wrapped in wet towels, and stored at –80°C for subsequent use. The titer of the frozen transformants was determined by plating serial dilutions on SD H^- W^- media. The number of CFUs was then counted after 3 days of growth at 30°C (~10^8 cells/200 µl).

4.4.7. Mating *S. cerevisiae* Strains EY93 and EY111

Mating between the haploid strain EY111 (that contained *lexA* K156A or S119A plasmid) and the haploid strain EY93 (that contained the *recA* library plasmid) was performed according to the Mating the Bait Strain and the Pre-transformed Library protocol (Serebriiskii *et al.*, 2005). Briefly, the haploid strain EY111 (that contained *lexA* K156A or S119A plasmid) was grown to an $OD_{600\ nm}$ of 0.7 in 50 ml SD H^- media (~10 $x10^8$ cells), and then the cells were harvested by centrifugation at 3,082 xg for 5 min at 20°C. The cell pellet was resuspended with sterile double distilled water in a 1 ml final volume. At the same time, the haploid strain EY93 (that contained the *recA* library plasmid) was thawed at 20°C. The two strains, EY111 and EY93 were mixed together (bait/prey ratio of 2:1; $x10^8$ cells), plated on a single 100-mm diameter YPD media, and incubated overnight at 30°C. On the following day, the CFUs on the YPD plates were suspended in sterile double-distilled water, pooled in a 50 ml falcon tube, and centrifuged at 3,082 xg for 5 min at 20°C. The cell pellet was resuspended with 1 volume of freeze down solution, then distributed in 200 µl aliquots, and stored at –80°C for future use. The titer for the frozen mated cells was determined by plating serial dilutions on SD H^- W^- media. The number of colony forming units was counted after 3 days of growth at 30°C (~0.5 $x10^8$ cells/200 µl).

4.4.8. Screening for hyper-active RecA Mutants

An aliquot of the mated cells was thawed at 20°C. One hundred microliters of the thawed cells were inoculated into 10 ml gal/sac H^- W^- media, and incubated for ~4 hr in a shaking incubator at 30°C. Due to the high level of background growth, only 10^6 cells* were plated on each five 100-mm diameter X-Gal gal/sac H^- W^- L^- media. The cells were grown for a maximum of 4 days at 30°C, and subsequently transferred and grouped on a SD H^- W^- master plate according to the day that they appeared.

4.4.8.1. First Confirmation of the Positive Interactions

The positive interactions from the master plate were first confirmed for the activation of the *LEU2* and *ADE2* reporter genes on gal/sac H^- W^- L^- A^- plates. Also, the samples were checked for the repression of the *LEU2* and *ADE2* reporter genes on SD H^-

* The number of cells in the liquid media was determined by vis-spectroscopy where an $OD_{600\ nm}$ of 1.0 ≈ 3 $x10^8$ cells.

W^- L^- A^- plates. The latter test determined if the galactose inducible promoter in the pJG4-5 vector was repressed in the absence of galactose, and/or if there was contamination in the mated cells.

4.4.8.2. Second Confirmation of Positive Interactions

Following the first confirmation of the positive interactions, the samples were reconfirmed in the haploid strain EY111 that contained the *lexA* K156A plasmid. The steps that are involved in the isolation of the plasmid from the positive interactions, purification of the plasmid, and transformation of the purified plasmid in the yeast strain EY111 (that contained the *lexA* K156A plasmid) are described in section 4.4.5. Briefly, the CFUs from the master plate were inoculated into 3 ml SD W^- media, and grown overnight at 30°C. The plasmid DNA was extracted from the yeast culture, transformed into *E. coli* XL1 blue, and grown overnight in a shaking incubator at 37°C. The plasmid was purified from the overnight cell culture, and then transformed into the haploid strain EY111 (that contained the *lexA* K156A plasmid) as described in section 4.4.4. Ten colonies from each transformation were transferred onto a single SD H^- W^-master plate, and grown for 3 days at 30°C. The samples from the master plate were transferred onto X-Gal gal/sac H^- W^- plates and grown for 3 days at 30°C, in order to test for the activation of the *lacZ* reporter gene. The samples from the master plate were also transferred onto gal/sac H^- W^- L^- A^- plates and grown for 3 days at 30°C, in order to test for the activation of the *LEU2* and *ADE2* reporter genes.

4.5. Analysis of the RecA/LexA Complex *in vitro*

4.5.1. Site Directed Mutagenesis by Overlap Extension PCR

The mutations identified from the yeast monohybrid screen were introduced into the wild-type *recA* or *recA* E96D gene by site-directed mutagenesis by overlap extension PCR as described in Sambrook and Russell (2001b), in order to clone the mutants into the pET28a plasmid (discussed later). Briefly, the overlap site in each 5'- and 3'-regions of the DNA fragments were generated from the wild-type *recA* or *recA* E96D gene with the N_{for}/N_{rev} (Table 4.4; PCR step 1a) and C_{for}/C_{rev} (Table 4.4; PCR step 1b) oligonucleotide pairs respectively. The conditions and composition of the mixture used

in the PCR are described in section 4.4.1, except that the extension time at 72°C was 2 min, and the template DNA consisted of 500 ng of *recA* or *recA* E96D.

In the second PCR step, each 5'- and 3'-region of the DNA fragments were fused together and amplified by the N_{for}/C_{rev} oligonucleotide pair (Table 4.4; PCR step 2), in order to generate the ORF of interest. The reaction conditions and composition of the mixture used in the second PCR step are described in section 4.4.1, except that the extension time at 72°C was 2 min and 20 sec. In all cases the ORF products were purified with the QIAquick PCR Purification Kit unless otherwise stated.

Table 4.4. The oligonucleotides used in generating the *recA* mutants.

PCR Step	Construct/ oligonucleotide	Oligonucleotide sequence (5'-3')	Template
	RecA K216E		
1a. N_{for} N_{rev}	T7 Pro RecA K216E (rev)	taa tac gac tca cta tag gg cag agg cgt aga att cca gcg cgt tac c	wild-type *recA*
1b. C_{for} C_{rev}	RecA K216E (for) T7 Ter	ggt aac gcg ctg gaa ttc tac gcc tct g gct agt tat tgc tca gcg g	wild-type *recA*
2. N_{for} C_{rev}	T7 Pro T7 Ter	taa tac gac tca cta tag gg gct agt tat tgc tca gcg g	5'-*recA* K216E & 3'-*recA* K216E
	RecA E96D K216E		
1a. N_{for} N_{rev}	T7 Pro RecA K216E (rev)	taa tac gac tca cta tag gg cag agg cgt aga att cca gcg cgt tac c	*recA* E96D
1b. C_{for} C_{rev}	RecA K216E (for) T7 Ter	ggt aac gcg ctg gaa ttc tac gcc tct g gct agt tat tgc tca gcg g	*recA* E96D
2. N_{for} C_{rev}	T7 Pro T7 Ter	taa tac gac tca cta tag gg gct agt tat tgc tca gcg g	5'-*recA* E96D K216E & 3'-*recA* E96D K216E
	RecA K198N		
1a. N_{for} N_{rev}	T7 Pro RecA K198N (rev)	taa tac gac tca cta tag gg cac acc aat att cat acg gat ctg	wild-type *recA*
1b. C_{for} C_{rev}	RecA K198N (for) T7 Ter	gat ccg tat gaa tat tgg tgt gat g gct agt tat tgc tca gcg g	wild-type *recA*
2. N_{for} C_{rev}	T7 Pro T7 Ter	taa tac gac tca cta tag gg gct agt tat tgc tca gcg g	5'-*recA* K198N & 3'-*recA* K198N

4.5.2. Molecular cloning and Transformation

The ORF (insert) generated from section 4.5.1 was digested for 15 hr at 20°C with NcoI and XhoI restriction endonucleases. The mixture was made up to a 50 µl final reaction volume that consisted of 2.0 µg insert (alternatively 1.0 µg pET28a), 25 Units NcoI, 25 Units XhoI, and 1X Buffer R^+. The purified insert was ligated into the pET28a vector at the *NcoI* and *XhoI* restriction sites (insert/vector ratio 3:1) for 15 hr at 20°C. The ligation mixture was made up to a 10 µl final reaction volume that consisted of 1X Ligation Buffer, 2 Units T4 DNA Ligase, ~20 ng of digested insert, and 2 ng of digested pET28a. On the following day, the XL1 Blue cells were transformed with 1 µl of the ligation mixture by electroporation (5 msec at 1,700 volts), and then recovered in 1 ml LB media for one hour at 37°C. Two hundred fifty microliters of the transformants were plated on LB media that contained 35 µg/ml kanamycin (kan) and grown overnight in a shaking incubator at 37ºC. On the following day, the CFUs that contained the insert of interest were determined by colony PCR (section 4.3.2), inoculated into 10 ml LB media that contained 35 µg/ml kan, and grown overnight in a shaking incubator at 37°C. The plasmid construct of interest was purified from the overnight culture with the QIAgen Miniprep Kit, and then sent for sequencing at the National Research Council (Saskatoon, SK).

4.5.3. BL21 Culture and Gene Induction

The plasmid construct of interest (*lexA* or *recA*) was transformed into *E. coli* BL21 (DE3) by electroporation (5 msec at 1,600 volts), and then recovered in 1 ml LB media for one hour at 37°C. The transformants were inoculated into 10 ml LB media that contained 35 µg/ml kan and 0.3% (w/v) D-glucose, and grown overnight in a shaking incubator at 37ºC. The overnight culture was then inoculated into 1 L LB media that contained 35 µg/ml kan, grown to an OD_{600} of ~0.6 at 37ºC, and then induced with 0.120 mM isopropyl thio-β-D-galactoside (IPTG) for 3 hrs in a shaking incubator at 30ºC. The culture was harvested by centrifugation at 4,648 xg for 15 min at 6ºC, and the cell pellet was stored at -20ºC for future use.

4.5.4. Cell lysis and Protein Purification

4.5.4.1. LexA Protein

The cell pellets that contained His-tagged LexA was thawed at 20°C and resuspended in ice-cold Binding buffer A (30 mM Tris-HCl pH 7.5, 0.5 M NaCl). The cell suspension was homogenized on ice by sonication for five rounds (3" pulse, 6" rest; 90" total) and then centrifuged at 21,289 xg for 30 min at 6ºC. The DNA and cell debris was removed from the supernatant with the DE52 anion exchange column that was pre-equilibrated with Binding buffer A. The flow through from the anion exchange column was loaded onto the Ni-chelating Sepharose fast flow column that was pre-equilibrated with the Binding buffer A. The Ni chelating column that contained the bound protein was washed with five column volumes of Wash buffer A[*]; and then stripped from the column with two column volumes of Elution buffer (30 mM Tris-HCl pH 7.5, 0.5 M NaCl, 300 mM imidazole). Fractions with the highest protein yield were pooled together as determined by visualization on a 15% SDS-polyacrylamide gel that was stained with Coomassie Brilliant Blue (section 4.3.3).

4.5.4.2. RecA Protein

The purification of His-tagged RecA is described in section 4.5.4.1, except that Binding buffer A consisted of 30 mM Tris-HCl pH 7.9, 0.5 M NaCl. Additionally, the bound protein in the Ni chelating column was washed with two column volumes of Wash buffer A1 (30 mM Tris-HCl pH 7.9, 0.5 M NaCl, 2 M Urea), followed by three column volumes of Wash buffer A2 (30 mM Tris-HCl pH 7.9, 0.5 M NaCl, 30 mM imidazole), and then stripped with two column voumes of Elution buffer (30 mM Tris-HCl pH 7.9, 0.5 M NaCl, 300 mM imidazole).

4.5.4.3. Thrombin cleavage

The histag was removed from the protein of interest with 0.5 Unit/mg of thrombin (optional for the LexA samples). The digestion for the RecA samples proceeded for 15 hr at 4ºC, and the digestion for the LexA samples proceeded for 15 hr at 20°C. The

[*] The column was washed as needed, until the residual protein was no longer detected by the 1X Bradford reagent.

completeness of the digestion was determined by visualization on a 12% SDS-polyacrylamide gel that was stained with Coomassie Brilliant Blue (section 4.3.3).

4.5.4.4. Gel Filtration and Storage of Protein

The protein sample was treated with 0.1% (v/v) β-mercaptoethanol and then precipitated with 35% (w/v) ammonium sulfate for at least 6 hrs at 4ºC. The sample was then centrifuged at 28,977 xg for 20 min at 4ºC, and the protein pellet (~60 mg) was resuspended in 4 ml of running buffer. (Trace amounts of protein that did not dissolve in the running buffer were removed by centrifugation at 15,700 xg for 1 min at 20°C. The running buffer for LexA consisted of 30 mM Tris-HCl pH 7.5, 0.2 M NaCl, and 0.1% (v/v) β-mercaptoethanol. On the other hand, the running buffer for RecA consisted of 30 mM Tris-HCl pH 7.9, 2.0 M NaCl, 2.0 M Urea, and 0.1% (v/v) β-mercaptoethanol.

The LexA and RecA samples were loaded onto a Äkta Prime Protein Purification System, and resolved on a HiPrep Sephacryl S-100 and S-300 HR columns (Amersham Biosciences) respectively at a flow rate of 1.0 ml/min. The fractions for the second peak of the LexA sample (dimer form) and the third peak of the RecA sample (hexamer form) were collected and pooled. The pooled samples were concentrated with an Amicon Ultra-4 centrifugal filter device (10,000 nominal Molecular Weight Limit; Millipore) at 3,901 xg, until a final concentration in the range of 16-25 mg/ml was reached. (The concentration of the samples was determined with a 1X Bradford Reagent at 595 nm). The samples were then quench-frozen with liquid nitrogen in a 500 µl PCR tube, and stored at –79ºC for subsequent use. A cryoprotectant [20% (w/v) sucrose] was also added to the RecA samples, in order to protect the protein against aggregation during the freezing and storing process (Cleland *et al.*, 2000).

4.5.5. ATPase Assay

The Malachite Green reagent used in the ATPase assay was prepared by mixing 10 ml of solution A [0.045% (w/v) Malachite Green oxalate] with 30 ml of solution B [4.2% (w/v) ammonium molybdate, 4 N HCl], and letting it sit for 30 min at 4ºC. Forty microlitres of the enzymatic reaction was added to the Malachite Green reagent in a 1 ml final reaction volume, and then developed for 1 min before measuring the OD at 620 nm for the amount of inorganic phosphate released in 30 min. The mixture for the enzymatic

reaction consisted of 150 mM MES [2-(4-morpholino)-ethane sulfonic acid] pH 6.9, 8 mM $MgCl_2$, 5 mM ATP, 15% (w/v) PEG 400, 10 μM RecA sample, and 40 μM LexA sample. All of the enzymatic reactions were incubated for 30 min at 37ºC, before mixing the samples with the Malachite Green reagent. The PEG gradient mixture was also similar, except that the PEG concentration varied from 0 to 15% (w/v) and NaCl concentrations remained constant at 0.2 M.

The standard, NaH_2PO_4 was used to determine the amount of inorganic phosphate (Pi) released during the enzymatic reaction. The calibration curve was constructed in the range of 0-1.0 mM NaH_2PO_4, where 40 μl of each standard was added to the Malachite Green reagent in a 1 ml final reaction volume. Each standard was developed for 1 min before measuring the OD at 620 nm.

4.5.6. Coprotease Assay

The reaction mixture for the coprotease assay was made up to a 20 μl final reaction volume that consisted of 150 mM HEPES pH 7.5, 8 mM $MgCl_2$, 15% (w/v) PEG 400, 1.5 mM ATP substrate (ATP, ATP-γ-S, or AMP-PNP), 10 μM RecA sample, and 40 μM His-tagged wild-type LexA. Also, RecA's coprotease activity was further stimulated with the addition of 15 μM dT_{36} oligonucleotide. The enzymatic reactions were incubated for 1 hr at 20°C, and stopped with 5 μl of 2X Loading buffer [100 mM Tris-HCl pH 6.8, 2% (v/v) β-mercaptoethanol, 4% (w/v) SDS, 0.2% (w/v) bromophenol blue, 20% (v/v) glycerol]. Six microlitres of this mixture was resolved on a 12% SDS-polyacrylamide gel and then stained with Coomassie Brilliant Blue (section 4.3.3), in order to visualize the resulting cleavage products of the LexA repressor. The PEG gradient mixture was also similar, except that the PEG concentration varied from 0 to 18% (w/v), and the ATP substrate consisted of 1.5 mM ATP-γ-S.

4.5.7. Inhibition Assay

The reaction mixture for the inhibition assay was made up to a 20 μl final reaction volume that consisted of 150 mM HEPES pH 7.5, 8 mM $MgCl_2$, 15% (w/v) PEG 400, and 1.5 mM ATP-γ-S substrate, 5 μM RecA sample, 40 μM His-tagged wild-type LexA, and 10 μM LexA inhibitor (K156A, or K156A dimer interface mutants). The enzymatic reactions were incubated for 1 hr at 20°C, and stopped with 5 μl of 2X Loading buffer.

Six microlitres of this mixture was resolved on a 12% SDS-polyacrylamide gel and then stained with Coomassie Brilliant Blue (section 4.3.3) in order to visualize the resulting cleavage products of the LexA repressor.

4.6. The Yeast Monohybrid Analysis of the LexA Dimer Interface Mutants

4.6.1. Constructing the *lexA* Dimer Interface Mutants by PCR

Before introducing the mutations at the dimer interface of *lexA*, the *lexA b42AD* fusion gene was constructed by overlap extension PCR. In the first PCR step, the wild-type *lexA* gene was amplified from the pEG202 plasmid with the N_{for}/N_{rev} oligonucleotide pair (Table 4.5; PCR step 1a), while the *b42AD* gene was amplified from the pJG4-5 plasmid with the C_{for}/C_{rev} oligonucleotide pair (Table 4.51b). The reaction conditions and composition of the mixture used in the first PCR step are described in section 4.4.1, except that the extension time at 72°C was 1 min, and the template DNA consisted of 250 ng of either pEG202 or pJG4-5 plasmid.

In the second PCR step, the 5'-region of the *lexA* gene was fused to the 3'-region of the *b42AD* gene, and amplified with the N_{for}/C_{rev} oligonucleotide pair (Table 4.5; PCR step 2), in order to generate the *lexA b42AD* fusion gene. The reaction conditions and composition of the mixture used in the second PCR step are described in section 4.4.1.

The *lexA b42AD* fusion gene was then used as a template to generate the mutations at the dimer interface of *lexA* by site-directed mutagenesis by overlap extension PCR as described in Sambrook and Russell (2001b). Briefly, the overlap site in the 5'-region of the *lexA* mutant fragment and 3'-region of the *lexA* mutant *b42AD* fragment were generated from the same *lexA* b42AD template with the N_{for}/N_{rev} (Table 4.5; PCR step 1a) and C_{for}/C_{rev} (Table 4.5; PCR step 1b) oligonucleotide pairs respectively. The reaction conditions and composition of the mixture used in the PCR are described section 4.4.1, except that the extension time at 72°C was 2 min, and the template DNA consisted of 250 ng of the *lexA* mutant *b42AD* fragment.

In the second PCR step, the 5'- and the 3'-regions of the DNA fragments were fused together and amplified with the N_{for}/C_{rev} oligonucleotides pair (Table 4.5; PCR step 2), which generated the *lexA* dimer interface mutant *b42AD* gene. The reaction

conditions and composition of the mixture used in the second PCR step are described in section 4.4.1.

Table 4.5. The oligonucleotides used in generating the fusion gene and interface mutants for the yeast monohybrid system.

PCR Step	Construct	Sequence (5'-3')	Template
	LexA B42AD		
1a. N_{for}	$ADH1_{Pro}$ (for)	tat acc aag cat aca atc aac tcc	pEG202
N_{rev}	$ADH1_T$ (rev)	ata aga aat tcg ccc gga a	
1b. C_{for}	B42 Recomb P1	ggc gac tgg ctg gaa ttc atc aat aaa gat-atc- gag ga	pJG4-5
C_{rev}	B42 Recomb P2	agg tcg act cga gtt agg gag agg cat aat-ctg- gca	
2. N_{for}	P1 pEG202 amp	gct tca cca ttg aag ggc tgg cgg ttg ggg tta- ttc gca acg gcg act ggc tgg aat tc	*LexA* &
C_{rev}	$ADH1_T$ (rev)	ata aga aat tcg ccc gga a	*b42AD* insert
	LexA V100D B42AD		
1a. N_{for}	$ADH1_{Pro}$ (for)	tat acc aag cat aca atc aac tcc	*lexA b42AD*
N_{rev}	LexA V100D (rev2)	gaa taa gga agg atc atc ctg ata atg acc-ttc	
1b. C_{for}	LexA V100D (for)	gaa ggt cat tat cag gat gat cct tcc tta tt-c aag	*lexA b42AD*
C_{rev}	$ADH1_T$ (rev)	ata aga aat tcg ccc gga a	
2. N_{for}	$ADH1_{Pro}$ (for)	tat acc aag cat aca atc aac tcc	5'-*lexA* V100D &
C_{rev}	$ADH1_T$ (rev)	ata aga aat tcg ccc gga a	3'-*lexA* V100D *b42AD*
	LexA V100K B42AD		
1a. N_{for}	$ADH1_{Pro}$ (for)	tat acc aag cat aca atc aac tcc	*lexA b42AD*
N_{rev}	LexA V100K (rev)	gga agg atc ttt ctg ata atg acc ttc	
1b. C_{for}	LexA V100K (for)	gaa ggt cat tat cag aaa gat cct tcc tta tt-c aag	*lexA b42AD*
C_{rev}	$ADH1_T$ (rev)	ata aga aat tcg ccc gga a	
2. N_{for}	$ADH1_{Pro}$ (for)	tat acc aag cat aca atc aac tcc	5'-*lexA* V100K &
C_{rev}	$ADH1_T$ (rev)	ata aga aat tcg ccc gga a	3'-*lexA* V100K *b42AD*
	LexA I196D B42AD		
1a. N_{for}	$ADH1_{Pro}$ (for)	tat acc aag cat aca atc aac tcc	*lexA b42AD*
N_{rev}	LexA I196D (rev)	cca gtc gcc gtt gcg atc aac ccc aac cgc-cag	
1b. C_{for}	LexA I196D (for)	ctg gcg gtt ggg gtt gat cgc aac ggc gac-tgg	*lexA b42AD*
C_{rev}	$ADH1_T$ (rev)	ata aga aat tcg ccc gga a	
2. N_{for}	$ADH1_{Pro}$ (for)	tat acc aag cat aca atc aac tcc	5'-*lexA* I196D &
C_{rev}	$ADH1_T$ (rev)	ata aga aat tcg ccc gga a	3'-*lexA* I196D *b42AD*

	LexA I196K B42AD		
1a. N_{for} N_{rev}	$ADH1_{Pro}$ (for) LexA I196K (rev)	tat acc aag cat aca atc aac tcc gtc gcc gtt gcg ttt aac ccc aac cgc cag-c	*lexA b42AD*
1b. C_{for} C_{rev}	LexA I196K (for) $ADH1_T$ (rev)	cgg ttg ggg tta aac gca acg gcg act gg ata aga aat tcg ccc gga a	*lexA b42AD*
2. N_{for} C_{rev}	$ADH1_{Pro}$ (for) $ADH1_T$ (rev)	tat acc aag cat aca atc aac tcc ata aga aat tcg ccc gga a	5'-*lexA* I196K & 3'-*lexA* I196K *b42AD*

4.6.2. Cloning Insert and transforming Plasmid into Yeast Cells

Both the *lexA b42AD* fusion and *lexA* dimer interface mutant *b42AD* genes were cloned into the backbone of the pEG202 vector *via* homologous recombination as described in section 4.4.4. The transformants were plated on SD H^- media and incubated for 3 days at 30°C. On the following day, several CFUs were picked from the SD H^- plates, inoculated into 3 ml SD H^- media, and grown overnight in a shaking incubator at 30°C. The steps that are involved in the isolation of the plasmid that contained the gene of interest from the yeast cells, transformation of the plasmid into XL1 blue cells by electroporation, and purification of the plasmid from the overnight cell culture are described in section 4.4.5. The purified plasmid was transformed into *S. cerevisiae* strain EY111 as described in section 4.4.4. Several transformants were then plated into SD H^- media and grown for 3 days at 30°C.

4.6.3. Activation of Reporter Genes

A single colony was picked from the SD H^- plates, inoculated into 3 ml SD H^- media, and grown overnight in a shaking incubator at 30°C. The overnight cell culture was standardized to an $OD_{600\ nm}$ of 0.2 in 3 ml SD H^- media, and subsequently grown to $OD_{600\ nm}$ of 0.8 in a shaking incubator at 30°C. Serial dilutions were performed on the standardized cell culture in the range of 10^{-1} to 10^{-4}-fold. Two microliters from each dilution was plated onto both X-Gal SD H^-, and X-Gal SD H^- L^- media; and grown for 3 days at 30°C.

4.7. Analysis of the LexA Dimer Interface Mutants *in vitro*

The procedures for isolating the LexA mutant proteins and testing for their ability to inhibit RecA-mediated cleavage of wild-type LexA *in vitro* are described in section 4.5, unless otherwise stated.

4.7.1. Site Directed Mutagenesis

The *lexA* dimer interface mutants were generated by site directed mutagenesis by overlap extension PCR as described in Sambrook and Russell (2001b)**.** Briefly, the overlap site in the 5'- and 3'-region of the *lexA* mutant fragments were generated from the Δ_{69}*lexA* K156A template with the N_{for}/N_{rev} (Table 4.6; PCR step 1a) and C_{for}/C_{rev} (Table 4.6; PCR step 1b) oligonucleotide pairs respectively. The reaction conditions and composition of the mixture used in the PCR are described in section 4.4.1, except that the extension time at 72°C was 1 min and 20 sec, and the template DNA consisted of 250 ng of Δ_{69}*lexA* K156A gene.

In the second PCR step, the 5'- and the 3'-region of the *lexA* mutant fragments were fused together and amplified with the N_{for}/C_{rev} oligonucleotides pair (Table 4.6; PCR step 2), which generated the *lexA* dimer interface mutant gene. The reaction conditions and composition of the mixture used in the second PCR step are described in section 4.4.1.

Table 4.6. Oligonucleotides used in generating the *lexA* dimer interface mutants.

PCR Step	Construct	PCR Step	Made by/Template
	Δ_{69}LexA K156A I196D		**I. Moya**
1a. N_{for}	$T7_{Pro}$ (for)	taa tac gac tca cta tag gg	Δ_{69}LexA K156A/
N_{rev}	LexA I196D (rev)	cca gtc gcc gtt gcg atc aac ccc- aac-cgc cag	
1b. C_{for}	LexA I196D (for)	ctg gcg gtt ggg gtt gat cgc aac- ggc-gac tgg	Δ_{69}LexA K156A
C_{rev}	$T7_{Ter}$ (rev)	gct agt tat tgc tca gcg g	
2. N_{for}	$T7_{Pro}$ (for)	taa tac gac tca cta tag gg	5'-*lexA* K156A I196D &
C_{rev}	$T7_{Ter}$ (rev)	gct agt tat tgc tca gcg g	3'-*lexA* K156A I196D
	Δ_{69}LexA K156A I196K		**G. Qian**
1. N_{for}	$T7_{Pro}$ (for)	taa tac gac tca cta tag gg	Δ_{69}*lexA* K156A
N_{rev}	P2 LexA I196K (rev)	gtc gcc gtt gcg ttt aac ccc aac- cgc-cag c	
2. C_{for}	P3 LexA I196K (for)	cgg ttg ggg tta aac gca acg gc-g act-gg	Δ_{69}*lexA* K156A

C_{rev}	P2-LexA *Xho*1 (rev)	ccg ctc gag tta cag cca gtc gcc- gtt-gc	
2. N_{for}	$T7_{Pro}$ (for)	taa tac gac tca cta tag gg	5'-*lexA* K156A I196K &
C_{rev}	P2-LexA *Xho*1 (rev)	ccg ctc gag tta cag cca gtc gcc- gtt-gc	3'-*lexA* K156A I196K
	Δ_{69}LexA K156A V100D		**I. Moya**
1. N_{for}	$T7_{Pro}$ (for)	taa tac gac tca cta tag gg	Δ_{69}*lexA* K156A
N_{rev}	LexA V100D (rev2)	gaa taa gga agg atc atc ctg ata- atg-acc ttc	
2. C_{for}	LexA V100D (for)	gaa ggt cat tat cag gat gat cct- tcc-tta ttc aag	Δ_{69}*lexA* K156A
C_{rev}	$T7_{Ter}$ (rev)	gct agt tat tgc tca gcg g	
2. N_{for}	$T7_{Pro}$ (for)	taa tac gac tca cta tag gg	5'-*lexA* K156A V100D &
C_{rev}	$T7_{Ter}$ (rev)	gct agt tat tgc tca gcg g	3'-*lexA* K156A V100D
	Δ_{69}LexA K156A V100K		**G. Qian**
1. N_{for}	$T7_{Pro}$ (for)	taa tac gac tca cta tag gg	Δ_{69}*lexA* K156A
N_{rev}	LexA V100K (rev)	gga agg atc ttt ctg ata atg acc- ttc	
2. C_{for}	LexA V100K (for)	gaa ggt cat tat cag aaa gat cct- tcc-tta ttc aag	Δ_{69}*lexA* K156A
C_{rev}	P2-LexA *Xho*1 (rev)	ccg ctc gag tta cag cca gtc gcc- gtt-gc	
2. N_{for}	$T7_{Pro}$ (for)	taa tac gac tca cta tag gg	5'-*lexA* K156A V100K &
C_{rev}	P2-LexA *Xho*1 (rev)	ccg ctc gag tta cag cca gtc gcc- gtt-gc	3'-*lexA* K156A V100K

5. RESULTS

5.1. Stimulation of RecA's Activity by Polyethylene Glycol

In previous studies, volume-excluding agents such as polyethylene glycol and polyvinyl alcohol have been shown to enhance RecA's binding affinity for ssDNA and filament formation (Lavery and Kowalczykowski, 1992). The volume-excluding agents exert their effect by reducing the energy barrier required to displace water between interacting molecules, thereby "squishing" them together (Zimmerman and Minton, 1993). A similar approach was taken in this study in order to reduce the energy barrier involved in the binding between RecA and the LexA repressor.

Specifically, enhancement of RecA's binding affinity for LexA K156A was examined with increasing concentrations of polyethylene glycol 400 (PEG 400)[*] *in vitro*. This was determined by measuring the level of RecA's ATPase activity. The rational behind this assay was based on the correlation between the level of RecA's ATPase activity (*i.e.* active form of RecA) and the extension of its helical pitch upon binding of its substrate such as salt, ssDNA, or the LexA repressor (DiCapua *et al.*, 1990a). To determine whether RecA's conformation had shifted towards the active form, the amount of inorganic phosphate (P_i) released during ATP hydrolysis was detected with a Malachite Green reagent at 620 nm. This assay also served as an indicator for detecting the formation of the RecA/LexA complex, since previous studies had shown that RecA's conformation in the presence of ssDNA was shifted towards the active form upon binding to the LexA protein (DiCapua *et al.*, 1990a). Additionally, 4-fold excess of the LexA protein was used throughout this experiment (the ATPase assay) and coprotease assay,[**] since it was the minimum concentration of protein that was required to saturate RecA's ATPase and coprotease activities.

---

[*]The volume-excluding agent, PEG 400 was selected for its low molecular weight since it did not affect the resolution of SDS-polyacrylamide gel when examining RecA's coprotease activity.

[**]Increasing concentrations of PEG did not facilitate the LexA protein to hydrolyze ATP during the ATPase assay, nor did it facilitate the cleavage of the LexA protein during the coprotease assay.

In the ATPase assay for wild-type RecA in the presence of Δ_{69}LexA K156A, there was a 6-fold increase in the amount of P_i released as the PEG 400 concentration increased from 0% to 15% (w/v; Figure 5.1a)[*]. One-third of this activity might be caused by an increase in self-polymerization of the RecA monomers as a result of dehydration (when examining RecA alone; Figure 5.1a) as proposed by Lavery and Kowalczykowski (1992). The remaining two-thirds of this activity was likely caused by an increase formation of the RecA/LexA complex as a result of dehydration at RecA's binding site when RecA and Δ_{69}LexA K156A were squished together (compare the difference between RecA in the presence and absence of LexA; Figure 5.1a). Thus, a volume-excluding agent, PEG 400 was able to enhance RecA's binding affinity for the Δ_{69}LexA K156A.

The effect of increasing PEG concentrations on RecA's coprotease activity was also tested *in vitro*, in order to detect the enhancement of RecA's binding affinity for the LexA repressor. Again the rational behind this assay is based on the correlation between the level of RecA's coprotease activity and the extension of its helical pitch upon binding to the substrate. The level of RecA's coprotease activity was determined by the amount of His-tagged wild-type LexA cleavage products generated, as visualized on a 15% SDS polyacrylamide gel that was stained with Coomassie Brilliant Blue.

In the coprotease assay, the level of RecA's coprotease activity was found to increase as the concentration of PEG increased from 0% to 15% (w/v; Figure 5.1b). Beyond 15% (w/v) PEG 400, the level of RecA's coprotease activity decreased, which might be attributed to the precipitation of RecA in the PEG 400 solution. Thus, the volume-excluding agent was most effective at a 15% (w/v) in order to enhance RecA's binding affinity for the LexA repressor.

In general, RecA's ATPase and coprotease activity did not require preactivation by ssDNA *in vitro*. The addition of a volume-excluding agent and the LexA substrate

[*]In the ATPase assay, PEG 400 concentrations greater than 15% (w/v) were not examined because RecA precipitates out of the solution. Consequently, precipitation during crystallization trials was expected to reduce the quality of the crystal.

a.

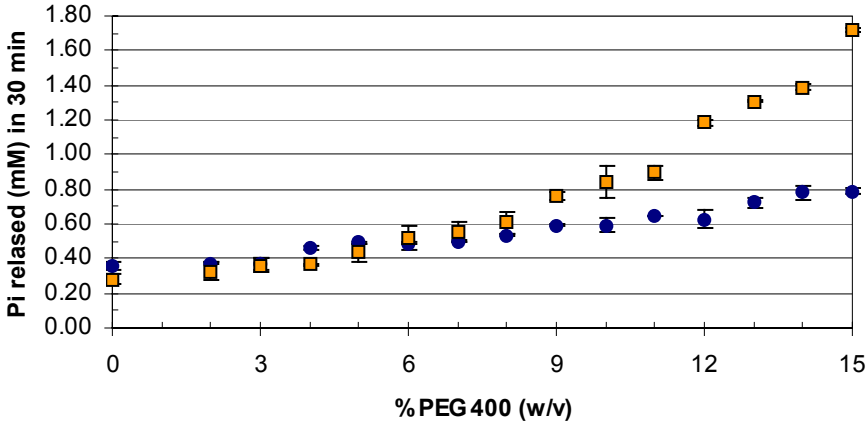

b.

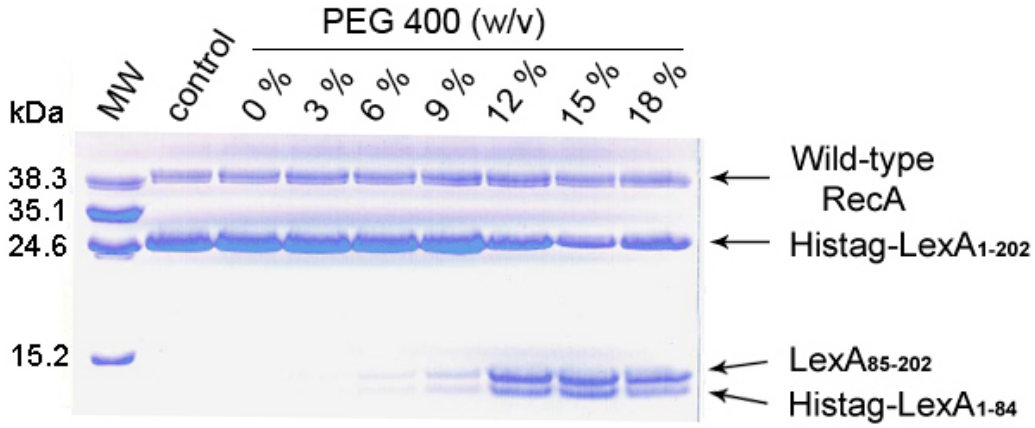

Figure 5.1. The effects of the increasing concentrations of PEG 400 on the ATPase and coprotease activity of wild-type RecA.

(a) The effect of increasing PEG 400 concentrations on the ATPase activity of wild-type RecA (10 μM) in the absence (●) and presence (■) of Δ_{69}LexA K156A (40 μM). The enzyme solutions contained 150 mM MES/NaOH pH 6.9 and 5 mM ATP, and were incubated for 30 min at 37°C. The amount of P_i released in 30 min was detected with a Malachite Green reagent at 620 nm, and the mean ±S.D was determined from two independent experiments. **(b)** The effect of increasing PEG 400 concentrations on wild-type RecA (10 μM) mediated cleavage of His-tagged wild-type LexA (40 μM). The enzyme solutions contained 150 mM HEPES/NaOH pH 7.5 and 1.5 mM ATP-γ-S, and were incubated for 1 hr at 20°C. The control experiment was the same as above, except that the solution lacked both PEG and ATP-γ-S. The reaction mixtures were resolved on a 15% SDS-polyacrylamide gel, and stained with Coomassie Brilliant Blue. RecA-mediated cleavage of His-tagged wild-type LexA produced a N-terminal fragment (histag-$LexA_{1-84}$) and a C-terminal fragment ($LexA_{85-202}$).

was able to activate RecA's enzymatic activities and enhance the stability of the RecA/LexA complex. These preliminary results led to the hypothesis that the formation of a RecA/LexA complex is a thermodynamic process that involves three steps. To confirm the first two steps (*i.e.* the active form of RecA and cleavable form of LexA), the effects of a hyper-active RecA mutant and a LexA K156A mutant on RecA's enzymatic activities were tested. These mutants are expected to enhance the stability of the RecA/LexA complex, because they are known to have a reduced energy barrier for their conformational change.

5.2. Isolating Hyper-active RecA Mutants

Based on the thermodynamic model, one approach to enhance the stability of the RecA/LexA complex was to shift the conformation of RecA towards the active form. For example, enhancement of the RecA/LexA complex was achieved by promoting RecA's hyper-activity with the E96D and F217Y mutants, which were situated at RecA's ATP binding core. However, these mutants were not sufficient to enhance the stability of the RecA/LexA complex, such that it was able to utilize a non-hydrolysable AMP-PNP substrate during crystallization trials. Therefore, the hyper-active RecA mutants were isolated from the yeast two-hybrid system, in order to further enhance the stability of the RecA/LexA complex.

The hyper-active RecA mutants were generated from the wild-type *recA* and *recA* E96D templates by random mutagenic PCR. The *recA* samples were cloned into the pJG4-5 vector *via* homologous recombination in the *S. cerevisiae* strain EY93 (prey strain), which created a library size of 4 x10^6 transformants. The *recA* gene was cloned down stream from the *b42* activation domain (*b42AD*). This *b42AD recA* fusion construct was under the control of the *GAL1* promoter (Figure 5.2a). The *lexA* K156A and *lexA* S119A genes were cloned into the backbone of a pEG202 vector *via* homologous recombination in *S. cerevisiae* strain EY93, and these genes were constitutively expressed under the *ADH1* promoter in *S. cerevisiae* strain EY111 (bait strain) (Figure 5.2b). The non-cleavable LexA mutants, K156A and LexA S119A were chosen for this study because they do not undergo self-cleavage during the selection of a stable RecA/LexA complex. Additionally, the LexA mutants are expected to moderate the stringency (*i.e.* RecA's binding affinity for LexA) in the yeast two-hybrid system.

For example, LexA S119A is expected to select for RecA mutants that have a very tight binding affinity, because RecA must overcome the energy barrier that is associated with the burial and deprotonation of ε-amino group of the K156 residue in LexA (Lin and Little, 1989; Luo *et al.*, 2001). On the other hand, this energy barrier is reduced in LexA K156A; therefore, the bait is expected to select for RecA mutants that have a weak binding affinity. This latter situation is avoided by using a more stringent reporter gene (*e.g. ADE2* or *lacZ*) since it contains more *lexA* operator sites (Estojak *et al.*, 1995) or by increasing the number of reporter genes that are activated (*e.g. LEU2* and *ADE2*) (Sambrook and Russell, 2001a). Finally, it is noteworthy to point out that the LexA mutants are not a "hybrid" (fusion) protein, but the interaction trap still has the same underlying principles as a traditional yeast two-hybrid system (*i.e.* a prey and a bait protein).

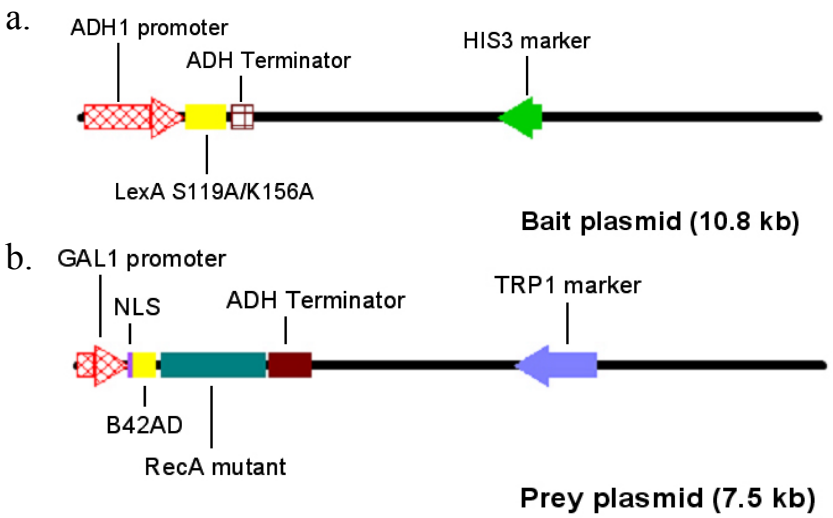

Figure 5.2. A linear plasmid drawing for the *recA* library, *lexA* S119A, and *lexA* K156A constructs.

(a) The *recA* library was under control of the inducible *GAL1* promoter. **(b)** The *lexA* S119A and *lexA* K156A gene were constitutively expressed under the *ADH1* promoter.

The prey strain that contained the *recA* library was mated with *S. cerevisiae* strain EY111 (bait strain) that contained either *lexA* K156A or S119A plasmid (Figure 5.3). However, the bait strain that contained the *lexA* K156A plasmid was used in the screening process, because there was an 8-fold increase in the number of interactions

obtained on X-Gal gal/sac H^- W^- L^- plates when compared to the bait strain that contained the *lexA* S119A plasmid. The activation of the *lacZ* reporter gene was also used in the screening process, because it was easier to distinguish between the background growth* and true positives.

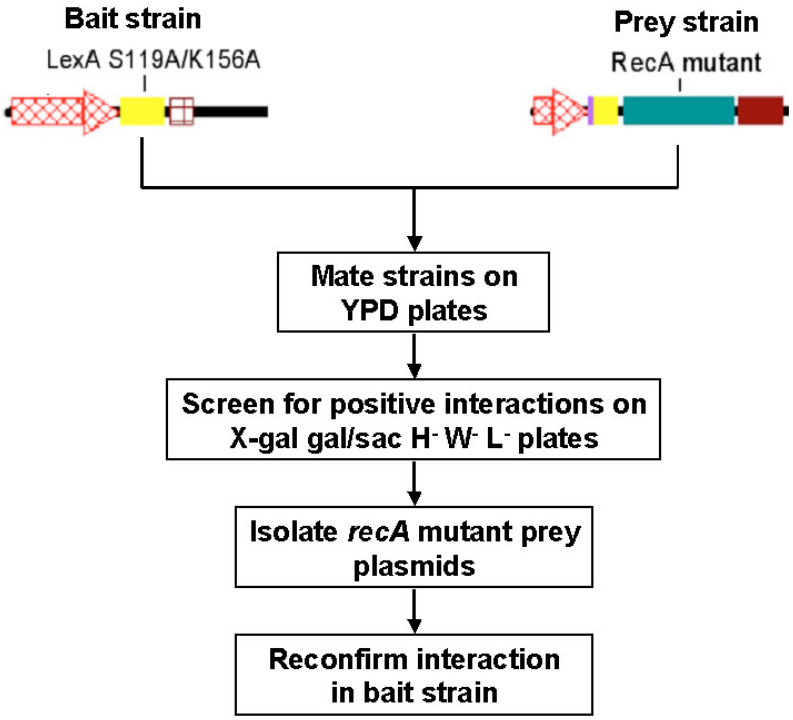

Figure 5.3. A Flow chart for isolating the hyper-active-RecA mutants from the yeast monohybrid screen.

In order to reconfirm the interactions from the yeast two-hybrid screen, the *recA* mutants were isolated and then transformed into the bait strain that contained LexA K156A. The binding affinity between the RecA mutant and LexA K156A was determined by their ability to activate the *lacZ* reporter gene or both the *LEU2* and *ADE2* reporter genes. The activation of the *lacZ* reporter gene was detected on X-Gal gal/sac H^- W^- plates, such that a blue phenotype served as an indicator for a strong-binding affinity, while a white phenotype served as an indicator for a weak-binding affinity between the RecA mutant and LexA K156A. The activation of both *LEU2* and *ADE2* reporter genes

* Background growth was observed on the control plates (SD H^- W^- L^- A^- media). These cells were found to carry the *recA* and *lexA* K156A plasmid, which suggested that the *GAL1* promoter for the prey plasmid was leaky.

was detected on gal/sac H^- W^- L^- A^- plates, which provided three different roles in the analysis. First, activation of the *LEU2* reporter gene allowed the cells to grow on L^- media. Second, activation of the *ADE2* reporter gene provided a white/red phenotype, such that a white phenotype served as an indicator for a strong-binding affinity, while a red phenotype served as an indicator for a weak-binding affinity between the RecA mutant and LexA K156A. Third, the activation of both *LEU2* and *ADE2* reporter genes was a more stringent selection method than activating a single reporter gene.

In this assay, the RecA mutants were able to activate either the *lacZ*, or both the *LEU2* and *ADE2* reporter genes on the X-Gal containing plates (Figure 5.4a) or L^- A^- plates (Figure 5.4b) respectively. The samples were then sequenced (National Research Council) in order to identify the mutations responsible for shifting RecA's conformation towards the active form. Most of the mutations within the *recA* library were found to occur at the monomer-monomer interface of RecA, such as E63G, K216E/I, E127Y,

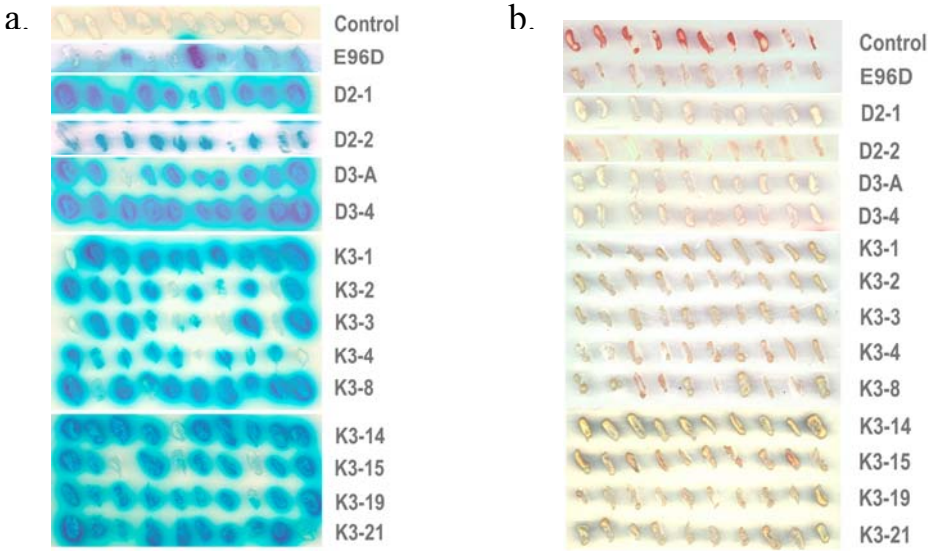

Figure 5.4. Reconfirming the isolated hyper-active RecA mutants in *S. cerevisiae* strain EY111 that contained LexA K156A.

Saccharomyces cerevisiae strain EY111 that contained both LexA K156A and the RecA mutants were grown on **(a)** X-Gal gal/sac H^- W^- plates or **(b)** gal/sac H^- W^- L^- A^- plates for 4 days at 30°C. The control cells contained LexA K156A, while the E96D cells contained both LexA K156A and RecA E96D.

Q118R, A219V and D112G (Table 5.1). Interestingly, the monomer-monomer interface mutant, K216E was a reoccurring mutation (5 out of 13 samples sequenced) and was generated from the E96D template. On the other hand, the K198N mutation was the only sample that was not generated from the *recA* E96D template (Table 5.1) but still capable of activating the reporter genes. Thus, RecA K216E and RecA K198N appeared to be good candidates for enhancing the stability of the RecA/LexA complex. Therefore, the *recA* mutants were cloned into the pET28a vector, such that the protein could be purified from BL21 cells, and examined for their hyper-activity *in vitro* by using the ATPase and coprotease assay (discussed later).

Table 5.1. DNA sequencing results for the *recA* samples that were reconfirmed in the yeast two-hybrid system.

Sample	Mutation	Sample	Mutation	Sample	Mutation	Sample	Mutation
D2-1	E63G E96D R176H E235G	**K3-1**	E96D K216E	**K3-8**	E96D E127Y K216E	**K3-19**	K198N A219V
D2-2	E96D R169P	**K3-2**	E96D Q124R K216E	**K3-14**	E96D A147Y K216E	**K3-21**	E96D F191E I195T A214G
D3-A	E96D M164T	**K3-3**	E96D K216I				
D3-4	E96D K216E E296G	**K3-4**	E96D M175T G211D	**K3-15**	E96D Q118R E156G F191S		

5.3. Stimulation of RecA's Activity by Other Substrates

In this section, various substrates were examined for their effect on the stability of the RecA/LexA complex. These include the effects of salt and ATP substrates in shifting RecA's conformation towards the active form, the effect of a hyper-active RecA mutant in preactivating RecA, and the effect of LexA K156A (the cleavable form) in promoting RecA's binding affinity. All of these substrates are expected to reduce the energy barrier that is associated at each step in the thermodynamic process, thereby enhancing the stability of the RecA/LexA complex and providing evidence for the thermodynamic

model. These effects were determined by measuring the level of RecA's ATPase and coprotease activity (discussed below).

Studies had shown that salt concentrations greater than 1.0 M were able to stimulate the ATPase activity of RecA in the absence of DNA, since the anions were believed to mimic the phosphate backbone of DNA (DiCapua *et al.*, 1990a; Pugh and Cox, 1988). A similar approach was taken in this study in order to determine the optimal salt concentration for a stabile RecA/LexA complex in a 15% (w/v) PEG 400 solution. These effects were monitored by measuring the level of RecA's ATPase activity in a Malachite Green reagent at 620 nm. The RecA proteins selected for this ATPase assay were wild type, K198N and K216E. The latter two mutants were selected because the results from the yeast two-hybrid screen suggested that these mutants might have a greater binding affinity for the LexA repressor. Additionally, the solutions were supplemented with either LexA S119A or K156A mutant* in order to examine RecA's binding affinity for each mutant.

The stability of the RecA/LexA complex was also reexamined with the coprotease assay at low salt concentrations. This assay semi-quantifies the level of RecA's coprotease activity (*i.e.* its mediated cleavage of the LexA repressor) by the amount of LexA cleavage products produced, as visualized on a 15% SDS-polyacrylamide gel that was stained with Coomassie Brilliant Blue. For example, high amounts of LexA cleavage products indicates that RecA has a tight-binding affinity for the LexA repressor; and therefore, a more stable RecA/LexA complex has formed. On the other hand, low amounts of cleavage products indicates that RecA has a weak-binding affinity for the LexA repressor; and therefore, a less stable RecA/LexA complex has formed.

Also, the effect of different ATP substrates (ATP, ATP-γ-S, or AMP-PNP) on the coprotease activity of RecA was tested. This assay will be useful for crystallization trials since the lifetime for a crystal structure is expected to be 3 months with AMP-PNP, as opposed to 3 days with ATP-γ-S, or 4 hours with ATP (Wu *et al.*, 2004). Thus, the second objective for this assay is to find a stable RecA/LexA complex that can utilize AMP-PNP in the absence of ssDNA or high salt concentrations during the crystallization

*The two LexA mutants do not undergo RecA-mediated cleavage since they are both defective in self-cleavage mechanism.

trials, since high salt concentrations will impair the binding of ssDNA (Weinstock *et al.*, 1981a) and excess ssDNA will impair the binding of the LexA protein (Rehrauer *et al.*, 1996).

5.3.1. Wild-type RecA Analysis

In the ATPase assay, the ATPase activity for wild-type RecA was found to increase by 15-fold as salt concentrations reached 0.4 M and 0.8 M in the presence of Δ_{69}LexA K156A and in the absence of Δ_{69}LexA K156A respectively (Figure 5.5). Under these conditions, the maximum turnover rate (k_{cat}, the number of ATP molecules hydrolyzed per RecA molecule per unit time) for RecA's ATPase activity was 8 min^{-1}, which was much lower than the reported values of 15-30 min^{-1} (Pugh and Cox, 1988). The differences in the turnover values were related to whether ADP was allowed to accumulate in the reaction, or regenerate into ATP by a coupling system that contained pyruvate kinase (Pugh and Cox, 1988). Thus, the lower turnover rate reported in this study was caused by the accumulation of ADP in the reaction mixture, which inhibits RecA's coprotease and ATPase activity (Moreau and Carlier, 1989; Weinstock *et al.*, 1981a). (This was also true for the two RecA mutants examined in the following subheadings, since a coupling system was not used in the regeneration of ADP to ATP).

Also, a lower salt concentration was able to stimulate RecA's ATPase activity in the presence of Δ_{69}LexA K156A when compared to RecA alone (Figure 5.5). This result suggests that the LexA mutant was able to stimulate the ATPase activity of RecA that may otherwise be influenced by a higher salt concentration. In the latter situation, complete stimulation of RecA's activity by a high salt concentration was observed at 0.8 M, where the two curves begin to overlap for RecA alone and RecA in the presence of Δ_{69}LexA K156A. Thus, the salt concentrations in the range of 0.4-0.8 M were optimal in promoting RecA's binding affinity for the LexA protein. On the other hand, salt concentrations above 0.8 M should be avoided, since the electrostatic-shielding effect may disrupt RecA's binding affinity for the LexA protein. In the presence of C-terminal His-tagged LexA S119A (LexA S119A), increasing salt concentrations did not improve the ATPase activity of RecA when compared to RecA alone (Figure 5.5). This may

suggest that wild-type RecA had a poor/no binding affinity for LexA S119A as salt concentrations were increased.

RecA's binding affinity towards either LexA K156A or S119A mutant (*i.e.* the inhibitor) was reexamined with the inhibition assay. This assay correlates the level of inhibition for RecA's coprotease activity (*i.e.* lack of wild-type LexA cleavage products) with its binding affinity towards the LexA mutant.

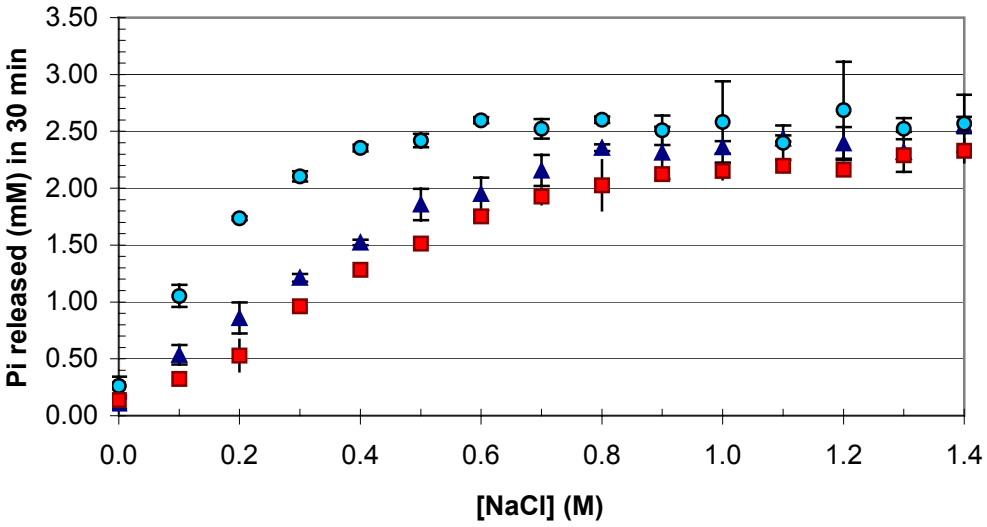

Figure 5.5. NaCl stimulation of the ATPase activity of wild-type RecA. The effect of increasing the salt concentrations on the ATPase activity of wild-type RecA (10 μM) in the absence (▲) and presence of Δ_{69}LexA K156A (●; 40 μM) or C-terminal His-tagged LexA S119A (■; 40 μM). The enzyme solutions contained 150 mM MES/NaOH pH 6.9, 15% (w/v) PEG 400, and 5 mM ATP; and were incubated for 30 min at 37°C. The amount of P_i released in 30 min was detected with a Malachite Green reagent at 620 nm, and the mean ±S.D was determined from two independent experiments.

In the inhibition assay, the two LexA mutants were able to decrease the amount of wild-type LexA cleavage products that was facilitated by RecA's coprotease activity, where Δ_{69}LexA K156A was a more effective inhibitor than LexA S119A (Figure 5.6). These results suggested that wild-type RecA had a greater binding affinity for Δ_{69}LexA K156A than LexA S119A, which were consistent with previous inhibition studies (Lin and Little, 1989; Slilaty and Little, 1987). Additionally, RecA's binding affinity towards LexA S119A appeared to be greater in the inhibition assay than the ATPase assay

(compare Figure 5.6 and Figure 5.5 respectively). These variations may be caused by a lack of salt used in the inhibition assay, or the differences in the energetic cost when stimulating RecA's ATPase activity than inhibiting its coprotease activity. In general, RecA had a greater binding affinity for Δ_{69}LexA K156A than LexA S119A as salt concentrations were increased. Therefore, Δ_{69}LexA K156A was used in the subsequent ATPase assays.

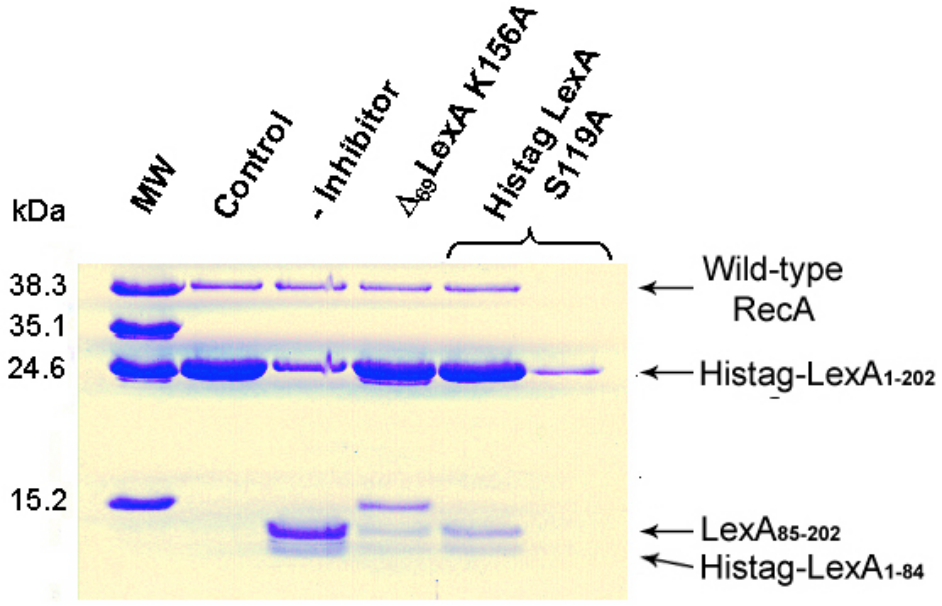

Figure 5.6. Inhibition of wild-type RecA's coprotease activity.
Inhibition of wild-type RecA (5 μM) mediated cleavage of His-tagged wild-type LexA (40 μM) by either Δ_{69}LexA K156A (10 μM) or His-tagged LexA S119A (10 μM). The enzyme solutions contained 150 mM HEPES/NaOH pH 7.5, 15% (w/v) PEG 400, and 1.5 mM ATP-γ-S; and were incubated for 2 hr at 20°C. The experiment for the Control or –Inhibitor was the same as above, except that it lacked both a LexA mutant and ATP-γ-S, or a LexA mutant respectively. The reaction mixtures were resolved on a 15% SDS-polyacrylamide gel, and stained with Coomassie Brilliant Blue. RecA-mediated cleavage of His-tagged wild-type LexA produced a N-terminal fragment (histag-LexA$_{1-84}$) and a C-terminal fragment (LexA$_{85-202}$). The last lane (right-hand side) contained Histag LexA S119A, in order to show the amount of sample loaded in the gel.

In the coprotease assay for wild-type RecA, the protein was able to utilize ATP-γ-S in the mediated-cleavage of wild-type LexA in the absence of dT_{36} oligonucleotides (Figure 5.7). On the other hand, in the presence of dT_{36} oligonucleotides, the protein was able to utilize all three ATP substrates (ATP, ATP-γ-S, and AMP-PNP) in the mediated-

cleavage of wild-type LexA (Figure 5.7). Thus, the RecA/LexA complex was not sufficiently stable enough to utilize AMP-PNP as a substrate in the absence of ssDNA. In general, the results for RecA's ATPase and coprotease assays served as a guideline to determine whether the RecA mutants were hyper-active in their enzymatic activities.

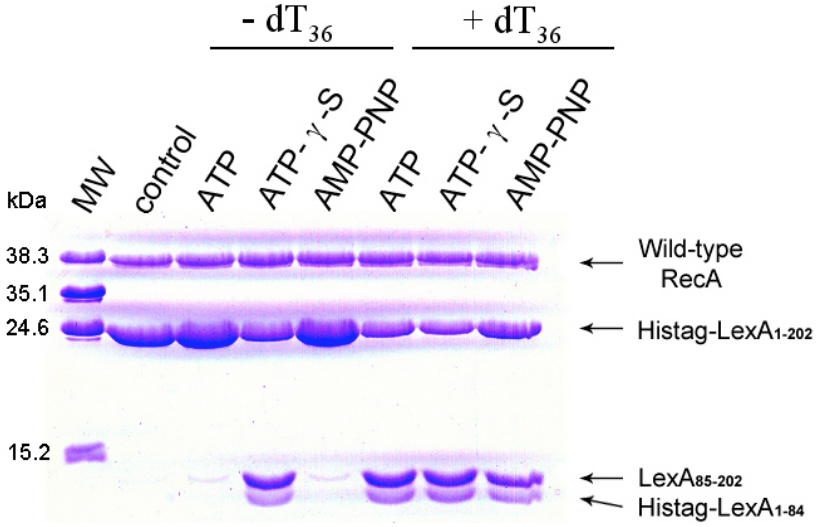

Figure 5.7. ATP substrates and ssDNA stimulation of the coprotease activity of wild-type RecA.

The effect of different ATP substrates (1.5 mM) on wild-type RecA (10 μM) mediated cleavage of His-tagged wild-type LexA (40 μM). The enzyme solutions contained 150 mM HEPES/NaOH pH 7.5, 15% (w/v) PEG 400, and ±15 μM dT_{36} oligonucleotides; and were incubated for 1 hr at 20°C. The control experiment was the same as above, except that the solution lacked an ATP substrate. The reactions were resolved on a 15% SDS-polyacrylamide gel, and stained with Coomassie Brilliant Blue. RecA-mediated cleavage of His-tagged wild-type LexA produced a N-terminal fragment (histag-$LexA_{1-84}$) and a C-terminal fragment ($LexA_{85-202}$).

5.3.2. RecA K216E Analysis

In the ATPase assay for RecA K216E, the turnover rate decreased by 42-fold in the range of 0.8 to 1.2 M salt when compared to wild-type RecA (compare Figure 5.8a and Figure 5.5 respectively). As the salt concentrations increased, the ATPase activity of RecA K216E decreased in the presence or absence of Δ_{69}LexA K156A (Figure 5.8a). This may suggest that the mutant was more sensitive to salt disruption when compared to wild-type levels. Thus, high salt concentrations did not enhance the activity of RecA K216E, nor did it improve the mutant's binding affinity for Δ_{69}LexA K156A.

In the coprotease assay, RecA K216E was able to utilize ATP-γ-S in the mediated-cleavage of wild-type LexA in the absence of dT_{36} oligonucleotides. On the other hand, in the presence of dT_{36} oligonucleotides, the mutant was able to utilize all three ATP substrates (ATP, ATP-γ-S, and AMP-PNP) in the mediated-cleavage of wild-type LexA (Figure 5.8b), but its activity was lower than wild-type levels (Figure 5.7). These results suggest that the activity for RecA was not enhanced with the K216E mutation. In general, the results indicate that RecA K216E was defective in its ATPase activity, and partially active in its coprotease activity. Therefore, the K216E mutation did not enhance RecA's binding affinity for the LexA protein when compared to wild-type levels.

The E96D mutation was also introduced into RecA K216E by site-directed mutagenesis, since the double mutant (E96D K216E) was isolated from the yeast two-hybrid screen and suspected of having hyper-activity (*i.e.* a potential candidate for enhancing the stability of the RecA/LexA complex). In the coprotease assay, RecA E96D K216E was able to utilize ATP-γ-S in the mediated-cleavage of wild-type LexA in the absence of dT_{36} oligonucleotides (Figure 5.9). On the other hand, in the presence of dT_{36} oligonucleotides, the double mutant was able to utilize all three ATP substrates (ATP, ATP-γ-S, and AMP-PNP) in the mediated-cleavage of wild-type LexA (Figure 5.9). Thus, the E96D mutation restores the defective coprotease activity of RecA K216E to wild-type levels (compare Figure 5.9 and Figure 5.7 respectively). It is also noteworthy to point out that the ATPase activity was not examined for this double mutant. The E96D mutation is known to reduce RecA's rate of ATP hydrolysis by a 100-fold (Campbell and Davis, 1999a), because the E96 residue acts as a general base for activating and positioning the water nucleophile for ATP hydrolysis (Wu *et al.*, 2005).

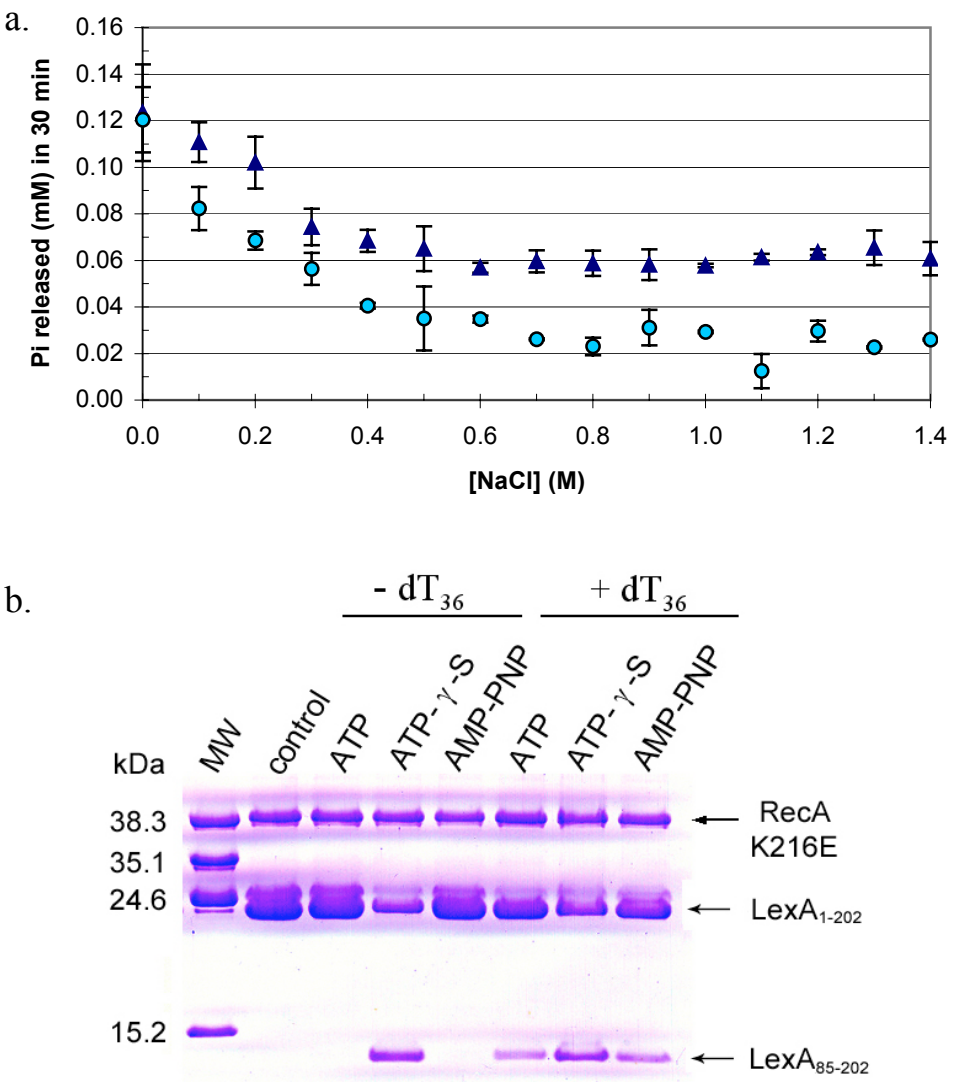

Figure 5.8. Stimulation of the ATPase and coprotease activity of RecA K216E.

(a) The effect of increasing the salt concentrations on the ATPase activity of RecA K216E (10 μM) in the absence (▲) and presence (●) of Δ_{69}LexA K156A (40 μM). The enzyme solutions contained 150 mM MES/NaOH pH 6.9, 15% (w/v) PEG 400, and 5 mM ATP; and were incubated for 30 min at 37°C. The amount of P_i released in 30 min was detected with a Malachite Green reagent at 620 nm, and the mean ±S.D was determined from two independent experiments. **(b)** The effect of different ATP substrates (1.5 mM) on RecA K216E (10 μM) mediated cleavage of wild-type LexA (40 μM). The enzyme solutions contained 150 mM HEPES/NaOH pH 7.5, 15% (w/v) PEG 400, and ±15 μM dT_{36} oligonucleotides; and were incubated for 1 hr at 20°C. The control experiment was the same as above, except that the solution lacked an ATP substrate. The reaction mixtures were resolved on a 12% SDS-polyacrylamide gel, and stained with Coomassie Brilliant Blue. RecA-mediated cleavage of wild-type LexA produced a N-terminal fragment ($LexA_{1-84}$) that has run off the gel, and a C-terminal fragment ($LexA_{85-202}$) that is present at the bottom of the gel.

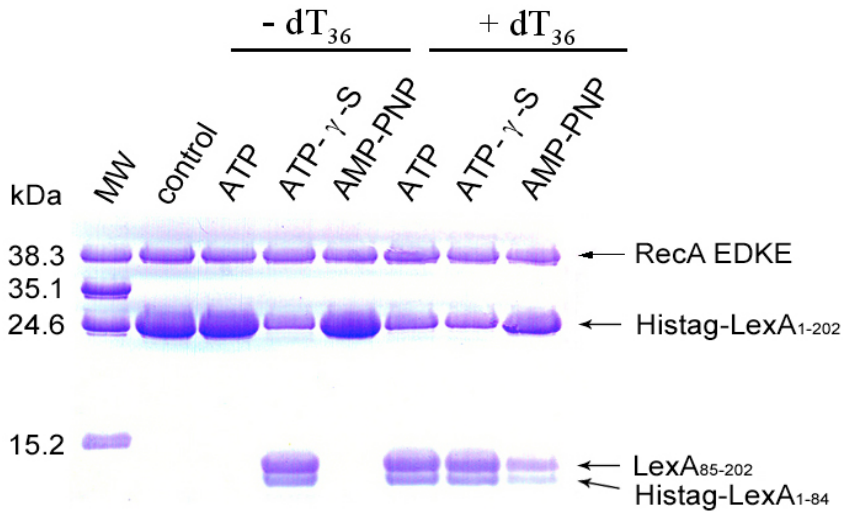

Figure 5.9. ATP substrates and ssDNA stimulation of the coprotease activity of RecA E96D K216E.

The effect of different ATP substrates (1.5 mM) on RecA E96D K216E (EDKE; 10 μM) mediated cleavage of His-tagged wild-type-LexA (40 μM). The enzyme solutions contained 150 mM HEPES/NaOH pH 7.5, 15% (w/v) PEG 400, and ±15 μM dT_{36} oligonucleotides; and were incubated for 1 hr at 20°C. The control experiment was the same as above, except that the solution lacked an ATP substrate. The reaction mixtures were resolved on a 15% SDS-polyacrylamide gel, and stained with Coomassie Brilliant Blue. RecA-mediated cleavage of His-tagged wild-type LexA produced a N-terminal fragment (histag-$LexA_{1-84}$) and a C-terminal fragment ($LexA_{85-202}$).

5.3.3. RecA K198N Analysis

In the ATPase assay for RecA K198N, increasing salt concentrations did not improve the protein's maximum turnover rate (6 min^{-1}) when compared to wild-type RecA (compare Figure 5.10a and Figure 5.5 respectively), nor did it improve with the addition of Δ_{69}LexA K156A when compared to wild-type RecA in the presence of Δ_{69}LexA K156A (compare Figure 5.10a and Figure 5.5 respectively). Thus, the results indicate that the ATPase activity of RecA K198N was comparable to wild-type levels.

In the coprotease assay for RecA K198N, the mutant was able to utilize ATP-γ-S in the mediated cleavage of wild-type LexA in the absence of dT_{36} oligonucleotides (Figure 5.10b). In the presence of dT_{36} oligonucleotides, the mutant protein was able to

a.

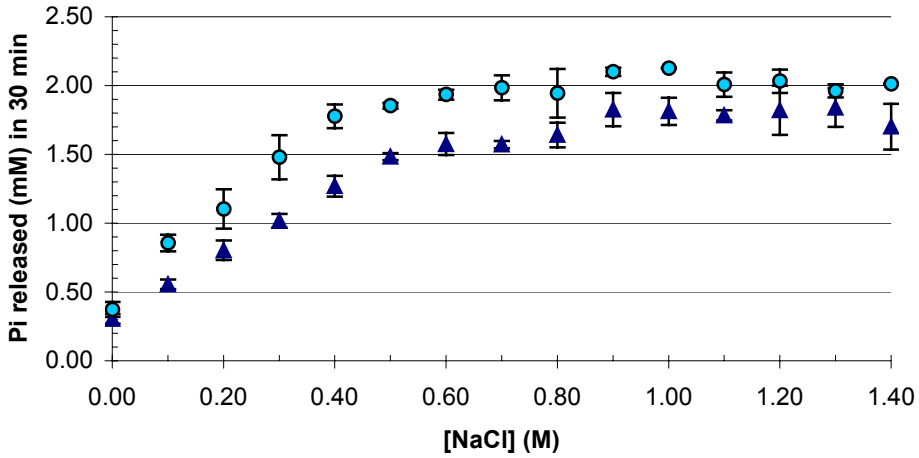

b.

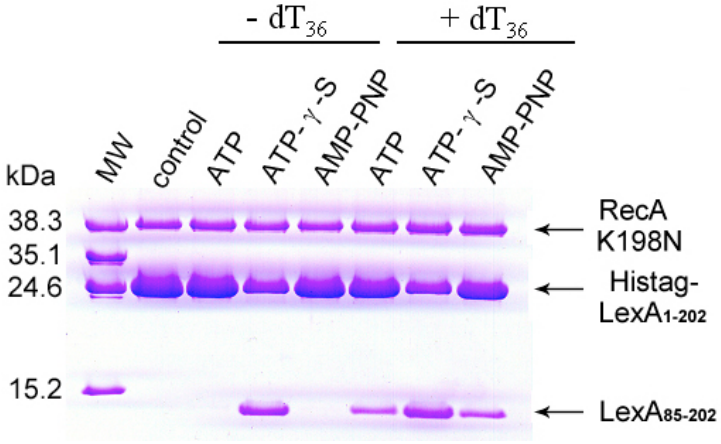

Figure 5.10. Stimulation of the ATPase and coprotease activity of RecA K198N. **(a)** The effect of increasing the salt concentrations on the ATPase activity of RecA K198N (10 μM) in the absence (▲) and presence(●) of Δ_{69}LexA K156A (40 μM). The enzyme solutions contained 150 mM MES/NaOH pH 6.9, 15% (w/v) PEG 400 and 5 mM ATP; and were incubated at 37°C for 30 min. The amount of P_i released in 30 min was detected with a Malachite Green reagent at 620 nm, and the mean ±S.D was determined from two independent experiments. **(b)** The effect of different ATP substrates (1.5 mM) on RecA K198N (10 μM) mediated cleavage of His-tagged wild-type LexA (40 μM). The enzyme solutions contained 150 mM HEPES/NaOH pH 7.5, 15% (w/v) PEG 400, and ±15 μM dT_{36} oligonucleotides; and were incubated for 1 hr at 20°C. The control experiment was the same as above, except that the solution lacked an ATP substrate. The reaction mixtures were resolved on a 12% SDS-polyacrylamide gel, and stained with Coomassie Brilliant Blue. RecA-mediated cleavage of His-tagged wild-type LexA produced a N-terminal (histag-$LexA_{1-84}$) fragment that has run off the gel, and a C-terminal ($LexA_{85-202}$) fragment that is present at the bottom of the gel.

utilize all three ATP substrates in the mediated cleavage of wild-type LexA (Figure 5.10b). The results indicate that the coprotease activity of RecA K198N was similar to wild-type levels (compare Figure 5.10 with Figure 5.7). In general, the two assays indicate that the ATPase and coprotease activity of the K198N mutant was similar to wild-type levels. Therefore, the K198N mutant did not improve RecA's binding affinity for the LexA protein.

5.4. LexA Dimer Interface Mutants Characterization

The dissociation constant for the LexA dimer (K_{dimer}) is in the picomolar range *in vitro* (Mohana-Borges *et al.*, 2000). This very low K_{dimer} value of 15 pM poses a problem when using standard techniques in detecting RecA's binding preference for the monomer or dimer form of LexA. To increase the K_{dimer} value of LexA, a single point mutation (either V100K, V100D, I196K, or I196D) was introduced at its dimer interface such that a charge-charge repulsion will disrupt the two interacting LexA monomers. The K156A mutation was also introduced into the dimer interface mutants in order to (1) improve the stability of the samples *in vitro*, since the proteins are defective in self-cleavage; and (2) shift the conformation of LexA towards the cleavable form. This study is related to the thermodynamic model for the formation of the RecA/LexA complex, since the stability of the RecA/LexA complex may be enhanced in the presence of the dimer interface mutants, as long as RecA has a greater binding affinity for the monomer form and not the dimer form of LexA.

5.4.1. Size-exclusion Chromatography

The purified LexA dimer interface mutants* were analyzed on a size-exclusion Protein-Pak 125 column, in order to determine if the mutants exist in the monomer or homodimer form. Approximately 1 mg/ml of protein was loaded onto the column that was pre-equilibrated with 100 mM phosphate buffer pH 7.0, and resolved at a flow rate of 1 ml/min. The control, Δ_{75}LexA K156A was used as a marker for the homodimer form of LexA; this protein was found to elute at 8.53 min. The two dimer interface mutants, Δ_{69}LexA K156A V100D and Δ_{69}LexA K156A V100K were found to elute between 8 to 9 min (Figure 5.11; a, b, and c respectively). When the elution times for the

* Samples were sent to Ron Geyer's lab for size exclusion and mass spectrometry analysis.

two mutants were compared with the control, the results suggested that the two mutants existed in the homodimer form. The other two mutants, Δ_{69}LexA K156A I196D and Δ_{69}LexA K156A I196K were found to elute between 11 to 12 min (Figure 5.11; c and d respectively). Since the elution time for these mutants proceeded after the homodimer peak, these results suggested that the two mutants existed in the monomer form. The variation in elution times was attributed to the mass differences in each LexA mutant, since some of the proteins contained an optional hexahistidine tag (Table 5.2).

Following size-exclusion chromatography, the mass of the monomer and homodimer peaks was then determined. Each mutant (1 mg/ml) was resolved onto a reverse phase column (Symmetry 300 C4 3.5 μm) and then analyzed with a micromass liquid chromatography time of flight mass-spectrometer. The mass for most of the samples agreed with the expected values listed in Table 5.2. However, Δ_{69}LexA K156A V100K and Δ_{69}LexA K156A I196K were found to have an additional mass of ~20.5 Da. This may have been caused by the formation of a Na-adduct (21.98 Da), since NaCl was used by the mass-spectrometer during the ionization process. Alternatively, this may have been caused by the oxidation of the tryptophan side chain residue to hydroxykynurenine (19.98 Da) (Berlett and Stadtman, 1997). In general, the results indicated that Δ_{69}LexA K156A I196D* and Δ_{69}LexA K156A I196K existed as a monomer, while Δ_{69}LexA K156A V100D and Δ_{69}LexA K156A V100K existed as a homodimer.

The two samples, 30 μM Δ_{69}LexA K156A I196K (monomer) and 30 μM Δ_{75}LexA K156A (dimer) were mixed together and tested for the formation of heterodimers. The mixture was incubated for 1 hr at 4°C and then resolved on a size-exclusion column. The mass of the mutants was then determined by mass-spectrometry as described above. The size-exclusion chromatograms showed that the dimer peak eluted at 8.67 min, and the monomer peak eluted at 12.5 min (Figure 5.12a). Upon analysis of the two peaks by mass-spectrometry, the dimer peak had only one molecular weight of 14.5 kDa (Figure 5.12b), which corresponded to Δ_{75}LexA K156A (Table 5.2). The monomer peak also

*No further analysis was conducted for Δ_{69}LexA K156A I196D, since the yield of the sample was very low following purification.

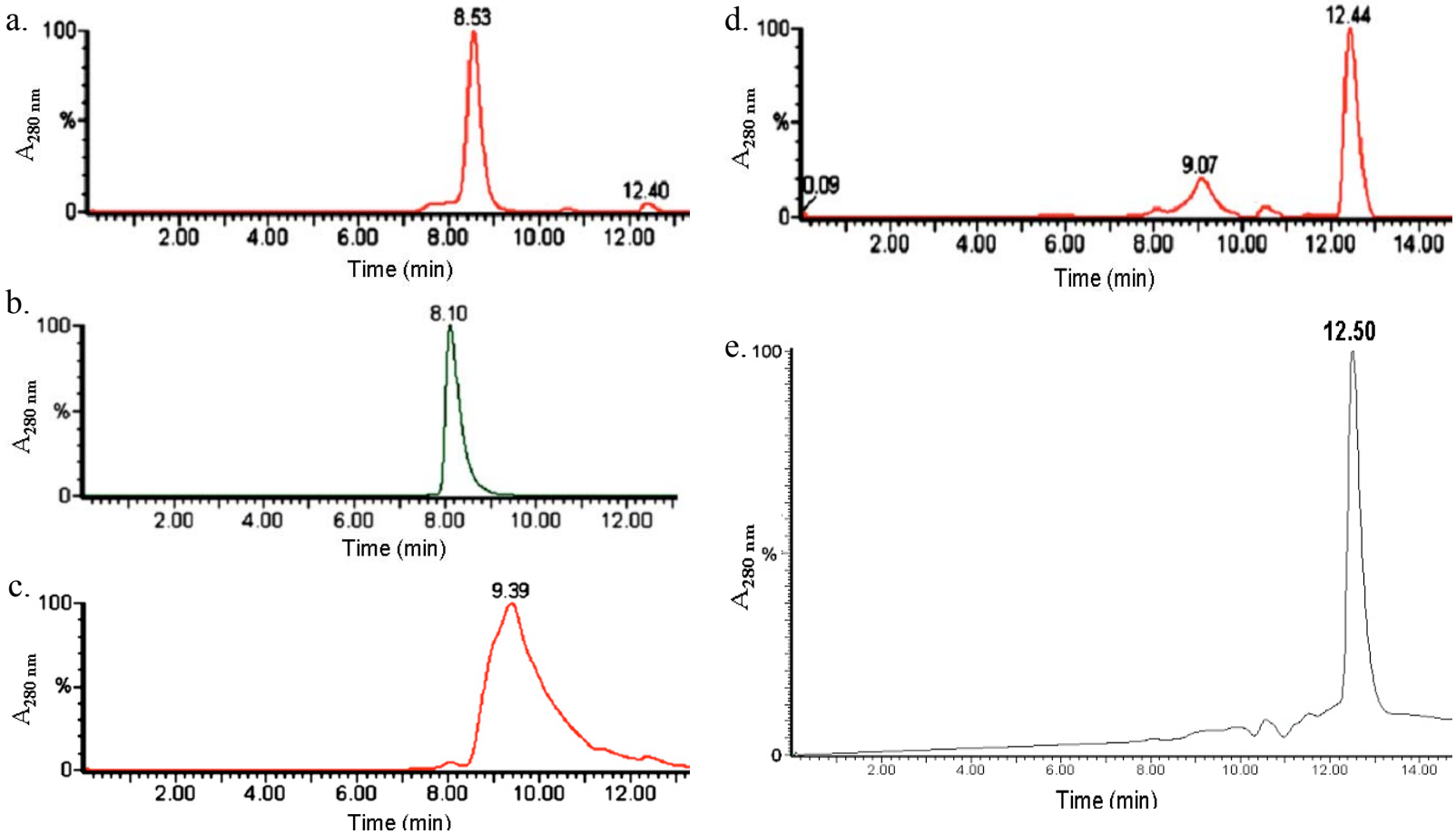

Figure 5.11. Size-exclusion chromatograms for the LexA dimer interface mutants.

(a) Δ_{75}LexA K156A, **(b)** Δ_{69}LexA K156A V100D, **(c)** Δ_{69}LexA K156A V100K, **(d)** Δ_{69}LexA K156A I196D, and **(e)** Δ_{69}LexA K156A I196K.

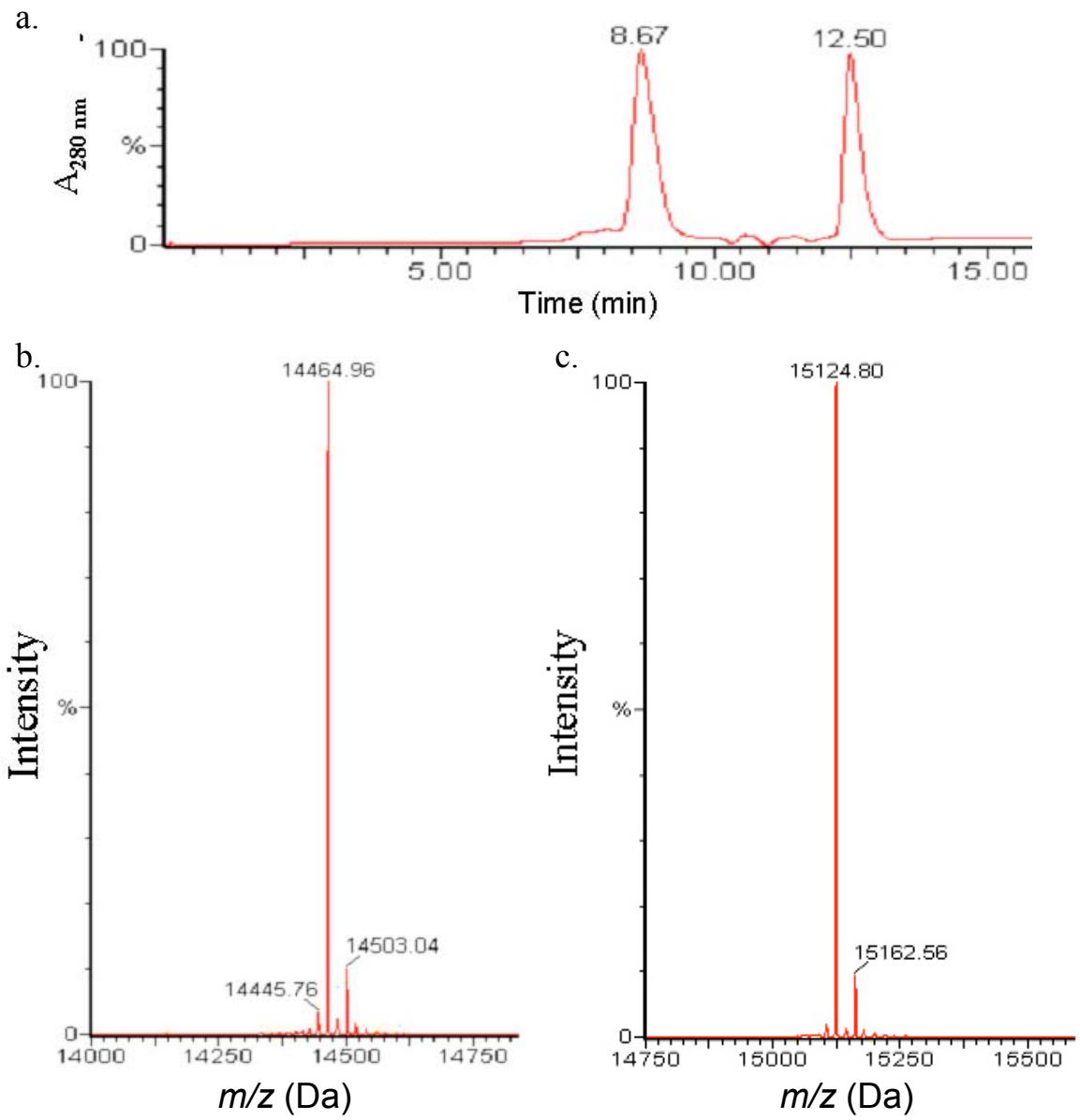

Figure 5.12. Size-exclusion chromatogram and MaxEnt spectra for a mixture that contained equal ratios of Δ_{75}LexA K156A and Δ_{69}LexA K156A I196K.

(a) Size exclusion chromatogram of the mixture that contained equal ratios of Δ_{75}LexA K156A (8.67 min) and Δ_{69}LexA K156A I196K (12.50 min), and MaxEnt spectra for a mixture that contained equal ratios of **(b)** Δ_{75}LexA K156A and **(c)** Δ_{69}LexA K156A I196K.

had only one molecular weight of 15.1 kDa (Figure 5.12c), which corresponded to Δ_{69}LexA K156A I196K (Table 5.2). Thus, there was a lack of heterodimer formation when Δ_{75}LexA K156A and Δ_{69}LexA K156A I196K were mixed together at equal ratios.

Table 5.2. Mass spectrometry results for the observed molecular masses, and the calculated molecular masses for the LexA mutants.

Sample	Comment	MW (Da)	
		Calculated	Observed
Δ75LexA K156A	-Histag	14,465.20	14,464.96
Δ69LexA K156A V100D	-Histag	15,125.70	15,125.44
Δ69LexA K156A V100K	+Histag	17,047.40	17,067.84
Δ69LexA K156A I196D	+Histag, -Met	16,889.00	16,888.64
Δ69LexA K156A I196K	+Histag	17,033.30	17,054.08
	-Histag	15,124.70	15,124.80

5.4.2. Yeast One-hybrid Analysis

In vivo, studies have shown that the dimer form of LexA has a 10-fold greater binding affinity for its DNA operator site than the monomer form of $LexA_{1-88}$ (*i.e.* the individual DNA binding domain) (Bertrand-Burggraf *et al.*, 1987; Brent and Ptashne, 1985; Golemis and Brent, 1992). Dimerization of the LexA repressor is believed to provide a favourable geometrical conformation for the DNA binding domain of LexA, such that the contacts with its operator site are optimized (Golemis and Brent, 1992); and also ensures that the two DNA strands do not melt (Silva and Silveira, 1993). If the dimer interface mutants exist in the dimer form, they are expected to have a high DNA-binding affinity as observed for the functional LexA repressor. On the other hand, if the dimer interface mutants exist in the monomer form, they are expected to have a low DNA-binding affinity as observed for $LexA_{1-88}$. This rational was applied to the LexA dimer interface mutants, in order to determine whether the mutants exist in the monomer or dimer form by using the yeast one-hybrid system. In other words, this system correlates the level of LexA's binding affinity for its operator site with the type of species present (*i.e.* the monomer or dimer form).

Single point mutations at LexA's dimer interface were introduced by site-directed mutagenesis by overlap extension PCR. The *b42* activation domain was also introduced at the C-terminal end of the LexA dimer interface mutants (Figure 5.13a). This served as an indicator for the mutants' binding affinity towards the *lexA* operator site. The *lexA* mutants were cloned into the backbone of the pEG202 vector (Figure 5.13a) *via* homologous recombination in *S. cerevisiae* strain EY93. The plasmid was then isolated from the *S. cerevisiae* strain EY93 cells and transformed into *S. cerevisiae* strain EY111, in order to test for their binding affinity towards the *lexA* operator site *in vivo*. If the dimer interface mutants do not dimerize, they are expected to have a reduced DNA-binding affinity, which is correlated to a reduced activation for the downstream reporter gene (Figure 5.13b). If the dimer interface mutants are able to dimerize, they are expected to have a normal DNA-binding affinity, which is correlated to a normal level of activation for the down stream reporter gene (Figure 5.13c).

The plasmid's high copy number (2 μm origin) will allow the fusion protein to reach an estimated nuclear concentration of 4.5 to 9.0 μM (Golemis and Brent, 1992).* This establishes a physiological LexA concentration in the yeast cells that is slightly higher than the intracellular levels in *E. coli*, which is reported to fluctuate during its growth cycle between 0.7 to 5 μM (Dri and Moreau, 1993).

In the yeast one-hybrid system, the mutants were tested for the activation of the *lacZ* reporter gene, which provides a blue-white colony assay on plates containing X-Gal. A blue phenotype suggests that LexA exists as a dimer (a strong binding affinity for its operator site), while a white phenotype suggests that LexA exists as a monomer (weak binding affinity for its operator site). The mutants were also tested for the activation of the *LEU2* gene, which allows the cells to grow on synthetic media that is lacking Leu. The latter assay is less stringent than the *lacZ* reporter gene; therefore, it will detect a weaker binding affinity between the LexA dimer interface mutants and their *lexA* operator site (Estojak *et al.*, 1995).

* The value for the estimated nuclear concentration is given for the LexA Gal4 fusion protein.

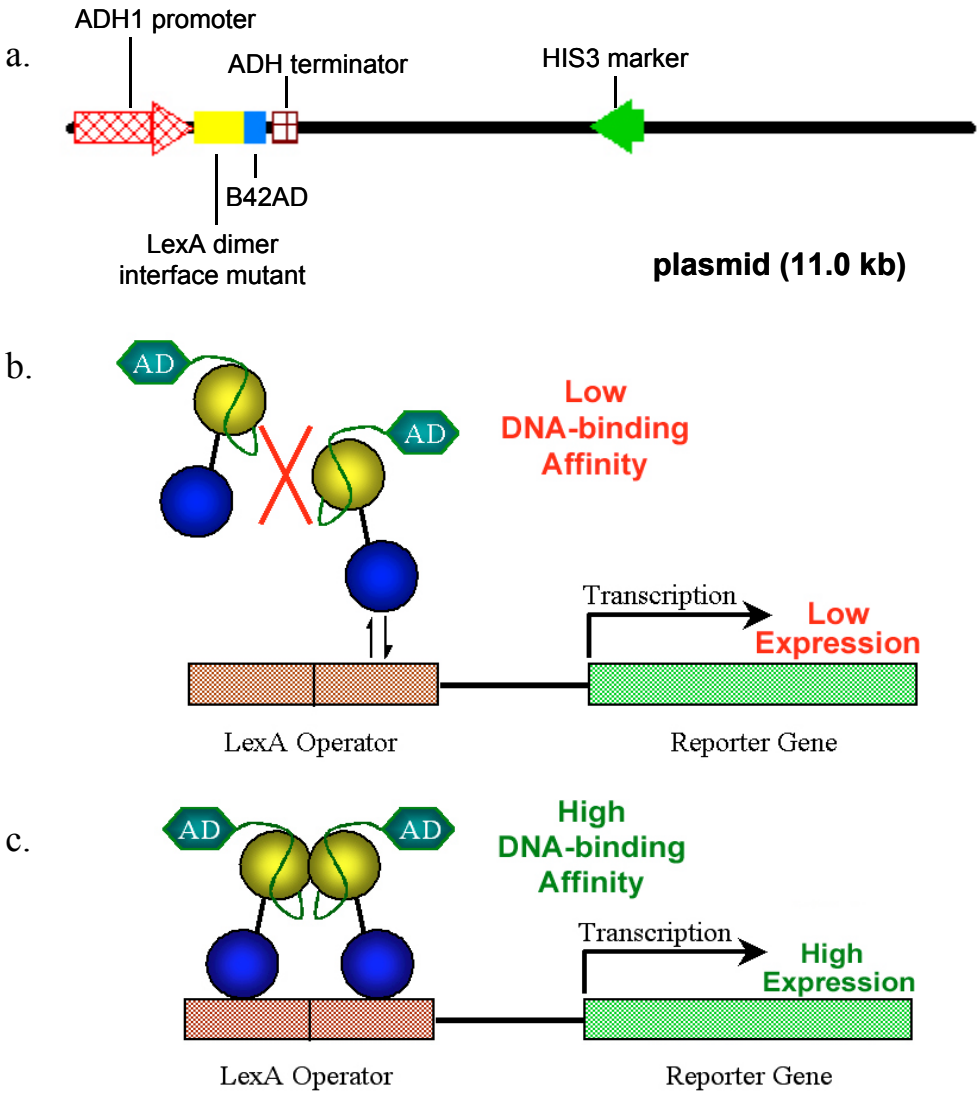

Figure 5.13. Schematic overview for the design of the LexA dimer interface mutants in the yeast one-hybrid system.

(a) A linear drawing of the plasmid that contains the *lexA* dimer interface mutant (V100D, V100K, I198D, or I198K) gene. Expression of the *lexA* gene was constitutively expressed with the ADH1 promoter. **(b)** The LexA dimer interface mutants that do not dimerize will have a low DNA-binding affinity, which leads to a low expression of the reporter gene. **(c)** The LexA dimer interface mutants that dimerize will have an high DNA-binding affinity, which leads to a high expression of the reporter gene.

The cells expressing the *lexA* mutants were plated on both X-Gal SD H^- and X-Gal SD H^- L^- media for 3 days at 30°C. The mutants were found to activate the *lacZ* reporter gene, which produced the following colour intensities: wild-type, V100D > V100K, I196K > I196D (Figure 5.14). Based on these colour intensities, the I196D mutation was more effective in destabilizing LexA's DNA binding affinity, but it may not prove that LexA I196D exists more frequently in the monomer form. In general, the point mutations V100D, V100K, and I196K did not significantly reduced LexA's DNA binding affinity when compared to the control. All of the mutants were found to activate the *LEU2* reporter gene, which suggested that the dimer interface mutants were able to bind to their operator site (Figure 5.14). More specifically, the results for the yeast one-hybrid system might imply that the LexA mutants, I196K and I196D existed as dimers *in vivo*. This was contrary to the size-exclusion results since the two mutants existed as monomers *in vitro*. In either case, the I196D and I196K mutants were good candidates for determining whether RecA is able to bind to the monomer form of LexA *in vitro*.

5.4.3. Inhibition Assay

RecA's binding preference for the monomer or dimer form of LexA was detected with the inhibition assay. The level of inhibition for RecA's coprotease activity (*i.e.* a lack of cleavage products for wild-type LexA) is correlated to its binding affinity for the LexA dimer interface mutants (inhibitor). In this assay, there was a high amount of wild-type LexA cleavage products generated in the presence of the dimer interface mutants when compared to Δ_{69}LexA K156A (Figure 5.15). These results suggested that RecA's coprotease activity was not inhibited by the dimer interface mutants when compared to the positive inhibitory control, Δ_{69}LexA K156A. Thus, a lack of inhibition for RecA's coprotease activity might suggest that the LexA dimer interface mutants acted as poor substrates for the binding of RecA.

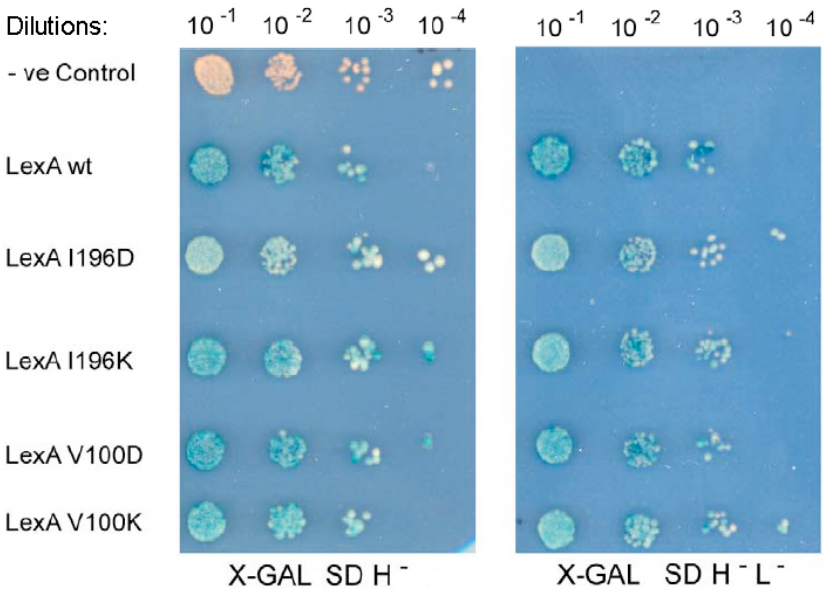

Figure 5.14. Yeast one-hybrid assay for the LexA dimer interface mutants.

Yeast strains EY111 that contained the *lexA b42AD* plasmids were grown on both X-Gal SD H^- and SD $H^- L^-$ plates for 3 days at 30°C. From top to bottom of the plate: negative control (wild-type LexA), wild-type LexA B42AD, and LexA B42AD dimer interface mutants (I196D, I196K, V100D, and V100K). Serial dilutions in the range of 10^{-1} to 10^{-4}–fold were performed on each sample.

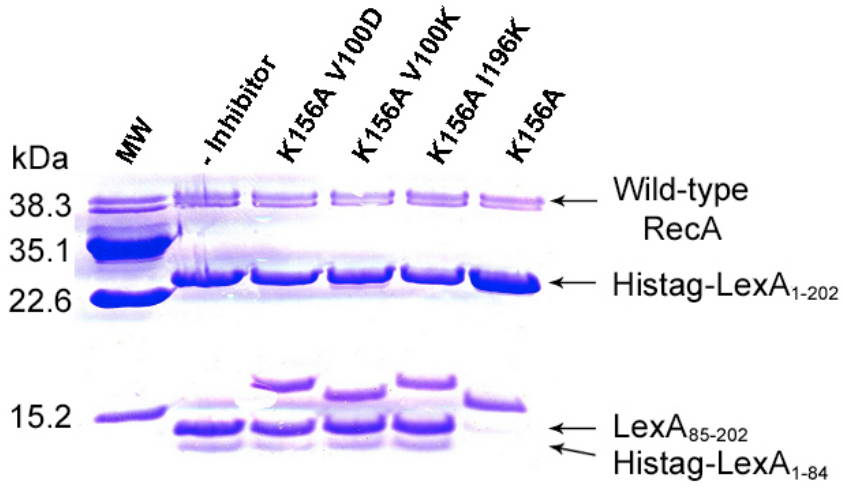

Figure 5.15. Inhibition of RecA's coprotease activity by the dimer interface mutants.

Inhibition of wild-type RecA (5 μM) mediated cleavage of His-tagged wild-type LexA (40 μM) by either the Δ_{69}LexA K156A dimer interface mutants (V100D, V100K, or I196K; 10 μM) or Δ_{69}LexA K156A (K156A; 10 μM). The enzyme solutions contained 150 mM HEPES/NaOH pH 7.5, 15% (w/v) PEG 400, and 1.5 mM ATP-γ-S; and were incubated for 2 hr at 20°C. The experiment for –Inhibitor was the same as above, except that it lacked a LexA mutant. The reaction mixtures were resolved on a 15% SDS-polyacrylamide gel and stained with Coomassie Brilliant Blue. RecA-mediated cleavage of His-tagged wild-type LexA produced a N-terminal fragment (histag-$LexA_{1-84}$) and a C-terminal fragment ($LexA_{85-202}$).

6. DISCUSSION

6.1. Enhancing the Stability of the RecA/LexA Complex

The formation of the RecA/LexA complex is a thermodynamic process that can be broken up into three steps: (1) self-activation of RecA (active form), (2) a change in LexA's conformation towards the cleavable form, and (3) the binding of the active form of RecA and the cleavable form of LexA. Evidence for this model was provided by the enhanced stability of the RecA/LexA complex, which was achieved by reducing the energy barrier at each step. For example, a volume excluding agent, PEG 400 was able to force the binding between the active form of RecA and the cleavable form of LexA (Figure 5.1 a and b); high concentrations of salt were able to promote the active form of RecA (Figure 5.5); and introducing the K156A mutation in LexA was able to promote the cleavable form of LexA (Figure 5.5 and Figure 5.6). On the other hand, LexA S119A did not improve the stability of the RecA/LexA complex as salt concentrations were increased (Figure 5.5). This result was also consistent with other inhibition assays, where LexA S119A had a weak inhibitory effect when compared to LexA K156A on the rate of RecA-mediated cleavage for the LexA repressor *in vitro* (Lin and Little, 1989; Slilaty and Little, 1987). This is not surprising if it is hypothesized that RecA is able to bind to the cleavable form of LexA. Thus, RecA may have a greater binding affinity for LexA K156A, because the energy barrier associated with the cleavable form of LexA is reduced (Luo *et al.*, 2001), *i.e.* an input of free energy is not spent on the neutralization of the ε-amino group of K156 since it is no longer a requirement with the K156A mutation, but it is spent on the burial of the K156A residue. As for LexA S119A, RecA may have a weaker binding affinity for this mutant because the energy barrier associated with the cleavable form of LexA is not reduced, *i.e.* an input of free energy is spent on the burial and neutralization of the ε-amino group of K156 in LexA upon binding of the RecA protein (Luo *et al.*, 2001). The stability of the RecA/LexA complex was enhanced in the

presence of LexA K156A but not in the presence of LexA S119A (Figure 5.5 and Figure 5.6).

Given that an anion is believed to mimic the polyanionic phosphate backbone of DNA (Menetski *et al.*, 1992; Pugh and Cox, 1988), high concentrations of anions may have a similar inhibitory effect as caused by either dsDNA or excess ssDNA on RecA's binding affinity for the LexA repressor (Rehrauer *et al.*, 1996; Takahashi and Schnarr, 1989). Thus, salt concentrations above 0.8 M should be avoided in facilitating stable RecA/LexA complexes (Figure 5.5) since the high ionic strengths may disrupt protein-protein interactions due to its electrostatic shielding effect.

6.1.1. Isolation of Hyper-active RecA Mutants

In the yeast two-hybrid system, there were two possibilities why LexA K156A did not select for hyper-active RecA mutants that were able to enhance the stability of the RecA/LexA complex. (1) A more stringent selection method was not used for the isolation of the hyper-active RecA mutants, such as the *ADE2* and *LEU2* reporter genes or LexA S119A. However, this approach was time consuming since there was an 8-fold decrease in the number of positive interactions with LexA S119A when compared to LexA K156A. (The same situation is expected when using the *ADE2* reporter gene as opposed to the *lacZ* reporter gene, since both genes are stringent reporter genes). (2) Screening for hyper-active RecA mutants may be biased towards external factors that bring about its activation. For example, hyper-coprotease activity has been observed for RecA mutants that have lost their substrate specificity, such that the mutants are able to utilize other nucleotides or RNA molecules as substrates (Campbell and Davis, 1999a, 1999b; Konola *et al.*, 1995). This is indeed the case for the RecA mutants, E96D, K198N, and K216I, since previous studies have shown that all of these mutants exhibit hyper-coprotease activity *in vivo* (Campbell and Davis, 1999a; McGrew and Knight, 2003). Therefore, the mutants may not influence the self-activation of RecA directly, but increase the number of substrates that are able to bring about its activation.

Mutations at the K198 position of RecA were found to slightly reduce RecA's coprotease and recombinase activity during UV-induced DNA damage *in vivo* (Hörtnagel *et al.*, 1999; Larminat *et al.*, 1992). These studies are also consistent with the results presented in this thesis for the K198N mutation. The mutant had a slightly reduced

ATPase activity (Figure 5.10a) and a normal coprotease activity (Figure 5.10b) when compared to wild-type levels *in vitro* (Figure 5.5 and Figure 5.7 respectively). The slight reduction in the mutant's activity may have been caused by the disruption in its L2 loop region, which is implicated in anion/DNA binding (Pugh and Cox, 1988; Story *et al.*, 1992). Alternatively, the K198N mutation may affect RecA's structure, which in turn impairs the binding of the anions. In either case, the K198N mutation leads to a partial activation of RecA and in turn reduces the stability of the RecA/LexA complex.

The RecA K216E mutant had a defective ATPase activity (Figure 5.8a) and a reduced coprotease activity (Figure 5.8b) when compared to wild-type levels *in vitro* (Figure 5.5 and Figure 5.7). This mutation may have impaired the conformational changes that are induced upon ATP binding, since it is situated at the helix G region (ATPase core). This idea is supported by: the changes in position of the helix G/L2 region when comparing the RecA-dimer model (Wu *et al.*, 2004) with the RecA filament model (VanLoock *et al.*, 2003b); the close proximity of the K216 residue to the triphosphate of ATP in the RecA filament model (VanLoock *et al.*, 2003b); and the limited extent to which RecA K216E is able to form ATP-induced polymers *in vivo* (Logan *et al.*, 1997). Thus, the mutation may impair some of the ATP-induced allosteric changes that are required for RecA's strand exchange activities, but these additional changes may not be an absolute requirement for its coprotease activity. This may explain why RecA K216E was found to be defective in its recombination activity for both UV-damaged DNA repair and λ-phage recombination *in vivo* (Larminat *et al.*, 1992; Skiba and Knight, 1994), while still functional in its coprotease activity *in vitro*.

Interestingly, the E96D K216E double mutant was found to increase RecA's coprotease activity (Figure 5.9) when compared to the K216E single mutant *in vitro* (Figure 5.8b). This was expected since RecA E96D was found to have a 100-fold decrease in its ATP hydrolysis rate and an increase in its binding affinity for ATP, which in turn preactivates the RecA filament (Campbell and Davis, 1999a, 1999b). Thus, a hyper-active RecA mutant such as the E96D mutation will enhance the stability of the RecA/LexA complex because the mutation will shift RecA's conformation towards the active form.

The binding of anions to RecA's primary ssDNA binding site is believed to stimulate its ATPase activity (Pugh and Cox, 1988). However, salt did not stimulate the ATPase activity of RecA K216E (Figure 5.8a). It is tempting to speculate that the lack of ATPase stimulation by salt is somehow associated with the loss of its ssDNA-binding sites by the K216E mutation. However, the coprotease assay suggests that RecA K216E is still capable of binding to ssDNA at very low salt concentrations (Figure 5.8b); therefore, the mutant is expected to bind to other polyanions. It is quite possible that RecA K216E may be more sensitive to preferential hydration, thereby making the active form of RecA less stable since it is disrupted by low ion concentrations. In general, the hyper-coprotease activity of RecA K216E or RecA E69D K216E is not sufficient to stabilize the RecA/LexA complex such that AMP-PNP can be used as a substrate during crystallization trials.

6.1.2. Significance of the Thermodynamic Model

The crystal structure for the inactive form of EcRecA was solved 14 years ago (Story *et al.*, 1992). Since then there has been no crystal structures reported for either the active form of RecA or the RecA/LexA complex. The thermodynamic model that is proposed in this thesis will hopefully overcome past failures during crystallization trials, and lead to a structural insight into the RecA/LexA complex. This complex is important in understanding a similar RecA/CI-phage repressor (a LexA homolog) complex that has been implicated in the epidemiology of STEC diseases. Therefore, a structural insight into the RecA/LexA complex will be useful in developing drugs that target the RecA/CI phage repressor complex, since there are no conventional drugs to treat STEC infections.

6.2. LexA Dimer Interface Mutants

In a recent paper, the preferred substrate for RecA-mediated cleavage of bacteriophage 434 repressor (a LexA homolog) was found to be the dimer form and not the monomer form (Pawlowski and Koudelka, 2004). Therefore, it is very likely that RecA will have a greater binding affinity for the dimer form of LexA. Despite that RecA's binding preference has been determined, the work presented here is still useful in understanding why RecA does not bind to the dimer interface mutants.

In this thesis, the charge-charge repulsion established at the dimer interface of LexA by either mutation, I196D or I196K was found to prevent the protein from forming homodimers *in vitro* (Figure 5.11; d and e respectively). The charged interface at LexA I196K was also found to prevent the protein from forming heterodimers with LexA K156A at equal ratios (Figure 5.12). On the other hand, i*n vivo*, the mutants, I196K, I196D, V100K and V100D might exist as dimers (Figure 5.14). The former and latter results indicated that both mutants, I196K and I196D existed in the monomer form *in vitro* and in the dimer form *in vivo* respectively. The *lexA* operator site in the yeast one-hybrid system may be responsible for the dimerization of these mutants *in vivo*, since the DNA binding site has been reported to reduce the K_{dimer} value of LexA by 750-fold *in vitro* (Mohana-Borges *et al.*, 2000). Alternatively, the monomer form of LexA I196K or I196D may have a similar binding affinity for its *lexA* operator site as observed for the functional LexA repressor (dimer form) due to their intracellular concentrations. This idea is based on the equation for the monomer repression of the *uvrA* gene (Bertrand-Burggraf *et al.*, 1987), which indicates that ~2 μM $LexA_{1-88}$ is required to occupy 98% of the *uvrA* operator site. Thus, LexA I196K or I196D is expected to have a similar DNA-binding affinity as $LexA_{1-88}$, because they are unable to dimerize *in vitro*. It is quite possible that the mutant will reach a concentration of 2 μM in the yeast one-hybrid system, since the estimated nuclear concentration of a fusion protein is expected to be in the range of 4.5 to 9.0 μM (Golemis and Brent, 1992). In general, it is very difficult to determine if the dimer interface mutants were able to prevent dimerization *in vivo*. The high intracellular concentration of either LexA species may be able to overcome its weak binding affinity for its *lexA* operator site, and its *lexA* operator site is known to improve the dimerization of LexA.

Finally, the dimer interface mutants were found to act as poor substrates for the RecA protein *in vitro*, since they failed to inhibit RecA's coprotease activity (Figure 5.15). Either the V100D or the V100K mutation (dimer form) may have disrupted the overall conformation of the LexA dimer, which may have impaired RecA's binding affinity for the LexA mutant and in turn decrease the stability of the RecA/LexA complex. The I196K mutation (monomer form) may have disrupted LexA's tertiary structure, since its hydrophobic dimer interface surface is exposed to the aqueous

environment as observed in a free energy study on the stability of phage repressors (LexA homologs) (Foguel and Silva, 1994; Rupert *et al.*, 2000). This may also explain why RecA does not bind to the monomer form of LexA I196K nor does it lead to a stable RecA/LexA complex. In general, it is difficult to say whether RecA's poor binding affinity for the LexA dimer interface mutants was the result of changes in LexA's overall structure or a lack of dimerization *in vitro*.

In conclusion, a LexA monomer was generated *in vitro* by introducing either the I196K or I196D mutation at LexA's dimerization interface. These mutants will be extremely useful in future crystallization trials and free energy studies in order to understand the proteins' stability in solution and affinity for their operator site. More importantly, understanding the stability of the dimer interface mutants in solution may influence the energy barrier that is associated at each step in the formation of the RecA/LexA complex.

7. REFERENCES

Aihara, H., Ito, Y., Kurumizaka, H., Terada, T., Yokoyama, S., and Shibata, T. (1997). An interaction between a specified surface of the C-terminal domain of RecA protein and double-stranded DNA for homologous pairing. J. Mol. Biol. *274*, 213-221.

Aihara, H., Ito, Y., Kurumizaka, H., Yokoyama, S., and Shibata, T. (1999). The N-terminal domain of the human Rad51 protein binds DNA: structure and a DNA binding surface as revealed by NMR. J. Mol. Biol. *290*, 495-504.

Battista, J. R., Ohta, T., Nohmi, T., Sun, W., and Walker, G. C. (1990). Dominant negative *umuD* mutations decreasing RecA-mediated cleavage suggest roles for intact UmuD in modulation of SOS mutagenesis. Proc. Natl. Acad. Sci. U.S.A. *87*, 7190-7194.

Berlett, B. S., and Stadtman, E. R. (1997). Protein oxidation in aging, disease, and oxidative stress. J. Biol. Chem. *272*, 20313-20316.

Bertrand-Burggraf, E., Hurstel, S., Daune, M., and Schnarr, M. (1987). Promoter properties and negative regulation of the *uvrA* gene by the LexA repressor and its amino-terminal DNA binding domain. J. Mol. Biol. *193*, 293-302.

Bianco, P. R., and Kowalczykowski, S. C. (2001). RecA protein (London, Nature Publishing Group).

Bianco, P. R., T.Tracy, R., and Kowalczykowski, S. C. (1998). DNA strand exchange proteins: A biochemical and physical comparison. Front. Biosci. *3*, 570-603.

Brenner, S. L., Zlotnick, A., and Griffith, J. D. (1988). RecA protein self-assembly. Multiple discrete aggregation states. J. Mol. Biol. *204*, 959-972.

Brent, R., and Ptashne, M. (1985). A Eukaryotic transcriptional activator bearing the DNA specificity of a Prokaryotic repressor. Cell *43*, 729-736.

Burckhardt, S. E., Woodgate, R., Scheuermann, R. H., and Echols, H. (1988). UmuD mutagenesis protein of *Escherichia coli*: overproduction, purification, and cleavage by RecA. Proc. Natl. Acad. Sci. U.S.A. *85*, 1811-1815.

Campbell, M. J., and Davis, R. W. (1999a). On the *in vivo* function of the RecA ATPase. J. Mol. Biol. *286*, 437-445.

Campbell, M. J., and Davis, R. W. (1999b). Toxic mutations in the *recA* gene of *E. coli* prevent proper chromosome segregation. J. Mol. Biol. *286*, 417-435.

Cazaux, C., Blanchet, J.-S., Dupuis, D., Villani, G., Defais, M., and Johnson, N. P. (1998). Investigation of the secondary DNA-binding site of the bacterial recombinase RecA. J. Biol. Chem. *273*, 28799-28804.

Clark, A. J., and Margulies, A. D. (1965). Isolation and characterization of recombination-deficient mutants of *Escherichia coli* K12. Proc. Natl. Acad. Sci. U.S.A. *53*, 451–459.

Cleland, J. L., Lam, X., Kendrick, B., Yang, J., Yang, T.-H., Overcashier, D., Brooks, D., Hsu, C., and Carpenter, J. F. (2000). A specific molar ratio of stabilizer to protein is required for storage stability of a lyophilized monoclonal antibody. J. Pharm. Sci. *90*, 310-321.

Cotterill, S. M., Satterthwait, A. C., and Fersht, A. R. (1982). recA protein from *Escherichia coli*. A very rapid and simple purification procedure: binding of adenosine 5'-triphosphate and adenosine 5'-diphosphate by the homogeneous protein. Biochemistry *21*, 4332-4337.

Courcelle, J., Khodursky, A., Peter, B., Brown, P. O., and Hanawalt, P. C. (2001). Comparative gene expression profiles following UV exposure in wild-type and SOS-deficient *Escherichia coli*. Genetics *158*, 41-64.

Cox, J. M., Abbott, S. N., Chitteni-Pattu, S., Inman, R. B., and Cox, M. M. (2006). Complementation of one RecA protein point mutation by another. J. Biol. Chem. *281*, 12968-12975.

Cox, M. M., and Lehman, I. R. (1981). Directionality and polarity in recA protein-promoted branch migration. Proc. Natl. Acad. Sci. U.S.A. *78*, 6018-6022.

De Zutter, J. K., Forget, A. L., Logan, K. M., and Knight, K. L. (2001). Phe217 regulates the transfer of allosteric information across the subunit interface of the RecA protein filament. Structure *9*, 47-55.

DiCapua, E., Cuillel, M., Hewat, E., Schnarr, M., Timmins, P. A., and Ruigrok, R. W. (1992). Activation of recA protein. The open helix model for LexA cleavage. J. Mol. Biol. *226*, 707-719.

DiCapua, E., Ruigrok, R. W., and Timmins, P. A. (1990a). Activation of recA protein: the salt-induced structural transition. J. Struct. Biol. *104*, 91-96.

DiCapua, E., Schnarr, M., Ruigrok, R. W., Lindner, P., and Timmins, P. A. (1990b). Complexes of RecA protein in solution. A study by small angle neutron scattering. J. Mol. Biol. *214*, 557-570.

Dong, Q., E.Blatter, E., W.Ebright, Y., Bister, K., and H.Ebright, R. (1994). Identification of amino acid-base contacts in the Myc-DNA complex by site-specific bromouracil mediated photocrosslinking. EMBO J. *13*, 200-204.

Dri, A.-M., and Moreau, P. L. (1993). Phosphate starvation and low temperature as well as ultraviolet irradiation transcriptionally induce the *Escherichia coli* LexA-controlled gene *sfiA*. Mol. Microbiol. *8*, 697-706.

Dutreix, M., Moreau, P. L., Bailone, A., Galibert, F., Battista, J. R., Walker, G. C., and Devoret, R. (1989). New recA mutations that dissociate the various RecA protein activities in *Escherichia coli* provide evidence for an additional role for RecA protein in UV mutagenesis. J. Bacteriol. *171*, 2415-2423.

Egelman, E. H. (2001). Does a stretched DNA structure dictate the helical geometry of RecA-like filaments? J. Mol. Biol. *309*, 539-542.

Eguchi, Y., Ogawa, T., and Ogawa, H. (1988). Cleavage of bacteriophage phi 80 CI repressor by RecA protein. J. Mol. Biol. *202*, 565-573.

Estojak, J., Brent, R., and Golemis, E. A. (1995). Correlation of two-hybrid affinity data with in vitro measurements. Mol. Cell. Biol. *15*, 5820-5829.

Foguel, D., and Silva, J. L. (1994). Cold denaturation of a repressor-operator complex: The role of entropy in protein-DNA recognition. Proc. Natl. Acad. Sci. U.S.A. *91*, 8244-8247.

Friedberg, E. C., Walker, G. C., and Siede, W. (1995). DNA Repair and Mutagenesis (Washington, DC, American Society for Microbiology Press).

Gardner, R. V., Voloshin, O. N., and Camerini-Otero, R. D. (1995). The identification of the single-stranded DNA-binding domain of the *Escherichia coli* RecA protein. Eur. J. Biochem. *233*, 419-425.

Geyer, C. R., and Brent, R. (2000). Selection of genetic agents from random peptide aptamer expression libraries. Meth. Enzymol. *328*, 171-210.

Golemis, E. A., and Brent, R. (1992). Fused protein domains inhibit DNA binding by LexA. Mol. Cell. Biol. *12*, 3006-3014.

Gonda, D. K., and Radding, C. M. (1986). The mechanism of the search for homology promoted by recA protein. J. Biol. Chem. *261*, 13087-13096.

Gonzalez, M., Rasulova, R., Maurizi, M. R., and Woodgate, R. (2000). Subunit-specific degradation of the UmuD/D' heterodimer by the ClpXP protease: the role of trans recognition in UmuD' stability. EMBO J. *19*, 5251-5258.

Haque, R., Huston, C. D., Hughes, M., Houpt, E., and Petri, W. A. (2003). Amebiasis. N. Engl. J. Med. *348*, 1565-1573.

Harmon, F. G., Rehrauer, W. M., and Kowalczykowski, S. C. (1996). Interaction of *Escherichia coli* RecA protein with the LexA repressor. J. Biol. Chem. *39*, 23874-23883.

Heuser, J., and Griffith, J. (1989). Visualization of RecA protein and its complexes with DNA by quick-freeze/deep-etch electron microscopy. J. Mol. Biol. *210*, 473-484.

Honigberg, S. M., Gonda, D. K., Flory, J., and Radding, C. M. (1985). The pairing activity of stable nucleoprotein filaments made from recA protein, single-stranded DNA, and adenosine 5'-(γ-thio)triphosphate. J. Biol. Chem. *260*, 11845-11851.

Horrii, T., Ogawa, T., Nakatani, T., Hase, T., Matsubara, H., and Ogawa, H. (1981). Regulation of SOS functions: purification of *E. coli* LexA protein and determination of its specific site cleaved by the RecA protein. Cell *27*, 515-522.

Hörtnagel, K., Voloshin, O. N., Kinal, H. H., Ma, N., Schaffer-Judge, C., and Camerini-Otero, R. D. (1999). Saturation mutagenesis of the *E. coli* RecA loop L2 homologous DNA pairing region reveals residues essential for recombination and recombinational repair. J. Mol. Biol. *286*, 1097-1106.

http://www.cdc.gov/epo/dphsi/casedef/hemolyticcurrent.htm (2005). Hemolytic Uremic Syndrome, post-diarrheal (Centers for Disease Control and Prevention).

Karlin, S., and Brocchieri, L. (1996). Evolutionary conservation of RecA genes in relation to protein structure and function. J. Bacteriol. *178*, 1881-1894.

Kim, B., and Little, J. W. (1993). LexA and lambda CI repressors as enzymes: specific cleavage in an intermolecular reaction. Cell *73*, 1165-1173.

Kimmitt, P. T., Harwood, C. R., and Barer, M. R. (2000). Toxin gene expression by Shiga toxin-producing *Escherichia coli*: the role of antibiotics and the bacterial SOS response. Emerging Infect. Dis. *6*, 458-465.

Konola, J. T., Nastri, H. G., Logan, K. M., and Knight, K. L. (1995). Mutations at Pro67 in the RecA protein P-loop motif differentially modify coprotease function and separate coprotease from recombination activities. J. Biol. Chem. *270*, 8411-8419.

Kowalczykowski, S. C. (1986). Interaction of RecA protein with a photoaffinity analogue of ATP, 8-Azido-ATP: determination of nucleotide cofactor binding parameters and of the relationship bwtweeen ATP binding and ATP hydrolysis. Biochemistry *25*, 5872-5881.

Kowalczykowski, S. C. (1987a). Mechanistic aspects of the DNA strand exchange activity of *E. coli* recA protein. Trends Biochem. Sci. *12*, 141-145.

Kowalczykowski, S. C. (1987b). Mechanistic aspects of the DNA strand exchange activity of *E. coli* recA protein. Trends Biochem. Sci. *12*, 141-146.

Kowalczykowski, S. C. (1991). Biochemistry of genetic recombination: energetics and mechanism of DNA strand exchange. Annu. Rev. Biophys. Biophys. Chem. *20*, 539-575.

Kowalczykowski, S. C., Dixon, D. A., Eggleston, A. K., Lauder, S. D., and Rehrauer, W. M. (1994). Biochemistry of homologous recombination in *Escherichia coli*. Microbiol. Rev. *58*, 401-465.

Kowalczykowski, S. C., and Eggleston, A. K. (1994). Homologous pairing and DNA strand-exchange proteins. Annu. Rev. Biochem. *63*, 991-1043.

Kuzminov, A. (1999). Recombinational repair of DNA damage in *Escherichia coli* and Bacteriophage λ. Microbiol. Mol. Biol. Rev. *63*, 751-813.

Larminat, F., Cazaux, C., Germanier, M., and Defais, M. (1992). New mutations in and around the L2 disordered loop of the RecA protein modulate recombination and/or coprotease activity. J. Bacteriol. *174*, 6264-6269.

Lavery, P. E., and Kowalczykowski, S. C. (1992). Enhancement of recA protein-promoted DNA strand exchange activity by volume-occupying agents. J. Biol. Chem. *267*, 9307-9314.

Leahy, M. C., and Radding, C. M. (1986). Topography of the interaction of recA protein with single-stranded deoxyoligonucleotides. J. Biol. Chem. *261*, 6954-6960.

Leonard, N. J. (1984). Etheno-substituted nucleotides and coenzymes: fluorescence and biological activity. Crit. Rev. Biochem. Mol. Biol. *15*, 125-199.

Lin, L.-L., and Little, J. W. (1989). Autodigestion and RecA-dependent cleavage of Ind^- mutant LexA proteins. J. Mol. Biol. *210*, 439-452.

Little, J. W. (1983). The SOS regulatory system: control of its state by the level of RecA protease. J. Mol. Biol. *167*, 791-808.

Little, J. W. (1993). LexA cleavage and other self-processing reactions. J. Bacteriol. *175*, 4943-4950.

Little, J. W., Edmiston, S. H., Pacelli, L. Z., and Mount, D. W. (1980). Cleavage of the *Escherichia coli* lexA protein by the recA protease. Proc. Natl. Acad. Sci. U.S.A. *77*, 3225-3229.

Liu, Y., Stasiak, A. Z., Masson, J.-Y., McIlwraith, M. J., Stasiak, A., and West, S. C. (2004). Conformational changes modulate the activity of human RAD51 protein. J. Mol. Biol. *337*, 817-827.

Logan, K. M., Skiba, M. C., Eldin, S., and Knight, K. L. (1997). Mutant RecA proteins which form hexamer-sized oligomers. J. Mol. Biol. *266*, 306-316.

Luo, Y., Pfuetzner, R. A., Mosimann, S., Paetzel, M., Frey, E. A., Cherney, M., Kim, B., Little, J. W., and Strynadka, N. C. J. (2001). Crystal structure of LexA: A conformational switch for regulation of self-cleavage. Cell *106*, 585-594.

Malkov, V. A., and Camerini-Otero, D. R. (1995). Photocross-links between single-stranded DNA and *Escherichia coli* RecA protein map to loops L1 (amino acid residues 157–164) and L2 (amino acid residues 195–209). J. Biol. Chem. *270*, 30230-30233.

McGrew, D. A., and Knight, K. L. (2003). Molecular design and funcitonal organization of the RecA protein. Crit. Rev. Biochem. Mol. Biol. *38*, 385-432.

Menetski, J. P., Bear, D. G., and Kowalczykowski, S. C. (1990). Stable DNA heteroduplex formation catalyzed by the *Escherichia coli* RecA protein in the absence of ATP hydrolysis. Proc. Natl. Acad. Sci. U.S.A. *87*, 21-25.

Menetski, J. P., and Kowalczykowski, S. C. (1985). Interaction of recA protein with single-stranded DNA. Quantitative aspects of binding affinity modulation by nucleotide cofactors. J. Mol. Biol. *181*, 281-295.

Menetski, J. P., and Kowalczykowski, S. C. (1987). Transfer of recA protein from one polynucleotide to another. J. Biol. Chem. *262*, 2093-2100.

Menetski, J. P., Varghese, A., and Kowalczykowski, S. C. (1988). Properties of the high-affinity single-stranded DNA binding state of the *Escherichia coli RecA* protein. Biochemistry *27*, 1205-1212.

Menetski, J. P., Varghese, A., and Kowalczykowski, S. C. (1992). The physical and enzymatic properties of *Escherichia coli* recA protein display anion-specific inhibition. J. Biol. Chem. *267*, 10400-10404.

Mikawa, T., Masui, R., and Kuramitsu, S. (1998). RecA protein has extremely high cooperativity for substrate in its ATPase activity. J. Biochem. *123*, 450-457.

Mirshad, J. K., and Kowalczykowski, S. C. (2003). Biochemical characterization of a mutant RecA protein altered in DNA-binding Loop 1. Biochemistry *42*, 5945-5954.

Mohana-Borges, R., Pacheco, A. B. F., Sousa, F. J. R., Foguel, D., Almeida, D. F., and Silva, J. L. (2000). LexA repressor forms stable dimers in solution. J. Biol. Chem. *275*, 4708-4712.

Moreau, P. L., and Carlier, M.-F. (1989). RecA protein-promoted cleavage of LexA repressor in the presence of ADP and structural analogues of inorganic phosphate, the fluoride complexes of aluminum and beryllium. J. Biol. Chem. *264*, 2302-2306.

Morimatsu, K., Takahashi, M., and Nordén, B. (2002). Arrangement of RecA protein in its active filament determined by polarized-light spectroscopy. Proc. Natl. Acad. Sci. U.S.A. *99*, 11688-11693.

Nastri, H. G., Guzzo, A., Lange, C. S., Walker, G. C., and Knight, K. L. (1997). Mutational analysis of the RecA protein L1 region identifies this area as a probable part of the co-protease substrate binding site. Mol. Microbiol. *25*, 967-978.

Nguyen, T. T., Muench, K. A., and Bryant, F. R. (1993). Inactivation of the recA protein by mutation of histidine 97 or lysine 248 at the subunit interface. J. Biol. Chem. *268*, 3107-3113.

Nohmi, T., Battista, J. R., Dodson, L. A., and Walker, G. C. (1988). RecA-mediated cleavage activates UmuD for mutagenesis: mechanistic relationship between transcriptional derepression and posttranslational activation. Proc. Natl. Acad. Sci. U.S.A. *85*, 1816-1820.

Ogawa, H., and Ogawa, T. (1986). General recombination: functions and structure of RecA protein. Adv. Biophys. *21*, 135-148.

Oppenheim, A. B., Kobiler, O., Stavans, J., Court, D. L., and Adhya, S. (2005). Switches in bacteriophage lambda development. Annu. Rev. Genet. *39*, 409-429.

Opperman, T., Murli, S., Smith, B. T., and Walker, G. C. (1999). A model for a *umuDC*-dependent prokaryotic DNA damage checkpoint. Proc. Natl. Acad. Sci. U.S.A. *96*, 9218-9223.

Pattanayek, R., Wang, J., Mori, T., Xu, Y., Johnson, C. H., and Egli, M. (2004). Visualizing a circadian clock protein: crystal structure of KaiC and functional insights. Mol. Cell *15*, 375-388.

Pawlowski, D. R., and Koudelka, G. B. (2004). The preferred substrate for RecA-mediated cleavage of bacteriophage 434 repressor is the DNA-bound dimer. J. Bacteriol. *186*, 1-7.

Phizicky, E. M., and Roberts, J. W. (1981). Induction of SOS functions: regulation of proteolytic activity of *E. coli* RecA protein by interaction with DNA and nucleoside triphosphate. Cell *25*, 259-267.

Pugh, B. F., and Cox, M. M. (1988). High salt activation of recA protein ATPase in the absence of DNA. J. Biol. Chem. *263*, 76-83.

Quillardet, P., and Hofnung, M. (1993). The SOS chromotest: a review. Mutat. Res. *297*, 235-279.

Rajagopalan, M., Lu, C., Woodgate, R., O'Donnell, M., Goodman, M. F., and Echols, H. (1992). Activity of the purified mutagenesis proteins UmuC, UmuD', and RecA in replicative bypass of an abasic DNA lesion by DNA polymerase III. Proc. Natl. Acad. Sci. U.S.A. *89*, 10777-10781.

Rehrauer, W. M., Lavery, P. E., Palmer, E. L., and Singh, R. N. (1996). Interaction of *Escherichia coli* RecA protein with LexA repressor. J. Biol. Chem. *271*, 23865-23873.

Reuven, N. B., Arad, G., Maor-Shoshani, A., and Livneh, Z. (1999). The mutagenesis protein UmuC is a DNA polymerase activated by UmuD', RecA, and SSB and is specialized for translesion replication. J. Biol. Chem. *274*, 31763-31766.

Riddles, P. W., and Lehman, I. R. (1985). The formaton of plectonemic joints by the recA protein of *Escherichia coli*. Requirement for ATP hydrolysis. J. Biol. Chem. *260*, 170-173.

Roberts, J. W., Roberts, C. W., and Craig, N. L. (1978). *Escherichia coli* recA gene product inactivates phage lambda repressor. Proc. Natl. Acad. Sci. U.S.A. *75*, 4714-4718.

Roland, K. L., Smith, M. H., Rupley, J., and Little, J. W. (1992). *In vitro* analysis of mutant LexA proteins with an increased rate of specific cleavage. J. Mol. Biol. *228*, 395-408.

Roman, L. J., and Kowalczykowski, S. C. (1986). Relationship of the physical and enzymatic properties of *Escherichia coli* RecA protein to its strand exchange activity. Biochemistry *25*, 7375-7385.

Rupert, P. B., Mollah, A. K. M. M., Mossing, M. C., and Matthews, B. W. (2000). The structural basis for enhanced stability and reduced DNA binding seen in engineered second-generation Cro monomers and dimers. J. Mol. Biol. *296*, 1079-1090.

Sambrook, J., and Russell, D. W. (2001a). Protocol 1: Two-hybrid and other two-component systems. In Molecular cloning: a laboratory manual (New York, Cold Spring Harbor Laboratory Press), pp. 18.16-18.47.

Sambrook, J., and Russell, D. W. (2001b). Protocol 6: Site-specific mutagenesis by overlap extension. In Molecular cloning: a laboratory manual (New York, Cold Spring Harbor Laboratory Press), pp. 13.36-13.39.

Sauer, R. T., Ross, M. J., and Ptashne, M. (1982). Cleavage of the λ and P22 repressors by recA protein. J. Biol. Chem. *257*, 4458-4462.

Schiestl, R. H., and Gietz, R. D. (1989). High efficiency transformation of intact yeast cells using single stranded nucleic acid as a carrier. Curr. Genet. *16*, 339-346.

Schuller, S., Frankel, G., and Phillips, A. D. (2005). New insights into the role of Shiga toxins in intestinal disease. Gastroenterology *129*, 4-5.

Selmane, T., Wittung-Stafshede, P., Maraboeuf, F., Voloshin, O. N., Nordeèn, B., Camerini-Otero, D. R., and Takahashi, M. (1999). The L2 loop peptide of RecA stiffens and restricts base motions of single-stranded DNA similar to the intact protein. FEBS Lett. *446*, 30-34.

Serebriiskii, I. G., Golemis, E. A., and Uetz, P. (2005). The Proteomics Handbook (Totowa (NJ), Humana Press).

Shin, D. S., Pellegrini, L., Daniels, D. S., Yelent, B., Craig, L., Bates, D., Yu, D. S., Shivji, M. K., Hitomi, C., Arvai, A. S., Volkmann, N., Tsuruta, H., Blundell, T. L., Venkitaraman, A. R., and Tainer, J. A. (2003). Full-length archaeal Rad51 structure and mutants: mechanisms for RAD51 assembly and control by BRCA2. EMBO J. *22*, 4566-4576.

Shinagawa, H., Iwasaki, H., Kato, T., and Nakata, A. (1988). RecA protein-dependent cleavage of UmuD protein and SOS mutagenesis. Proc. Natl. Acad. Sci. U.S.A. *85*, 1806-1810.

Silva, J. L., and Silveira, C. F. (1993). Energy coupling between DNA binding and subunit association is responsible for the specificity of DNA-Arc interaction. Protein Sci. *2*, 945-950.

Silver, M. S., and Fersht, A. R. (1982). Direct observation of complexes formed between recA protein and a fluorescent single-stranded deoxyribonucleic acid derivative. Biochemistry *21*, 6066-6072.

Silver, M. S., and Fersht, A. R. (1983). Inverstigation of binding between recA protein and single-stranded ploynucleotides with the aid of a fluorescent deoxyribonucleic acid derivative. Biochemistry *22*, 2860-2866.

Skiba, M. C., and Knight, K. L. (1994). Functionally important residues at a subunit interface site in the RecA protein from *Escherichia coli*. J. Biol. Chem. *269*, 3823-3828.

Skiba, M. C., Logan, K. M., and Knight, K. L. (1999). Intersubunit proximity of residues in the RecA protein as shown by engineered disulfide cross-links. Biochemistry *38*, 11933-11941.

Slilaty, S. N., and Little, J. W. (1987). Lysine-156 and serine-119 are required for LexA repressor cleavage: a possible mechanism. Proc. Natl. Acad. Sci. U.S.A. *84*, 3987-3991.

Slilaty, S. N., and Vu, H. K. (1991). The role of electrostatic interactions in the mechanism of peptide bond hydrolysis by a Ser-Lys catalytic dyad. Protein Eng. Des. Sel. *4*, 919-922.

Story, R. M., Weber, I. T., and Steitz, T. A. (1992). The structure of the *Escherichia coli* RecA protein monomer and polymer. Nature *355*, 318-325.

Takahashi, M., Maraboeuf, F., and Nordén, B. (1996). Locations of functional domains in the RecA protein overlap of domains and regulation of activities. Eur. J. Biochem. *242*, 20-28.

Takahashi, M., and Schnarr, M. (1989). Investigation of RecA-polynucleotide interactions from the measurement of LexA repressor cleavage kinetics. Eur. J. Biochem. *183*, 617-622.

Tang, M., Pham, P., Shen, X., Taylor, J. S., O'Donnell, M., Woodgate, R., and Goodman, M. F. (2000). Roles of *E. coli* DNA polymerases IV and V in lesion-targeted and untargeted SOS mutagenesis. Nature *404*, 1014-1018.

Tang, M., Shen, X., Frank, E. G., O'Donnell, M., and Woodgate, R. (1999). UmuD'$_2$C is an error-prone DNA polymerase, *Escherichia coli* pol V. Proc. Natl. Acad. Sci. U.S.A. *96*, 8919-8924.

Tateishi, S., Horii, T., Ogawa, T., and Ogawa, H. (1992). C-terminal truncated *Escherichia coli* RecA protein RecA5327 has enhanced binding affinities to single- and double-stranded DNAs. J. Mol. Biol. *223*, 115-129.

Tombline, G., Heinen, C. D., Shim, K.-S., and FishelDagger, R. (1990). Biochemical characterization of the human RAD51 protein. J. Biol. Chem. *277*, 14434-14442.

VanLoock, M. S., Yu, X., Yang, S., Galkin, V. E., Huang, H., Rajan, S. S., Anderson, W. F., Stohl, E. A., Seifert, H. S., and Egelman, E. H. (2003a). Complexes of RecA with LexA and RecX differentiate between active and inactive RecA nucleoprotein filaments. J. Mol. Biol. *333*, 345-354.

VanLoock, M. S., Yu, X., Yang, S., Lai, A. L., Low, C., Campbell, M. J., and Egelman, E. H. (2003b). ATP-mediated conformational changes in the RecA filament. Structure *11*, 187-196.

Vershon, A. K., Liao, S.-M., McClure, W. R., and Sauer, R. T. (1987). Interaction of the bacteriophage P22 Arc repressor with operator DNA. J. Mol. Biol. *195*, 323-331.

Voloshin, O. N., Wang, L., and Camerini-Otero, R. D. (1996). Homologous DNA pairing promoted by a 20-amino acid peptide derived from RecA. Science *272*, 868-872.

Walker, G. C. (1985). Inducible DNA repair systems. Annu. Rev. Biochem. *54*, 425-457.

Wang, W.-B., and Tessman, E. S. (1986). Location of functional regions of the *Escherichia coli* RecA protein by DNA sequence analysis of RecA protease constitutive mutants. J. Bacteriol. *168*, 901-910.

Weinstock, G. M., McEntee, K., and Lehman, I. R. (1981a). Hydrolysis of nucleoside triphosphates catalyzed by the recA protein of *Escherichia coli*. Characterization of ATP hydrolysis. J. Biol. Chem. *256*, 8829-8834.

Weinstock, G. M., McEntee, K., and Lehman, I. R. (1981b). Hydrolysis of nucleoside triphosphates catalyzed by the recA protein of *Escherichia coli*. Steady state kinetic analysis of ATP hydrolysis. J. Biol. Chem. *256*, 8845-8849.

Weisemann, J. M., and Weinstock, G. M. (1988). Mutations at the cysteine codons of the *recA* gene of *Escherichia coli*. DNA *7*, 389-398.

Witkin, E. M. (1991). RecA protein in the SOS response: milesontes and mysteries. Biochemie *1991*, 133-141.

Wong, C. S., Jelacic, S., Habeeb, R. L., Watkins, S. L., and Tarr, P. I. (2000). The risk of hemolytic-uremic syndrome after antibiotic treatment of *Escherichia coli* O157:H7 infections. N. Engl. J. Med. *342*, 1930-1936.

Wu, Y., He, Y., Moya, I. A., Qian, X., and Luo, Y. (2004). Crystal structure of archaeal recombinase RadA: A snapshot of its extended conformation. Mol. Cell *15*, 423-435.

Wu, Y., Qian, X., He, Y., Moya, I. A., and Luo, Y. (2005). Crystal structure of an ATPase-active form of Rad51 homolog from *Methanococcus voltae*. J. Biol. Chem. *280*, 722-728.

Yu, X., and Egelman, E. H. (1992). Structural data suggest that the active and inactive forms of the RecA filament are not simply interconvertable. J. Mol. Biol. *227*, 334-346.

Yu, X., and Egelman, E. H. (1993). The LexA repressor binds within the deep helical groove of the activated RecA filament. J. Mol. Biol. *231*, 29-40.

Yu, X., Jacobs, S. A., West, S. C., Ogawa, T., and Egelman, E. H. (2001). Domain structure and dynamics in the helical filaments formed by RecA and Rad51 on DNA. Proc. Natl. Acad. Sci. U.S.A. *98*, 8419-8424.

Zimmerman, S. B., and Minton, A. P. (1993). Macromolecular crowding: biochemical, biophysical, and physiological consequences. Annu. Rev. Biophys. Biomol. Struct. *22*, 27-65.